Max-Planck-Institut für Meteorologie

REPORT No. 244

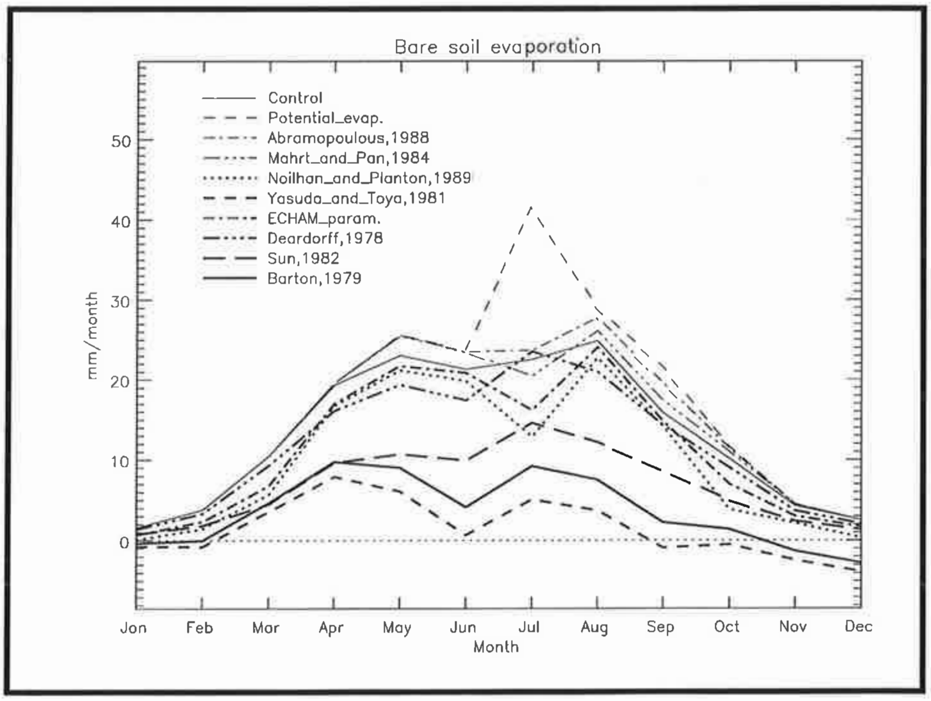

COMPARISON AND SENSITIVITY STUDIES OF THE LAND-SURFACE SCHEMES IN THE ECHAM GENERAL CIRCULATION MODEL AND THE EUROPA-MODELL

by

A. Roesch • J.-P. Schulz • M. Wild

HAMBURG, December 1997

AUTHORS:

Andreas Roesch
Martin Wild

Swiss Federal Institute of Technology
Department of Geography
Zürich
Switzerland

Jan-Peter Schulz

Max-Planck-Institut für Meteorologie
Hamburg
F. R. Germany

MAX-PLANCK-INSTITUT
FÜR METEOROLOGIE
BUNDESSTRASSE 55
D-20146 HAMBURG
F.R. GERMANY

Tel.: +49 - (0)40 - 411 73 - 0
Telefax: +49 - (0)40 - 411 73 - 298
E-Mail: <name>@dkrz.de

Comparison and Sensitivity Studies of the Land-Surface Schemes in the ECHAM General Circulation Model and the Europa-Modell

A. Roesch[a], J.-P. Schulz[b], M. Wild[a]

[a] Swiss Federal Institute of Technology, Department of Geography, Zürich, Switzerland
[b] Max-Planck-Institut für Meteorologie, Hamburg, Germany

ISSN 0937-1060

Contents

List of Figures

List of Tables

0.1 Abstract

This study presents the comparison of largely different land-surface schemes in the ECHAM GCM and the Europa-Modell (EM). The model runs were performed in an off-line mode using the Cabauw observational data as forcing at the lowest atmospheric model level. A detailed study on the sensitivities, over the entire physically possible range, of different key parameters gives insight into the differences in the two land-surface schemes. Emphasis is placed on the comparison of annual and diurnal cycles for the surface energy and water budget, as well as a detailed discussion of the differences in the parameterization equations. The study shows that sensitivity studies should not only focus on monthly means but also on diurnal cycles. Moreover, it is not sufficient to test a sensitivity for a certain value, but extend the investigation over the whole range because of its nonlinearity. In general, the sensitivity of both models is decreasing with increasing values of roughness length, leaf area index and field capacity. ECHAM generally shows higher sensitivity with respect to leaf area index and roughness length when compared to EM. This is mainly due to different parameterization of the transpiration. The sensitivity of the evaporation from the skin reservoir is higher in ECHAM for all varied surface parameters due to very efficient infiltration in EM. Total winter runoff is predominantly higher in ECHAM due to the implementation of 'fast drainage'. It has been shown that the different assessment of soil water largely influences the sensitivities. In addition, ECHAM shows more distinct summer drying than EM. The boundary layer parameterization is typically the same in both models. However, differences in the von-*Kármán*-constant k can produce distinct differences in turbulent fluxes.

Address of correspondence
Andreas Roesch
Geographisches Institut der ETH, Zürich
Winterthurerstrasse 190
8057 Zürich
Switzerland
Ph.: +41-0-257.52.36
Fax: +41-0-362.51.97
e-mail: aroesch@geo.umnw.ethz.ch

0.2 Introduction

While the capability of climate models to reproduce observed climate has significantly increased in recent years, numerous problems related to model physics remain. Among these problems, the interaction of the land surface with the overlying atmosphere is of increasing interest, particularly in the case of land-use changes, which today have a strong anthropogenic component. The inclusion of realistic land-surface schemes in numerical models has taken on an added importance in recent times because of the increased interest in land-use activities and their impact on climate. Therefore, numerous land surface models for GCMs have been developed during recent years, e.g., Dickinson (1978), SIB [Sellers et al. (1986)], BATS [Dickinson et al. (1986)], BEST [Pitman et al. (1991)], CLASS [Verseghy (1991)] and SECHIBA [Ducoudré et al. (1993)]. Numerous investigations have demonstrated that the simulated surface climate by general circulation models, numerical weather prediction models and regional atmospheric modelling systems is very much dependent on the formulation of the land surface schemes (e.g. Meehl and Washington, 1988; Gallimore and Kutzbach, 1989; Yamazaki, 1989; Barnett et al., 1989).

The three land-surface properties - albedo, roughness and hydrology (degree of soil wetness) - have been the subject of individual sensitivity studies. Rowntree (1983) reviewed 11 studies with emphasis on surface albedo and soil moisture content. The paper of Garratt (1993) provides an overall summary of current GCM surface schemes and the main results from many sensitivity studies undertaken with GCMs in the last two decades. He mentions the well-known relationship that continental evaporation and precipitation tend to decrease with increased albedo and decreased soil-moisture availability. For example, results from numerous studies give an average decrease in continental precipitation of 1 mm/day in response to an average albedo increase of 0.13.

Many studies deal with the impact of deforestation in tropical and boreal forests (e.g. Henderson-Sellers and Gornitz, 1984; Mylne and Rowntree, 1991; Bonan et al., 1992). In testing the sensitivity to vegetation cover, Dickinson (1978) found that evapotranspiration can increase by a factor of two as the amount of vegetation cover increases. Jacquemin and Noilhan (1990) found vegetation cover to be the most sensitive surface parameter, strongly influencing the Bowen ratio and the amount of sensible and latent heat flux. Contrary to this result, Wetzel and Chang (1988) and Siebert et al. (1992) noted a higher sensitivity to the amount of soil water content rather than to vegetation. Pitman (1994) claims that it is impossible to give a general ranking of the sensitivity to surface parameters. Moreover, he emphasized that surface-atmosphere feedbacks are significant for the determination of these sensitivities. Additionally, it is obvious that the type of model simulation and the model complexity strongly influences sensitivity results.

Many sensitivity studies have shown that the regional and global climate is strongly influenced by albedo, surface roughness, soil moisture content and vegetation cover. However, most of the studies are based on short time integration in the range of several weeks or months, and only study the influence on one single parameter. Furthermore, most of the studies only use the maximum and minimum values of the range and therefore can not specify the non-linear responses to the surface parameters.

The present study is based on an exhaustive analysis of the surface parameterization in the ECHAM3 General Circulation Model (GCM) and the Europa-Modell (EM).

ECHAM is based on the ECMWF spectral weather forecast model and has been extensively modified for climate application at the MPI in Hamburg. It has been used for climate-related investigations by the ETH Climate Modeling Group in Switzerland through a joint collaboration. The EM, on the other hand, is an operational weather forecast model developed at the DWD (German Weather Service). Both models were run in an off-line mode to exclude effects resulting from feedbacks within the atmosphere.

The objective of this study is to show the dependencies of different important model variables on certain input parameters. The emphasis lies on a detailed description of the parameterizations used, a comparison of the model results and the sensitivities to different parameters. Testing the sensitivity is a useful tool to detect important differences and similarities between land-surface models. Since changing more than one variable will obscure the sensitivity in the experiments, only one land surface parameter has been changed at the same time what does not correspond to reality. For example, changing the vegetation ratio also implies a change in the surface albedo, the surface roughness length and the soil-moisture availability. The inclusion of a land surface parameterization implies that the number of parameters required to provide initial and boundary conditions for a numerical simulation increases substantially. The uncertainty of the parameters is often quite large (e.g. leaf area index or field capacity). Therefore, it is of major importance to understand the impact of these parameters on the surface and soil temperatures, fluxes of latent and sensible heat, or runoff. Without such assessments, it is very difficult to correctly interpret comparisons of model output and observations. The present study allows the evaluation of the effect of land surface changes on regional climate characteristics simulated by ECHAM or EM, and to understand the main differences of the land-surface schemes in these models.

Chapter 1

Comparison of the land-surface schemes of ECHAM and EM

The models used in this study are the land-surface schemes of the ECHAM3 GCM of the Max Planck Institute for Meteorology, Hamburg, described in detail in Roeckner et al. (1992) and the Europa-Modell (EM), which is described very detailed in Edelmann et al. (1995). For better understanding, a description and comparison of the land-surface schemes is given in this chapter.

1.1 Soil temperature and soil heat flux

The calculation of soil temperature is based on totally different methods in both the EM and ECHAM models. The ECHAM includes five layers (of increasing thickness with depth) for temperature. The uppermost layer is 6.5cm thick, whereas the lowest one has a thickness of 5.7m. The thickness of the uppermost layer is very important when determining the surface heat flux and the diurnal cycle of surface temperature. The discretized heat conduction equations are

$$\frac{\delta T_1}{\delta t} = \frac{F_s}{\rho_g C_g \Delta z_1} + \frac{2\kappa(T_2 - T_1)}{\Delta z_1(\Delta z_1 - \Delta z_2)} \quad \text{(layer 1)} \tag{1.1}$$

$$\frac{\delta T_i}{\delta t} = \frac{-2\kappa(T_i - T_{i-1})}{\Delta z_i(\Delta z_{i-1} - \Delta z_i)} + \frac{2\kappa(T_{i+1} - T_i)}{\Delta z_i(\Delta z_i - \Delta z_{i+1})} \quad \text{(layers 2 to 5)} \tag{1.2}$$

with

$\rho_g C_g$	Heat capacity of soil per unit volume	2.4 x 10^6Jm^{-3} K^{-1}
F_s	Sum of the radiative and turbulent fluxes at the surface if there is no snow; heat flux from the snow to the deep soil if snow depth exceeds 0.025m water equivalent	[Wm^{-2}]
T_i	Temperature of the i-th soil layer	[K]

κ	Thermal diffusivity of the soil	7.5 x 10^{-7}m^{2}s^{-1}
Δz_i	Thickness of soil layer i	[m]

At the bottom of the lowest layer a zero heat flux condition is applied. This ensures that no artificial heat sources and sinks may affect the energy balance. The surface temperature is set equal to the temperature of the uppermost soil layer temperature for snow free condition. In case of snow, the surface temperature is extrapolated from the temperature T_{S_n} in the middle of the snow pack.

The Europa-Modell (EM) includes only two soil layers for temperature. The equations for the temperatures in the middle of the soil layers are (positive fluxes are directed towards the surface)

$$\frac{(\rho c\Delta z)_S}{2}\frac{\delta}{\delta t}(T_S + T_B) = G_S - G_{SB} + G_{melt} \tag{1.3}$$

$$\frac{(\rho c\Delta z)_B}{2}\frac{\delta}{\delta t}(T_B + T_M) = G_{MB} + (1 - r_S)G_B + r_S G_{SB} + G_{melt} \tag{1.4}$$

$$\frac{(\rho c\Delta z)_M}{2}\frac{\delta}{\delta t}(T_M + T_U) = G_{UM} - G_{MB} \tag{1.5}$$

with

B	Subscript for upper soil layer
G_B	Sum of radiative and turbulent fluxes at the snow free surface [Wm^{-2}]
G_{melt}	Heat flux produced by a redistribution of heat caused by melting snow [Wm^{-2}]
G_{MB}	Heat flux across the boundary between upper and lower soil layer [Wm^{-2}]
G_S	Sum of radiative and turbulent fluxes at the snow surface [Wm^{-2}]
G_{SB}	Heat flux from soil to snow [Wm^{-2}]
G_{UM}	Heat flux across lower boundary of lower soil layer [Wm^{-2}]
M	Subscript for lower soil layer
r_S	Snow covered fraction of the grid element
S	Subscript for snow
T_B	Temperature of snow free surface [K]
T_M	Temperature at the boundary between upper and lower soil layers [K]
T_S	Temperature of the snow surface [K]
T_U	Temperature at the lower boundary of the lower soil layer [K]
Δz	Thickness of soil layer [m]
ρc	Heat capacity of the soil per unit volume [Jm^{-3} K^{-1}]

Temperature is linearly interpolated for snow and soil layers. In EM, the heat conduction equation will be solved by the so-called "Extended Force Restore"-Method (EFR-Method) (Jacobsen and Heise, 1982). This method is able to simulate the surface temperature for two preselected frequencies of harmonic forcing without amplitude or phase error as compared to the equation of heat conduction. The thicknesses of the soil layers are dependent on the chosen harmonic forcing with the forcing periods τ_1 and τ_2.

$$\begin{aligned} \Delta z_B &= \frac{D_{1,2}}{1+x} \\ \Delta z_M &= \Delta z_B(\frac{\alpha_s}{\beta_m} - 1) \end{aligned} \tag{1.6}$$

with

$$
\begin{aligned}
D_{1,2} &= \sqrt{\frac{2\lambda}{\rho c \omega_{1,2}}} \\
\omega_1 &= \frac{2\pi}{\tau_1} \\
\omega_2 &= \frac{2\pi}{\tau_2}
\end{aligned}
$$

and

$$
\begin{aligned}
\alpha_s &= \omega_1(1 + x + x^2) \\
\beta_m &= \omega_1 x \sqrt{x + x^2} e^{\frac{x}{1+x}} \\
x &= \frac{\tau_1}{\tau_2}
\end{aligned}
$$

λ Heat conductivity of the soil [$\mathrm{WK^{-1}m^{-1}}$]

For the ECHAM, soil heat fluxes can be directly determined by taking into account the fact that the heat flux at the lower boundary of the deepest soil layer must be zero. Therefore, the ground heat flux at the surface can be computed as

$$
G_{ECHAM} = \sum_{K=1}^{5} \rho_g C_g \Delta z_K \frac{\delta T_K}{\delta t} \tag{1.7}
$$

with

C_g	Specific heat of soil [$\mathrm{Jkg^{-1}K^{-1}}$]
K	Number of soil layers
T_K	Temperature of soil layer K [K]
t	Time [s]
Δz_K	Depth of soil layer K [m]
ρ_g	Density of soil (dependent on soil type) [$\mathrm{kgm^{-3}}$]

EM applies a different method to calculate the soil heat fluxes. The EFR-method allows the computation of the soil heat fluxes as

$$
\begin{aligned}
G_{UM} &= -\frac{\lambda}{D_2^2} \frac{\Delta z_B + \Delta z_M}{1 + x + x^2}(T_M - T_U) \qquad (1.8) \\
G_{MB} &= G_{UM} - \frac{\lambda}{D_1^2} \Delta z_M [-x(T_M - T_U) + (1 + x + x^2) \\
&\quad \frac{\Delta z_B}{\Delta z_B + \Delta z_M}(T_S - T_U)]
\end{aligned}
$$

where G_{MB} represents the soil heat flux at a depth of Δz_B while G_{UM} is the corresponding flux at the lower boundary of the (modeled) soil. We recognize that, in contrast to ECHAM, the heat flux at the lowest layer boundary is not zero. This distinction is one of the main differences of climate and weather forecast models and is based mainly on the request of the forecast model to save computer time.

With equations (1.6), some transformations of equation (1.8) lead to

$$
\begin{aligned}
G_{UM} &= -\sqrt{\lambda\rho c/\tau_1}\frac{\sqrt{\pi}x}{(1+x)\sqrt{1+x^2}}e^{\frac{x}{1+x}}(T_M - T_U) &(1.9)\\
G_{MB} &= -\sqrt{\lambda\rho c/\tau_1}\frac{\sqrt{\pi}}{1+x}\{-[\sqrt{1+x^2}e^{\frac{x}{1+x}} - x](T_M - T_U) &(1.10)\\
&\quad [(1+x+x^2) - x\sqrt{1+x^2}e^{\frac{x}{1+x}}](T_S - T_U)\}
\end{aligned}
$$

The meaning of the variables is mostly defined in the context of equation (1.6). The temperature at the surface is called T_S, at a depth of Δz_B T_M and at the lower boundary of the soil T_U. Equations (2.9) and (2.10) can be greatly simplified by setting the period τ_1=24 h and $\tau_2=5\tau_1$:

$$
\begin{aligned}
G_{UM} &= -\sqrt{\lambda\rho c/\tau_1}[0.68(T_M - T_U)] &(1.11)\\
G_{MB} &= -\sqrt{\lambda\rho c/\tau_1}[-1.28(T_M - T_U) + 1.58(T_S - T_U)] &(1.12)
\end{aligned}
$$

The parameters show typical values of λ and ρc of λ=1.5WK^{-1}m^{-1} and ρc=1.8 $\cdot$ 10 ^{6}JK^{-1}m^{-3} at the location of Cabauw. This assumption leads to an estimate of

$$
\begin{aligned}
G_{UM} &= 3.8\ Wm^{-2}K^{-1}(T_M - T_U) \quad and\\
G_{MB} &= 7.2\ Wm^{-2}K^{-1}(T_M - T_U) - 8.8\ Wm^{-2}K^{-1}(T_S - T_U)
\end{aligned}
$$

The heat flux at the lowest layer boundary increases by about 4Wm^{-2} when T_M changes by 1°C.

1.2 Soil hydrology

The soil hydrology in ECHAM is based on three budget equations representing only one layer for

i. Snow amount S_n (m water equivalent) accumulated at the surface
ii. Water amount W_l intercepted by the vegetation during rain or snow melt episodes (the so-called skin reservoir)
iii. Soil water amount W_s

The rate of the water equivalent of the snow layer is computed over land from

$$\frac{\delta S_n}{\delta t} = \frac{J_{qS_n} + P_{S_n} - M_{S_n}}{\rho_w} \tag{1.13}$$

with

J_{qS_n}	Evaporation rate per unit area over the snow pack [$kgm^{-2}s^{-1}$]
M_{S_n}	Snow melt rate per unit area [$kgm^{-2}s^{-1}$]
P_{S_n}	Snow fall rate per unit area [$kgm^{-2}s^{-1}$]
ρ_w	Density of water [$1000kgm^{-3}$]

Over glaciers and sea ice the snow depth does not change.

The maximum content of the skin reservoir is calculated by

$$W_{lmx} = W_{lmax}((1 - C_v) + (C_v LAI)) \tag{1.14}$$

with

C_v	Grid fraction covered with vegetation
LAI	Leaf area index
W_{lmax}	Maximum amount of water held in one layer of leaves or bare ground [2 x 10^{-4} m]
W_{lmx}	Maximum skin reservoir content [m]

The rain water and melting snow on the leaves is intercepted by the vegetation until its water holding capacity W_{lmx} is exceeded. The budget equation is given by

$$\frac{\delta W_l}{\delta t} = \frac{J_{q_{vi}} + C_{ip} C_v (C_a P_R + M_{S_n})}{\rho_w} \tag{1.15}$$

with

C_a	Fractional area wetted by rain during a time step (currently 100% for large-scale rain and 50% for convective rain)
C_{ip}	Coefficient of efficiency of rain and snow interception (currently 100%)
C_v	Fraction of the grid box covered with vegetation
$J_{q_{vi}}$	Evaporation rate from the skin reservoir [$kgm^{-2}s^{-1}$]
P_R	Rainfall rate per unit area [$kgm^{-2}s^{-1}$]

The amount of rain and snow melt which does not enter the skin reservoir is used to calculate the amount of soil infiltration and surface runoff. The soil water content is determined by

$$\frac{\delta W_s}{\delta t} = \frac{J_{q_v} - J_{q_{vi}} + P_R - P_{Ri} + M_{S_n} - M_{S_{ni}} - R_R - R_D}{\rho_w} \tag{1.16}$$

with

J_{q_v}	Grid-mean evaporation rate per unit area
$M_{S_{ni}}$	Snow melt rate per unit area intercepted by the skin reservoir
P_{Ri}	Rainfall rate per unit area intercepted by the skin reservoir
R_R	Surface runoff rate per unit area from precipitation events and snow melt
R_D	Runoff rate per unit area from drainage processes

This fundamental equation shows that the soil reservoir is filled by precipitation and snow melt subtracted by the intercepted amount plus the net evaporation flux minus the surface runoff and drainage.

The drainage calculation distinguishes fast and slow drainage. Fast drainage occurs when the soil moisture is larger than 90% of the field capacity; slow drainage takes place for soil moisture between 5% and 90% of the saturated value. The exact formulae are

$$\frac{R_D(slow)}{\rho_w} = d_{min}\frac{W_s}{W_{smax}} \qquad \text{if } (W_{smin} < W_s < W_{dr}) \tag{1.17}$$

$$\frac{R_D(fast)}{\rho_w} = d_{min}\frac{W_s}{W_{smax}} + (d_{max} - d_{min})\left(\frac{W_s - W_{dr}}{W_{smax} - W_{dr}}\right)^d \qquad \text{if } (W_s \geq W_{dr}) \tag{1.18}$$

with

$d = 1.5$
$d_{min} = 0.0005 \mathrm{mmhr}^{-1}$
$d_{max} = 0.05 \mathrm{mmhr}^{-1}$
$W_{dr} = 0.9 \times W_{smax}$
$W_{smin} = 0.05 \times W_{smax}$

The surface runoff is calculated following a scheme by Dümenil and Todini (1992) which takes into account the sub-grid scale heterogeneity of the grid box by introducing a structure parameter b. This parameter depends on the standard deviation of the terrain height. The important feature is the non zero surface runoff for not fully saturated soils, introduced by defining a fractional saturated area s/S:

$$\frac{s}{S} = 1 - \left(1 - \frac{W_s}{W_{smax}}\right)^b \tag{1.19}$$

with

b	Structure parameter
s	Saturated area of the grid box
S	Total area of the grid box

For rainfall events, runoff occurs for the fractional saturated area s/S, while in the area $1 - (s/S)$ rain water infiltrates.

The EM has a totally different set of parameterization formulae for soil hydrology. The main reason is due to the structure of the soil in the EM. There are two or more soil layers for soil moisture instead of the bucket assumption of ECHAM. Similar in both models is that there are prognostic equations for snow amount, skin reservoir and soil moisture. These equation are

$$\rho_W \frac{\delta W_S}{\delta t} = PR_S + r_S EP_S - ABF_{WS} - FL_{SI} \tag{1.20}$$

$$\rho_W \frac{\delta W_I}{\delta t} = PR_R + r_I EP_I - ABF_{WI} - INFIL + FL_{SI} \tag{1.21}$$

$$\rho_W \Delta z_{WB,1} \frac{\delta W_1}{\delta t} = (1 - r_S - r_I)(EV + TR_1) - ABF_1 + INFIL + FL_2 \tag{1.22}$$

and for the deeper soil layers (K=2,...,NLWB):

$$\rho_W \Delta z_{WB,K} \frac{\delta W_K}{\delta t} = (1 - r_S - r_I) TR_K - ABF_K + FL_{K+1} - FL_K \tag{1.23}$$

with

ABF	Runoff
EP	Potential evaporation (EP > 0 implies the formation of dew or hoarfrost) [$kgm^{-2}s^{-1}$]
EV	Bare soil evaporation [$kgm^{-2}s^{-1}$]
FL_K	Water flux between soil layers K-1 and K [$kgm^{-2}s^{-1}$] (positive fluxes are directed toward the surface)
FL_{SI}	Flux from snow to skin reservoir caused by melting and freezing processes [$kgm^{-2}s^{-1}$]
$INFIL$	Infiltration [$kgm^{-2}s^{-1}$]
PR	Precipitation (index S: snow, R: rain) [$kgm^{-2}s^{-1}$]
r_I	Water covered fraction of the grid element
r_S	Snow covered fraction of the grid element
TR_K	Transpiration [$kgm^{-2}s^{-1}$]
W_I	Water content of the skin reservoir [m]
W_K	Water content of soil layer K [m]
W_S	Water equivalent of the snow layer [m]
$\Delta z_{WB,K}$	Depth of soil layer K [m]
ρ_W	Density of water ($1000kgm^{-3}$).

The maximum skin reservoir content is calculated by

$$W_{I,max} = W_{I,MB}(1 + 5\sigma_{PLNT}) \tag{1.24}$$

with $W_{I,MB}$=0.5mm. The vegetated area of the grid element is represented by σ_{PLNT}. Therefore, the maximum content of the skin reservoir amounts to 3mm. The formula incorporates no dependence on the leaf area index. Setting the leaf area index equal to 2, equation (1.14) gives a corresponding maximum value of only 0.4mm for ECHAM.

The EM allows a water flux between the different soil layers. The transpiration originates not only from the uppermost soil layer but also from lower ones (depending on the root depth of plants). The units of all above listed equations is $kgm^{-2}s^{-1}$ (or mms^{-1}). A basic principle is that only the snow or the skin reservoir can contain a non zero filling.

The surface runoff includes the following components:
- precipitation which exceeds the infiltration capacity
- runoff if the skin reservoir is overfilled
- melt water of snow which is not able to infiltrate
- runoff of the uppermost soil layer.

The maximum infiltration rate is determined by a simplified Holtan equation (only for surface temperatures above freezing point):

$$N_{max} = SVORO \cdot \max(0.5, \sigma_{PLNT}) K_1 \frac{PV - W_1}{PV} + K_2 \tag{1.25}$$

K_1	Parameter for hydraulic conductivity [$kgm^{-2}s^{-1}$]
K_2	Minimum infiltration rate [$kgm^{-2}s^{-1}$]
N_{max}	Maximum infiltration rate [$kgm^{-2}s^{-1}$]
PV	Porosity (total water-holding capacity) [m^3m^{-3}]
$SVORO$	Influence of sub-grid scale orography (presently set equal to 1)
W_1	Relative water content of the uppermost soil layer
σ_{PLNT}	Vegetated area of the grid element

If more than half of the grid is vegetated, the maximum infiltration rate is linearly increasing with vegetated area. N_{max} and the relative soil moisture are also linear.

The infiltration of water from the skin reservoir into the soil is parameterized as

$$VERS_{IN} = \begin{cases} 0 & ; \; T_B \leq T_0 \\ W_I' \frac{\rho_W}{\tau_{VER}} & ; \; T_B > T_0 \end{cases} \tag{1.26}$$

with

T_B	Temperature of snow free surface [K]
T_0	Freezing temperature [273.15K]
$VERS_{IN}$	Infiltration of water into soil [$kgm^{-2}s^{-1}$]
W_I'	Initial skin reservoir content reduced by the evaporation [m]
τ_{VER}	Time constant (set equal to 1000s)
ρ_W	Density of water [$1000kgm^{-3}$]

This equation states that after approximately 15minutes, the whole interception reservoir is empty. Experiments have shown that nearly all (greater than 99%) precipitation or melt water will immediately infiltrate into soil. A five times higher time constant τ_{VER} will slow down the infiltration by the factor five, the average of the skin reservoir content rises by a factor 5 and evaporation from the skin reservoir increases more than twice. This is the reason why runoff due to an overfilled skin reservoir occurs very rarely.

If rain falls on to an unfrozen soil, the part αPR_R of the rain will rise the skin reservoir content whereas the remainder $(1-\alpha)PR_R$ will infiltrate. The parameter α depends on the current and the maximum skin reservoir content:

$$\alpha = \left(1 - \frac{W_I}{W_{I,max}}\right)^{0.5} \tag{1.27}$$

A special correction term is added so that the skin reservoir content can not decrease while raining. Experiments show that α is very rarely less than 0.9. This means that only a very small amount of rain goes this direct way of oozing.

All the components of surface runoff are of negligible importance (at least for the Cabauw site) except runoff from the uppermost soil layer. Runoff occurs when the field capacity of a soil layer is exceeded. If one sets FL_1=$-INFIL$, where $INFIL$ is the infiltration into the soil, the difference of water fluxes can be written as

$$\Delta FL_K = FL_{K+1} - FL_K \tag{1.28}$$

If $\Delta FL_K > 0$ and $W_K >$ FC then

$$ABF_K = \frac{W_K - FC}{PV - FC}\Delta FL_K \tag{1.29}$$

where ABF_K is runoff out of soil layer K.

The transport of water between the soil layers is calculated with the Darcy equation, which includes the influence of gravity and capillary force:

$$FL = -\rho_W[D_W(W)\frac{\delta W}{\delta z} + K_W(W)] \tag{1.30}$$

with the hydraulic diffusivity D_W ([m^2s^{-1}]) and the hydraulic conductivity K_W (unit ms^{-1}). These parameters are parameterized as

$$D_W(W) = D_0 e^{D_1 \frac{PV-\overline{W}}{PV-ADP}} \tag{1.31}$$

$$K_W(W) = K_0 e^{K_1 \frac{PV-\overline{W}}{PV-ADP}} \tag{1.32}$$

The four constants D_0, D_1, K_0 and K_1 depend on the soil type. For determining D_W and K_W at the boundary of the layers a weighted average of soil water content $\overline{W}$ is used. Formulae (1.31) suggests an exponential increase of K_W and D_W between the air dryness point ADP and the porosity. The water flux between the layers is not allowed to exceed a threshold of 10% of the porosity during one time step.

1.3 Prediction of snow temperature and albedo Parameterization of snow melt processes

The surface temperature in ECHAM is set equal to the temperature of the uppermost soil layer for snow free conditions. This assumption is probably a main reason for the large differences between modeled and observed surface temperatures. In case of snow, the skin temperature is extrapolated from the temperature T_{S_n} in the middle of the snow pack. The snow pack temperature is calculated differently depending on whether the snow cover is more than or less than 0.025m water equivalent. For a snow pack of less than 0.025m water equivalent, equation (1.1) is solved assuming the characteristics of bare soil. For the snow depth deeper than 0.025m, an extra heat conduction equation is evolved according to

$$\frac{\delta(T_{Sn})}{\delta t} = \frac{F_S}{\rho_{Sn} C_{Sn} Sn} \tag{1.33}$$

with

F_S	Sum of the radiative and turbulent fluxes at the surface
Sn	Depth of the snow pack
T_{Sn}	Temperature in the middle of the snow pack
$\rho_{Sn} C_{Sn}$	Heat capacity of the snow per unit volume (using a density of snow ρ_{Sn}=300kgm^{-3})

EM uses a more sophisticated equation for the determination of snow temperature (see Eq. (1.3)). In addition to the ECHAM, the heat equation for the snow pack in EM allows a heat flux from snow to soil and a heat flux resulting from melting snow and refreezing melt water. However, the contribution of these additional fluxes will be small for thick snow layers.

In ECHAM, the surface albedo is constant for every grid element under snow free conditions. Therefore, the albedo does not depend on land use. In snow-covered regions, the surface albedo is modified according to

$$\alpha_{surf} = \alpha_{sb} + (\alpha_s - \alpha_{sb}) \frac{S_n}{S_n + S_n^*} \tag{1.34}$$

with

S_n^*	Critical snow depth [0.01m]
α_s	Snow albedo
α_{sb}	Background albedo

The albedo of snow and ice surfaces α_s is a function of the surface type, the surface temperature and fractional forest area (Equation (1.35)). A maximum value α_{smax} for temperatures below T_m=263.15K and a minimum value α_{smin} for temperatures above the freezing point T_0 is assumed. A linear interpolation is used between these two extremes. Over land, a weighted albedo of the fraction covered with forest and the remaining part of the grid element is applied.

$$\alpha_s = \alpha_{smax} - (\alpha_{smax} - \alpha_{smin}) \frac{T_S - T_0}{T_m - T_0} \tag{1.35}$$

with

$$\alpha_{smin}(a_f) = a_f \alpha_{smin}(a_f = 1) + (1 - a_f)\alpha_{smin}(a_f = 0)$$
$$\alpha_{smax}(a_f) = a_f \alpha_{smax}(a_f = 1) + (1 - a_f)\alpha_{smax}(a_f = 1)$$

where

a_f	Fractional forest area
T_0	=273.15K
T_m	=263.15K

The EM parameterization of albedo is distinctly different. The albedo of snow free grid elements is not a constant as in the ECHAM, but depends on the soil water content of the uppermost soil layer, as well as the albedo of vegetation and bare soil. The albedo under snow free conditions is computed from

$$\alpha_{sf} = \sigma_{PLNT}\alpha_{PLNT} + (1 - \sigma_{PLNT})\left(\alpha_{bas} - \frac{LKW_1}{KR}\right) \tag{1.36}$$

with

KR	Term which includes heat capacity and heat conductivity of the soil
LK	Linear decrease coefficient
W_1	Relative water content of the uppermost soil layer
α_{bas}	Solar base albedo (for dry soil, dependent on soil type)
α_{PLNT}	Albedo of vegetated areas (constant, equal to 0.15)
σ_{PLNT}	Fraction of vegetated area
α_{sf}	Albedo under snow free conditions.

The albedo under snow covered conditions is parametrized much more simply than in the ECHAM model:

$$\alpha_{surf} = \sigma_s\alpha_s + (1 - \sigma_s)\alpha_{sf} \tag{1.37}$$

with

α_s	Albedo of snow (set to 0.7)
σ_s	Snow covered fraction of grid element.

The striking difference is the missing temperature dependence of snow albedo and the fact that there is no distinction between vegetated and forested areas. Figure (1.1) shows the difference between the two models under snow free conditions.

Figure (1.2) shows the dependence of the albedo under snow covered condition in dependence of the fractional forest area.

Another difference between ECHAM and EM is that the snow covered fraction of the grid element is calculated in a different way (see Fig. (1.3)). Whereas ECHAM assumes a nearly linear dependence, the EM requires an exponential law between snow water equivalent and snow covered fraction. We recognize that for a powdery snow pack of about 5cm height (corresponding to 0.5cm water equivalent), the EM has a snow covered fraction of about 90% whereas the ECHAM grid element has only about 30% covered with snow.

The parameterization of snow melt is also solved differently in ECHAM and EM. In ECHAM, snow melts when both the temperature in the middle of the snow pack and the temperature of the uppermost soil layer reach 0°C. Snow which is thinner than 0.025m may melt if the temperature of the uppermost soil layer equals 0°C.

The EM distinguishes snow melt from the upper and lower boundary of the snow pack. A rather sophisticated algorithm with the possibility of a vertical redistribution of heat in the snow pack and the uppermost soil layer guarantees a realistic parameterization of snow melt. Two cases

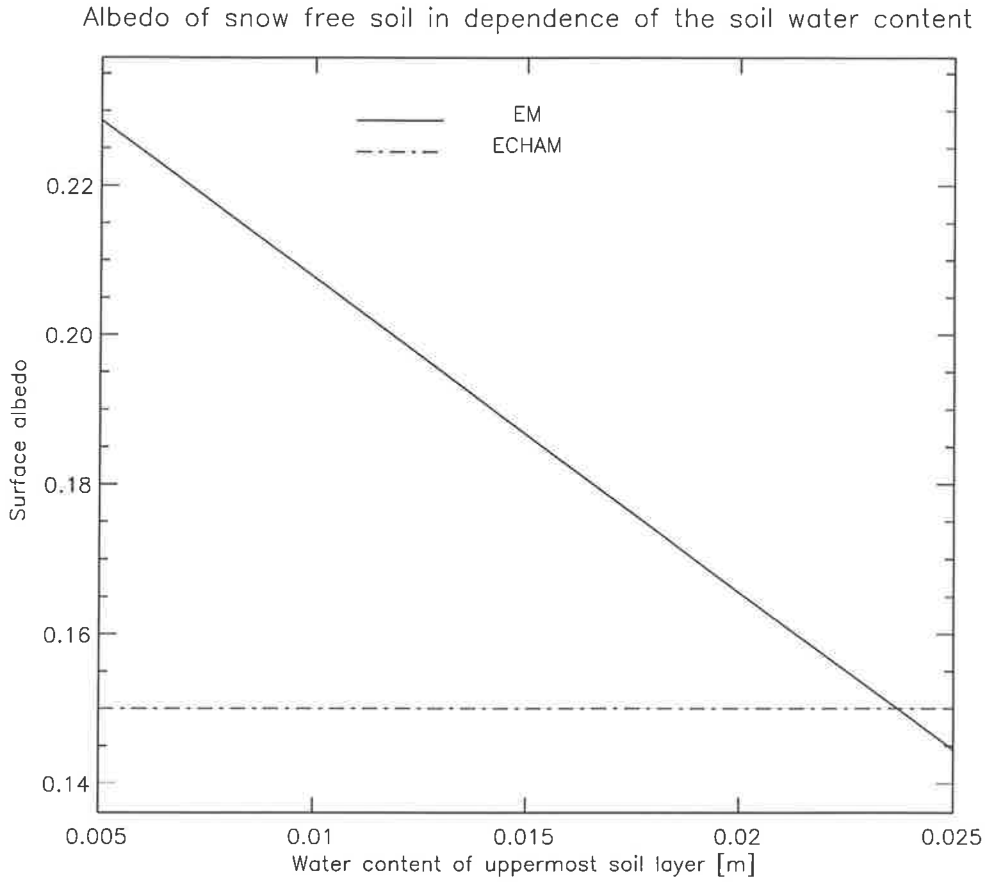

Figure 1.1: *Albedo in ECHAM and EM under snow free conditions. Albedo of ECHAM is equal to 0.15, albedo of dry bare soil is supposed to be 0.25 in EM.*

are distinguished:
1. If the temperature of the upper boundary of the snow layer ($T_{S,N}$) is above 0°C, but the temperature of the lower boundary of the snow pack ($T_{B,N}$) below the freezing point, no snow melt will occur. A vertical redistribution of heat, which leads to a higher $T_{B,N}$, will occur. Only if $T_{B,N}$ exceeds 0°C snow melt can take place.
2. If $T_{S,N}$ is below the melting point, but $T_{B,N}$ above 0°C, there is the following amount of energy available for snow melt:

$$WN_M = WM_S + WM_B \tag{1.38}$$

Snow can melt only when $WN_M > 0$, . If the middle temperature of the snow pack is above 0°C, the heat release of the snow pack which can be used for melting the snow will be

$$WM_S = \rho_S c_S \Delta z_S \left[\frac{T_{S,N} + T_{B,N}}{2} - (T_0 - \epsilon) \right] \tag{1.39}$$

with

c_S Heat capacity of snow [$\mathrm{Jkg^{-1}K^{-1}}$]

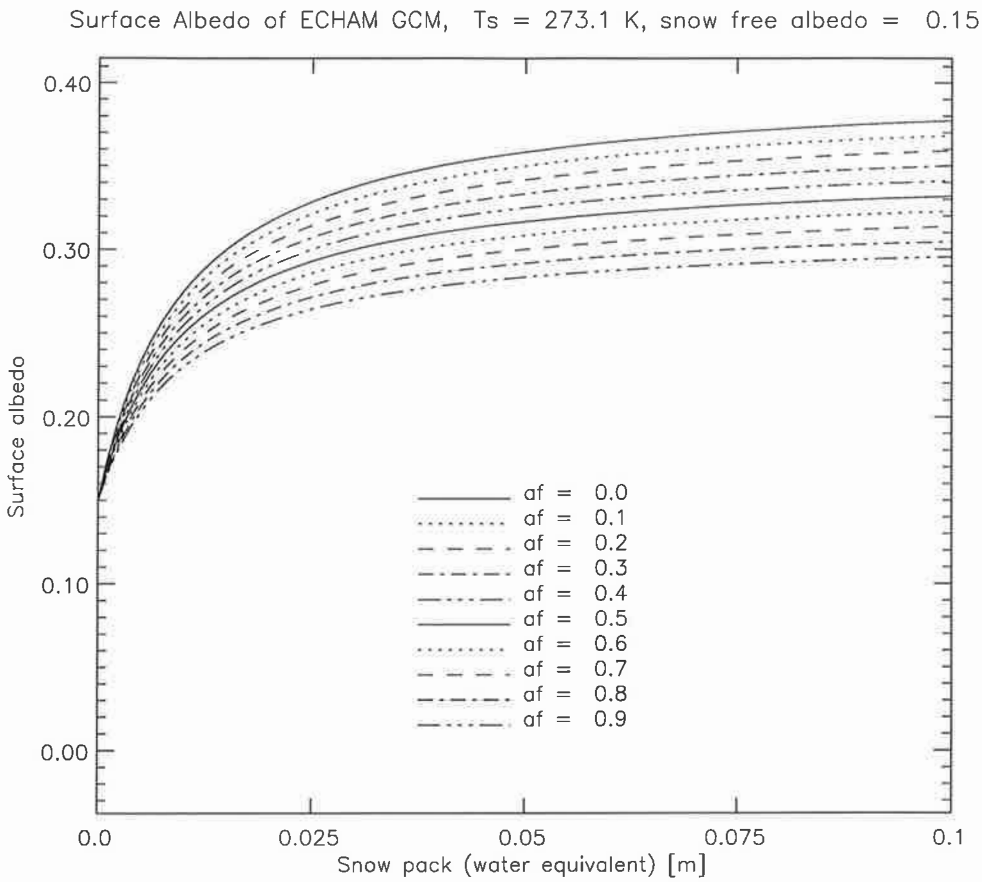

Figure 1.2: *Surface albedo of ECHAM for different fractional forest areas under snow covered conditions.*

S	Subscript for snow
$T_{B,N}$	Temperature of lower boundary of the snow pack [K]
$T_{S,N}$	Temperature of upper boundary of the snow pack [K]
T_0	Melting point (273.15K)
Δz_S	Snow depth [m]
ϵ	Very small number (set equal to 1.E-10K)
ρ_S	Density of snow.

In the upper soil layer, the following heat amount released by a cooling of $T_{B,N}$ down to the freezing point is available for the melt process:

$$WM_B = (\rho c \Delta z)_B [T_{B,N} - (T_0 - \epsilon)] \tag{1.40}$$

When calculating snow depth from snow water equivalent, it is important to know that ECHAM uses a constant snow density of $300 \mathrm{kgm}^{-3}$, whereas EM introduces a dependence on the water equivalent:

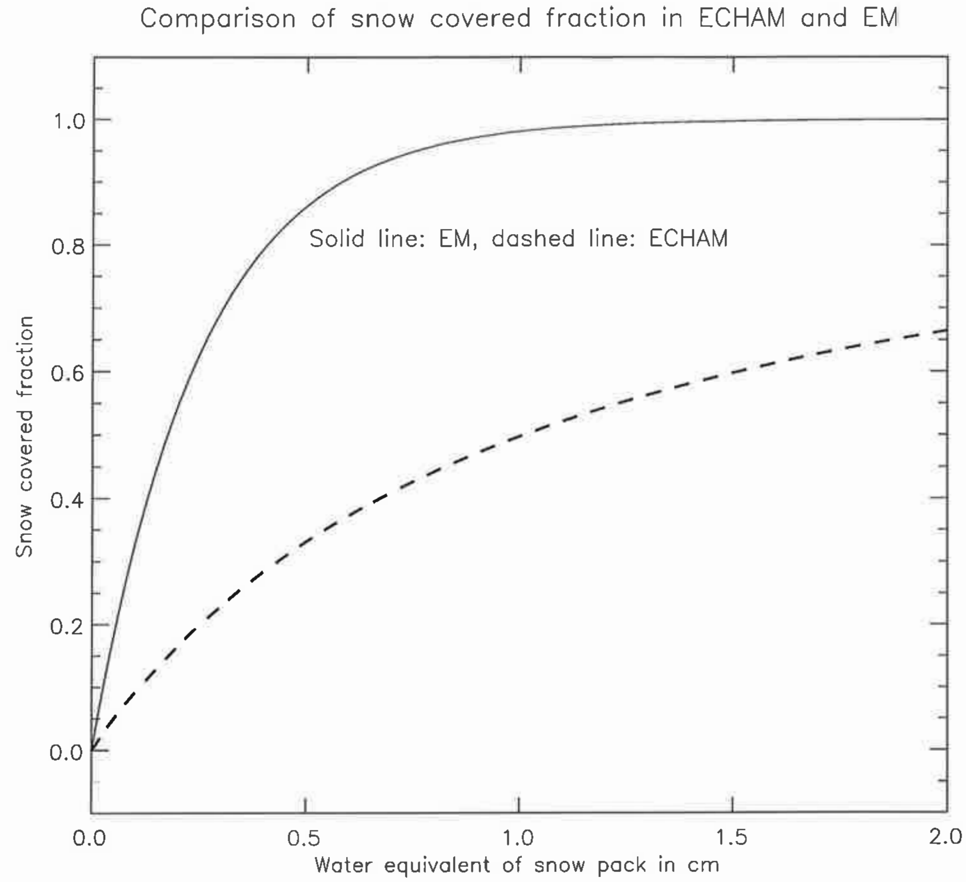

Figure 1.3: *Snow covered fraction of the grid element for ECHAM and EM.*

$$\rho_S = \rho_{S_0} + \min(\rho_{S_{max}}, W_S \frac{\delta \rho_S}{\delta W_S}) \tag{1.41}$$

with

ρ_S	Density of snow pack
ρ_{S_0}	Minimum snow density (500kgm^{-3})
$\rho_{S_{max}}$	Maximum snow density (800kgm^{-3})
$\frac{\delta \rho_S}{\delta W_S}$	Coefficient of snow density change with water equivalent of snow pack

This formula describes a linear increase of snow density with snow water equivalent. The maximum snow density is attained for W_S=1m.

1.4 Parameterization of water vapour fluxes

In ECHAM and EM, the different evaporation processes are parameterized using a heat transfer coefficient C_h. However, the parameterization formulae are not similar.

Evaporation from snow and the skin reservoir is at the potential rate (both in ECHAM and EM)

$$J_{q_v} = \rho C_h |v_h| (q_v - q_{sat}) \tag{1.42}$$

where C_h is the heat transfer coefficient, q_v the water vapour mixing ratio, q_{sat} the water vapour mixing ratio at saturation and v_h the horizontal wind vector. The water vapour mixing ratio q_v and $|v_h|$ refers to the lowest atmospheric model level whereas q_{sat} refers to the surface temperature T_S and surface pressure p_S.

For the evaporation from dry bare soil (no water in the skin reservoir) in ECHAM, the relative humidity at the surface h is introduced.

$$J_{q_v} = \rho C_h |v_h| (q_v - h q_{sat}) \tag{1.43}$$

where h is defined as

$$h = \max\left[0.5(1 - \cos(\frac{\pi W_s}{W_{smax}})), \min(1, \frac{q_v}{q_{sat}})\right] \tag{1.44}$$

The relative humidity takes into account the fact that evaporation from bare soil can be divided into two regimes: an almost saturated surface evaporating similarly to a free water surface and; the rate of evaporation determined by atmospheric demand ("atmospheric control"). If the surface layer is "dry", evaporation will be controlled by the hydraulic properties of the soil ("soil-control"). The bare soil evaporation stops when the term in brackets in equation (1.43) is equal to 0. This is the case when $h = q_v/q_{sat}$.
The formulation in (1.43) is called the 'bulk aerodynamic formulation', in contrast to the 'threshold formulation'. The threshold parameterization is based on the assumption that during a drying phase, evapotranspiration always tends towards the maximum sustainable, or threshold rate (Wetzel and Chang, 1987). An example of a threshold parameterization is the Dickinson formulation for evaporation.

EM computes the bare soil evaporation with a simple parameterization:

$$EV \quad = \quad (\beta_E)^2 \rho C_h |v_h| (q_v - q_{sat}) \tag{1.45}$$

For the soil type 1 (ice), EV is equal to the potential evaporation, whereas for soil type 2 (rocks), there is no evaporation. The coefficient β_E is a linear function of the soil water content of the uppermost soil layer between the air dryness point (β_E=0 => no evaporation) and field capacity (β_E=1 => evaporation at potential rate).
The evaporation from dry vegetated areas is called transpiration and is parameterized in ECHAM with the stomatal resistance and the water stress factor:

$$J_{q_v} = \rho C_h |v_h| E (q_v - q_{sat}) \tag{1.46}$$

The evaporation efficiency E is expressed as:

$$E = \left[1 + \frac{C_h |v_h| R_{co}(PAR)}{F(W_s)}\right]^{-1} \tag{1.47}$$

where the water stress factor $F(W_s)$ is a function of soil moisture and R_{co} is dependent on the photosynthetically active radiation (PAR), which is 55% of the net shortwave radiation at the surface. The water stress factor is set to 1 if the soil moisture is above the critical value

(50% of the field capacity) and to 0 for soil moisture under the point where plants start to wilt (permanent wilting point, equal to 20% of the field capacity in the control simulation).

EM applies a much simpler parameterization for transpiration.

$$TR_K = (\beta_{B,K})^2 r_{WT,K} \rho C_h |v_h| (q_v - q_{sat}) \tag{1.48}$$

For soil types 1 and 2 (ice and rock) and surface temperatures below 0°C, transpiration is zero. The potential evaporation is reduced by a too low soil water content ($\beta_{B,K}$) and rooting depth ($r_{WT,K}$). The factor $\beta_{B,K}$ is represented similar to β_E. This function increases linearly between the permanent wilting point (β_E=0 => transpiration stops) and the so-called turgor loss point, which is dependent on the soil type and potential evaporation. Above this point, β_E is set to 1. This means that water stress of plants has finished. The function $r_{WT,K}$ controls the water uptake of the roots in the different soil layers and lies strictly between 0 and 1. This factor $r_{WT,K}$ is responsible for the very strong dependence of transpiration on rooting depth.

$$r_{WT,K} = min(BWT, \Delta z_{WB,1}) / \sum_{k=1}^{NLWB} \Delta z_{WB,k} \qquad ; K = 1 \tag{1.49}$$

$$r_{WT,K} = (BWT - \sum_{k=1}^{K-1} \Delta z_{WB,k}) / \sum_{k=1}^{NLWB} \Delta z_{WB,k} \quad ; K > 1 \tag{1.50}$$

with

BWT	Rooting depth
$NLWB$	Number of hydrological soil layers
$\Delta z_{WB,K}$	Depth of (hydrological) soil layer K

It has to be emphasized that EM allows a more sophisticated parameterization of transpiration and bare soil evaporation to be switched on: a simplified version of the Dickinson parameterization.

1.5 Parameterization of boundary layer transport

In both ECHAM and EM, the parameterization of the boundary layer is based on Louis (1979). The surface fluxes of heat, moisture and momentum are calculated from Monin-Obukhov theory. It calculates the transfer coefficients for heat and momentum which are dependent on roughness length z_0, the von-Kármán-constant k and a stability-correction function f.

The transfer coefficient C_h for heat and moisture reads

$$C_h = \left(\frac{k}{ln(z/z_0)}\right)^2 f_h \tag{1.51}$$

and for momentum

$$C_m = \left(\frac{k}{ln(z/z_0)}\right)^2 f_m \tag{1.52}$$

In EM, the formula of C_h is modified by introducing a special roughness length z_h for heat and moisture. So far however, the one dimensional model uses the same values for z_0 and z_h. The operational EM uses different values for z_0 and z_h.

The correction functions are based on Louis (1982) and are given by

$$f_m = 1 - \frac{2bRi}{1 + 3bc[\frac{k}{ln(z/z_0)+1}]^2 \sqrt{(z/z_0 + 1)|Ri|}} \tag{1.53}$$

for ECHAM and

$$f_m = 1 - \frac{2bRi}{1 + 3bc[\frac{k}{ln(z/z_0)+1}]^2 [(z/z_0)^{(1/3)} - 1]^{3/2}|Ri|} \tag{1.54}$$

for EM in the unstable range. The function f_h are very similar with one minor difference in the numerator:

$$f_h = 1 - \frac{3bRi}{1 + 3bc[\frac{k}{ln(z/z_0)+1}]^2 \sqrt{(z/z_0 + 1)|Ri|}} \tag{1.55}$$

for ECHAM and

$$f_h = 1 - \frac{3bRi}{1 + 3bc[\frac{k}{ln(z/z_0)+1}]^2 [(z/z_0)^{(1/3)} - 1]^{3/2}|Ri|} \tag{1.56}$$

for EM in the unstable range. The formulae for f_h and f_m in both models are nearly the same. However, a minor simplification has been implemented into ECHAM because the lowest atmospheric model level is much higher than the roughness length. This simplication has been omitted in the EM.
For the stable range the formulae for ECHAM and EM are identical:

$$\begin{aligned} f_m &= \frac{1}{1 + 2bRi/\sqrt{1 + dRi}} \\ f_h &= \frac{1}{1 + 3bRi/\sqrt{1 + dRi}} \end{aligned} \tag{1.57}$$

with the constants b=c=d=5.0. The important difference is the value of the von-Kármán-constant k. The ECHAM model uses $k = 0.4$ whereas EM sets $k = 0.36$. For the stable range, this makes a difference of $(0.4^2/0.36^2 - 1)$ x $100\% = 23\%$ for the transfer coefficient. Since the bare soil evaporation and skin reservoir evaporation are linearly dependent on C_h, this leads to 23% higher fluxes for ECHAM than for EM (under omission of all the other differences). For the unstable range, the following chart (1.4) shows the difference between both models.

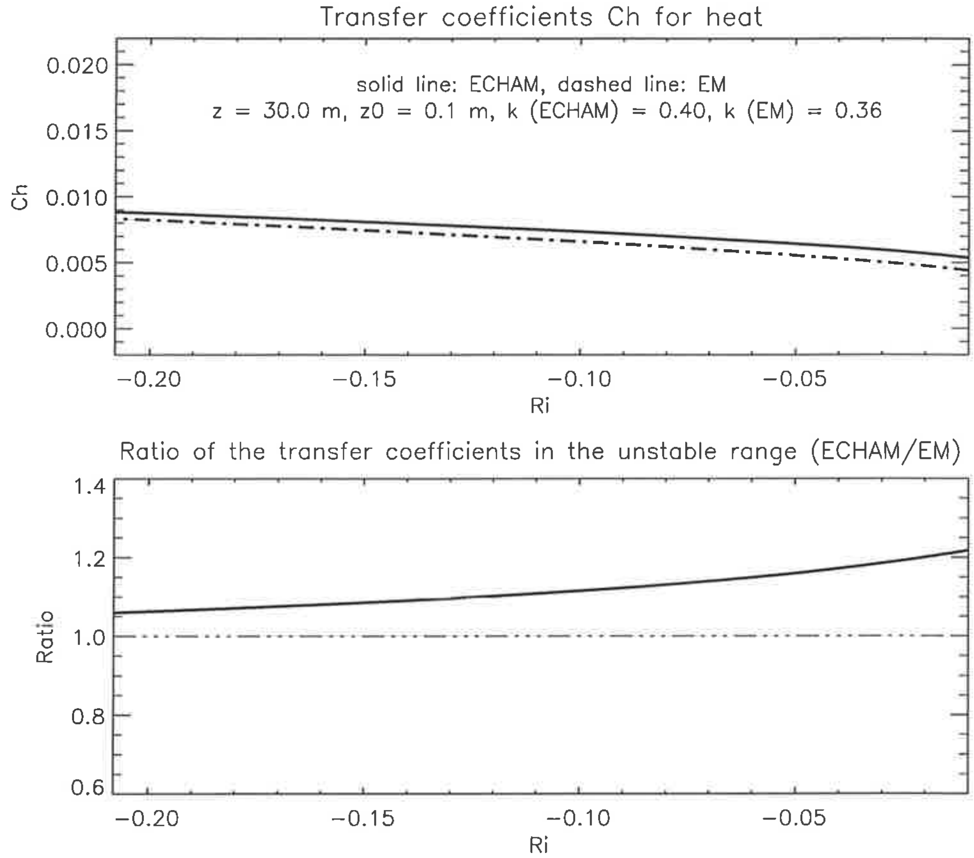

Figure 1.4: *Transfer coefficient for heat in the unstable range for ECHAM and EM.*

Chapter 2

Comparison of the sensitivities of ECHAM and EM

The sensitivity of a certain quantity f with respect to a parameter x is defined as (in discrete form)

$$Sens = \frac{f(x_2) - f(x_1)}{x_2 - x_1} \tag{2.1}$$

This is nothing other than the derivative written in the discrete form. All the results drawn from model experiments are based on Equation (2.1). Sensitivities can be computed exactly by the derivative of the parameterization formula ($\frac{\delta f}{\delta x}$).
There are different possibilities to study and compare sensitivities:
It is obvious that model experiments can be performed with changing values of model parameters. At first, a control set-up was defined (see Chapter (2.1)). Then, only one parameter was changed for each experiment. The following parameters have been varied:

Table 2.1: *List of varied parameters for the sensitivity study. In the second and third column, the examined range and step width are presented*

parameter	range	step width
albedo	0.15 - 0.35	0.05
snow albedo	0.5 - 0.9	0.05
roughness length	0.1 - 0.7m	0.05m
leaf area index	1 - 6	1
vegetation ratio	0.0 - 1.0	0.1
field capacity	0.20 - 0.40m	0.05m
wilting point	10 - 40% (of the field capacity)	5%
critical value	30 - 70% (of the field capacity)	10%
maximum amount of water per leaf layer	0.05 - 0.25mm	0.05mm
coefficient of interception of precipitation	0.0 - 1.0	0.2

The last four quantities are less important and only influence the model results slightly in the chosen ranges. The sensitivity of these quantities has only been tested for the ECHAM model (not shown). For most quantities, the values of these parameters are of less importance than the others. Moreover, the operational version of EM does not include the leaf area index and so the maximum amount of water held on one leaf layer. Therefore, the EM shows no dependence on the leaf area index at all. This obvious deficiency can be eliminated by switching on the so-called Dickinson parameterization for evaporation. This model version has not yet been tested. However, for this study, the Dickinson parameterization has been chosen, but only

for the sensitivity study concerning the leaf area index.
Another possibility to make sensitivities more plausible is to analytically determine the derivative of the different parameterization formulae with respect to the influencing parameters and to discuss the results. This method does not take into account the different feedbacks (which is possible by examining model results) but gives more insight into the model parameterization and structure. Moreover, it is possible to compute the sensitivity not only for some discrete values but for all values.
Finally, it is interesting to see how sensitive the models react to the substitution of a parameterization. The influence of replacing some special formulae can give more insight into the quality of the parameterization.

2.1 Description of the control simulations

It was not easy to define the values of the parameters in the control experiments. Most problems were produced by the different structures of the soil models in ECHAM and EM. The parameters of the standard configuration for Cabauw are listed in table (2.2).

Table 2.2: *List of the parameters used in the ECHAM and EM Land-Surface Scheme for the control experiment at Cabauw.*

parameter	description	ECHAM 3	EM
ALB	Albedo	0.156	depends on soil moisture
AZO	roughness length	0.15m	0.15m
VGRAT	vegetation ratio	0.886	0.886
FORESTM	fractional forest area	0.0	-
WLMAX	maximum moisture content of the skin reservoir	0.2mm	0.5mm
WSMAX	maximum soil moisture content	0.2m	1)
CVLT	leaf area index	2.0	2.0
CWCRIT	begin of water stress	0.5xWSMAX	2)
CWPWP	permanent wilting point	0.2xWSMAX	10 Vol%
CVINTER	efficiency of interception of precipitation	1.0	1.0
CVA, CVB	constants for definition of stomatal resistance	2582.01 rsp. 1.09	-
CVC	minimum stomatal resistance	110.0sm−1	-
ZEMISS	emissivity of soil	0.996	0.996
ALBSN	min./max. of snow albedo (bare soil)	0.4 rsp. 0.8	0.7 (constant)
ALBSNVEG	min./max. of snow albedo (vegetated areas)	0.3 rsp. 0.4	-
SNCRIT	critical snow depth	0.01m	-
SNDENS	density of snow	$300 kgm^{-3}$	500 - $800 kgm^{-3}$
SNHEAT	heat capacity of snow per unit volume	$0.6345 \times 10^6 Jm^{-3} K^{-1}$	Eq. (1.41)
CRGCG	heat capacity of soil per unit volume	$2.4 \times 10^6 Jm^{-3} K^{-1}$	3)
B	structure parameter (Eq. (1.19)) in the runoff scheme	0.2	-

Figures 1) to 3) in the last column of the table (2.2) correspond to the following description:
1) Whereas for ECHAM the maximum soil water content is easily defined (bucket model), the EM-parameterization includes two different parameters for the maximum soil water content. The absolute maximum is attained when all the pores in the soil are filled (porosity). However, potential evaporation of bare soil is already reached if the so-called field capacity is exceeded. This value is defined as the water content the soil can hold for more than one to two days after the last rainfall. As soon as this threshold is exceeded, runoff out of the soil layers sets in. Therefore, it is not easy to decide if, for calculation of the relative soil moisture, the ratio of soil water to the field capacity or the porosity should be taken. Most authors compute the ratio

of the soil water content to the field capacity. Thus the results of this report are based on this assumption. This definition allows a relative water contents above 1. The soil parameters in EM were taken as defined for the soil type of loamy sand which is the most frequent soil type in Western Europe.
2) The water stress in EM is computed by a formula which is dependent on the soil type and the potential evaporation.
3) In EM, the heat capacity is treated as a function of the soil water content. The value of dry soil depends on the soil type.

The data used in this study have been collected at the 213m meteorological mast at Cabauw (51°58'N, 4°56'E) in the Netherlands and cover a one year period from 1.1.1987-31.12.1987. This site is located in flat terrain consisting mainly of grassland interrupted by narrow ditches. Up to a distance of 200m from the mast, there are no obstacles or perturbations of any importance; further away scattered trees and houses are located in most directions (see Driedonks et al. (1978) for a more detailed description).
The model simulations were all run with a forcing at the lowest atmospheric model level (about 30m above the ground). Averages over 30 minute intervals of the following quantities were used :

- downward shortwave radiation
- downward longwave radiation
- total precipitation at the surface
- atmospheric temperature at the lowest model level
- zonal and meridional wind at the lowest model level
- specific humidity at the lowest model level.

Each model run comprises a period of five years. The forcing was cyclically repeated each year. The model results of the fifth year are presented in this study. This procedure is used to ensure that both models are in an equilibrium state.
The EM additionally needs the prescription of the temperature at the lowest soil layer (T_U). In a first step, the measured temperatures at a depth of 2cm at Cabauw were smoothed using a 31 day running mean. Then, the heat conduction equation (Eq. (4.1)) was used to calculate the phase lag between the temperature at a soil depth of 2cm and 47cm what is the soil depth where T_U (see Fig. (2.1)) is prescribed in EM. The second value corresponds to the depth where the temperature T_U is determined (the soil type in the control experiment is loamy sand). The calculation led to a phase lag of 34 days.
In the following chapters the terms
- 'temperature of second soil layer' and
- 'temperature of third soil layer'
sometimes appear. These terms are related to the definition of soil layers in ECHAM. The corresponding values for EM have been linearly interpolated from the temperatures T_B, T_M, and T_U (see Fig. (2.1)). Temperature T_3 in ECHAM will be compared to T_U in EM.

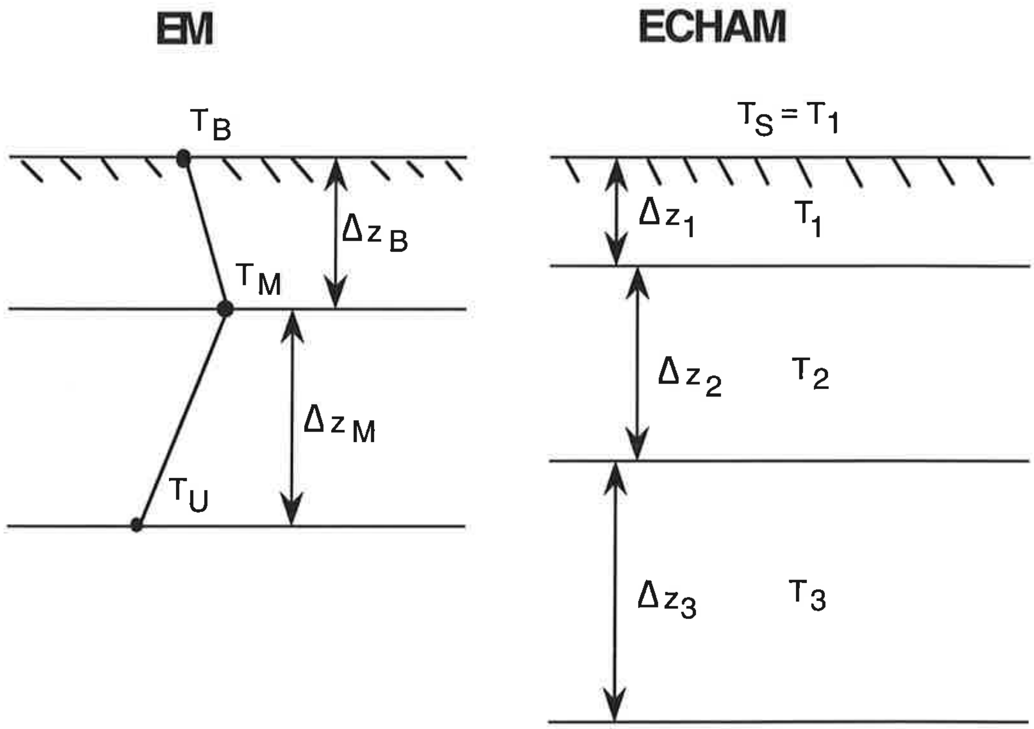

Figure 2.1: *Soil layers and temperatures in ECHAM (only the upper three soil layers are shown) and EM for snow free conditions. The soil type of EM is 'loamy sand' and the inherent layer depths are Δz_B=10.3cm and Δz_M=37.0cm for the control experiment.*

2.2 Sensitivity to the roughness length

The roughness length z_0 is an important parameter for GCMs and weather forecast models. The surface fluxes of momentum, heat and moisture are strongly determined by the roughness length. However, relatively little is known concerning exact values of roughness lengths for momentum, heat and moisture. The roughness length of momentum is distinctly larger than for heat and moisture. Nevertheless, in ECHAM3 and ECHAM4, there is no distinction between these values. In the EM, distinction is possible but in the version used here both values are set on the same value. It should be emphasized that although the roughness length is closely related to the geometry and height of the surface roughness elements, it is actually a matter of empirical coefficients. This emphasizes the importance of completing sensitivity studies for this parameter.

In this study, the roughness length was altered from 0.1m to 1.0m, with a step width of 0.1m. These values correspond to a field and a forest in spring.

The model uses the roughness length in the formulae for the different surface fluxes. They appear in the parameterization of the drag coefficient and the transfer coefficient for heat (Equation (1.51) to (1.56)). The transfer coefficient for heat (C_h) plays a major role in determining the water vapour fluxes and the sensible heat flux.

Figure (2.2) depicts the typical characteristics of the sensitivity for increasing roughness lengths. The general structure of the sensitivities can be better discussed on the basis of annual means because short time characteristics and accidental results can be avoided. Therefore, the following results are based on annual means (or sums). However, annual and diurnal characteristics should also be discussed.

It may be noticed that the sensitivity of both water vapour and sensible heat fluxes are decreasing for increasing roughness lengths. Both models clearly show this typical exponential decay. This means that for smooth areas, it is more important to know z_0 exactly. The decrease is distinct. Latent and sensible heat flux show a higher (absolute) sensitivity in ECHAM whereas transpiration and bare soil evaporation are more sensitive in EM. This characteristic can be explained with the derivative of the parameterization equations to the roughness length. The equation for water vapour fluxes and sensible heat flux incorporate the transfer coefficient C_h only as a function which is directly dependent on the roughness length. The transfer coefficient increases for all situations with increasing roughness. This is reasonable because turbulence is larger over rough than over smooth regions and so are the turbulent fluxes. The derivative $\frac{\delta C_h}{\delta z_0}$ (Fig. (2.3)) is high for low roughness lengths. It decreases rapidly at first with rougher surfaces and goes asympotically to zero for very high (unrealistic) z_0. The same characteristic is found for stably stratified boundary layers.

An important difference exists between the parameterizations of transpiration in ECHAM and EM. While the simple parameterization of EM puts the entire dependence on z_0 into the potential evaporation, the more sophisticated parameterization of the ECHAM model incorporates the evaporation efficiency E which is again a function of z_0. This function E becomes smaller with increasing roughness length, and therefore reduces the sensitivity of transpiration with respect to z_0. A typical situation is shown in Figure (2.4). It is obvious that the curve of the derivative goes very rapidly to values near zero and barely changes for z_0 >0.2m. Therefore, the sensitivity of transpiration with respect to z_0 decreases faster in the EM (Fig. (2.2)). Additionally, it should be added that the order of change in sensitivity is correctly represented compared to the theoretically obtained results.

Most other quantities show a similar characteristic of the sensitivity: surface runoff, drainage, soil moisture, surface temperature and net radiation. For smooth areas, a fixed change in roughness length has a larger influence than the same change for a rough area. Naturally, it is of interest to know how large the absolute sensitivity for the examined quantities are. Fig. (2.5) shows the change caused by an increase in z_0 from 0.1m to 0.2m. These two values contain the range of the roughness length's uncertainty for the Cabauw site.

The evaporation fluxes from plants (transpiration), bare soil, the skin reservoir and snow

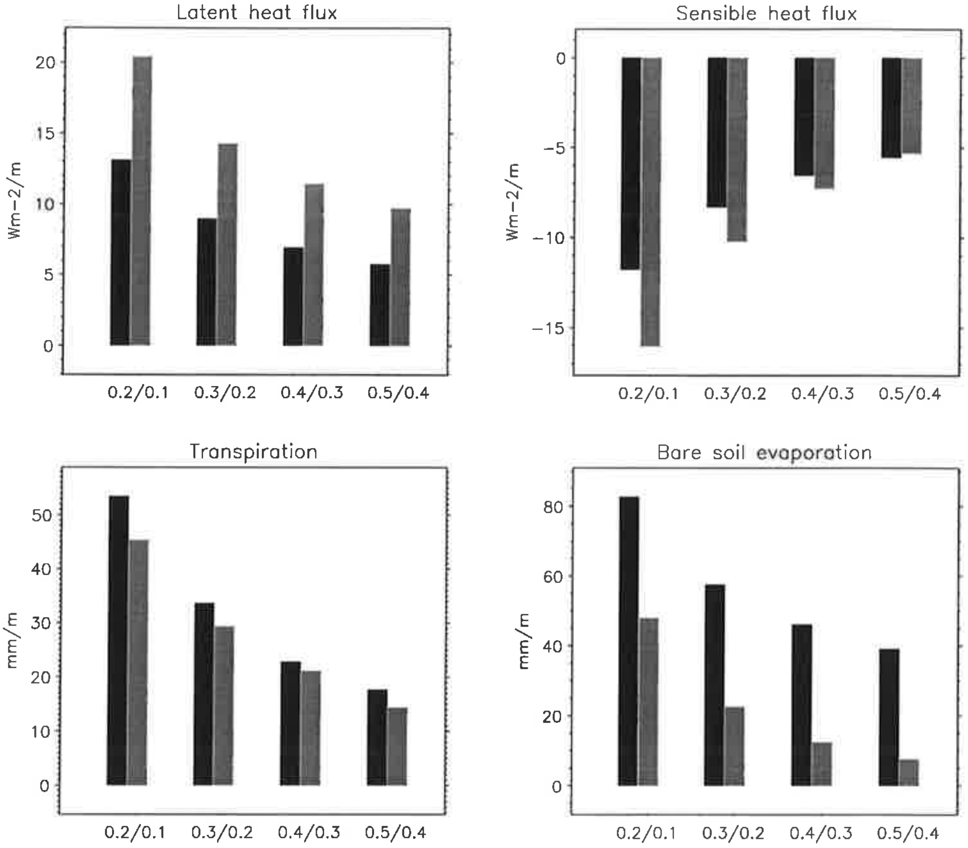

Figure 2.2: *Sensitivity of latent and sensible heat flux (annual averages), transpiration and bare soil evaporation (annual totals) for different roughness lengths. X-axis labels show which roughness lengths [unit: m] were used in the model runs to calculate the height of the presented bars. Left bar: EM; right bar: ECHAM.*

show a clear positive signal. The rougher the surface, the more turbulence is produced which leads to higher turbulent fluxes. The ECHAM model is typically more sensitive. The relative change in skin reservoir evaporation is more pronounced than transpiration and bare soil evaporation. This is due to the direct dependence of potential evaporation on the roughness length. Transpiration and bare soil evaporation incorporate dependences other than the potential evaporation. This leads to a reduced (relative) sensitivity to z_0. The absolute change in bare soil evaporation is larger in the ECHAM-model, but the relative change is smaller because the annual bare soil evaporation of ECHAM is less than 60% of EM. The (absolute) sensitivity of the skin reservoir is more than fifty times higher in ECHAM. The reason is the very fast infiltration of skin reservoir water in the EM. Therefore, the time to evaporate at the potential rate is much shorter and thus, the sensitivity to the roughness length is smaller.
Surface temperature and albedo, as well as short- and longwave net radiation are barely changed. The annual mean of surface temperature decreases by about 0.01°C for an increase in roughness length of 0.1 to 0.2m. The changes are very similar in both models. The main reason for low changes in surface temperature is the described forcing temperature at a height of 30m above

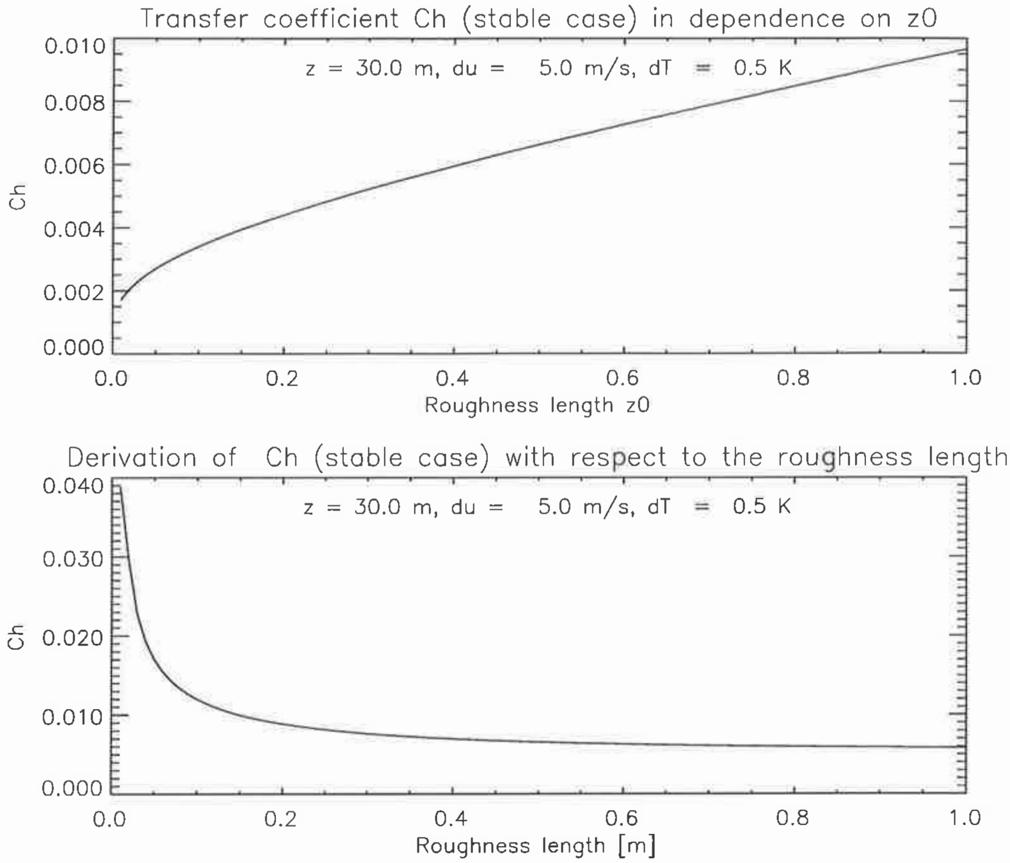

Figure 2.3: *Transfer coefficient (unstable case) in dependence on roughness length and the derivative to* z_0 (ECHAM). The wind speed difference between the lowest atmospheric model level z is du, the corresponding value for temperature is called dT.

ground. It could possibly be higher if a three dimensional run had been examined. This is clearly a deficiency in the model experiments and should be done later. Because of the low changes in surface temperature, there is practically no change in soil temperatures or ground heat fluxes. The ECHAM albedo experiences changes from an altered snow depth, whereas the EM albedo is additonally influenced by soil moisture in the uppermost soil layer. Nevertheless, the albedo of ECHAM is more sensitive. This is the reason why the snow conditions response is much more sensitive to roughness changes in ECHAM.

In order to fulfil the energy balance, the higher latent heat flux must be compensated by a lower sensible heat flux. In the ECHAM model, the annual average of latent heat increases by barely $2\mathrm{Wm}^{-2}$ for a 0.1m rougher grid element while the sensible heat flux decreases by a similar amount. The relative change is larger for the sensible heat flux because of a much lower annual average. Since over rougher surfaces more water is extracted out of the soil by evapotranspiration, the soil moisture and runoff fluxes decrease (this is shown by the negative values in Figure (2.5)). Since the sensitivity for water vapour fluxes is larger for the ECHAM model, the same applies (in order to have a correct water balance) to runoff at the surface and drainage processes. While the absolute change of runoff is similar for both models, surface runoff

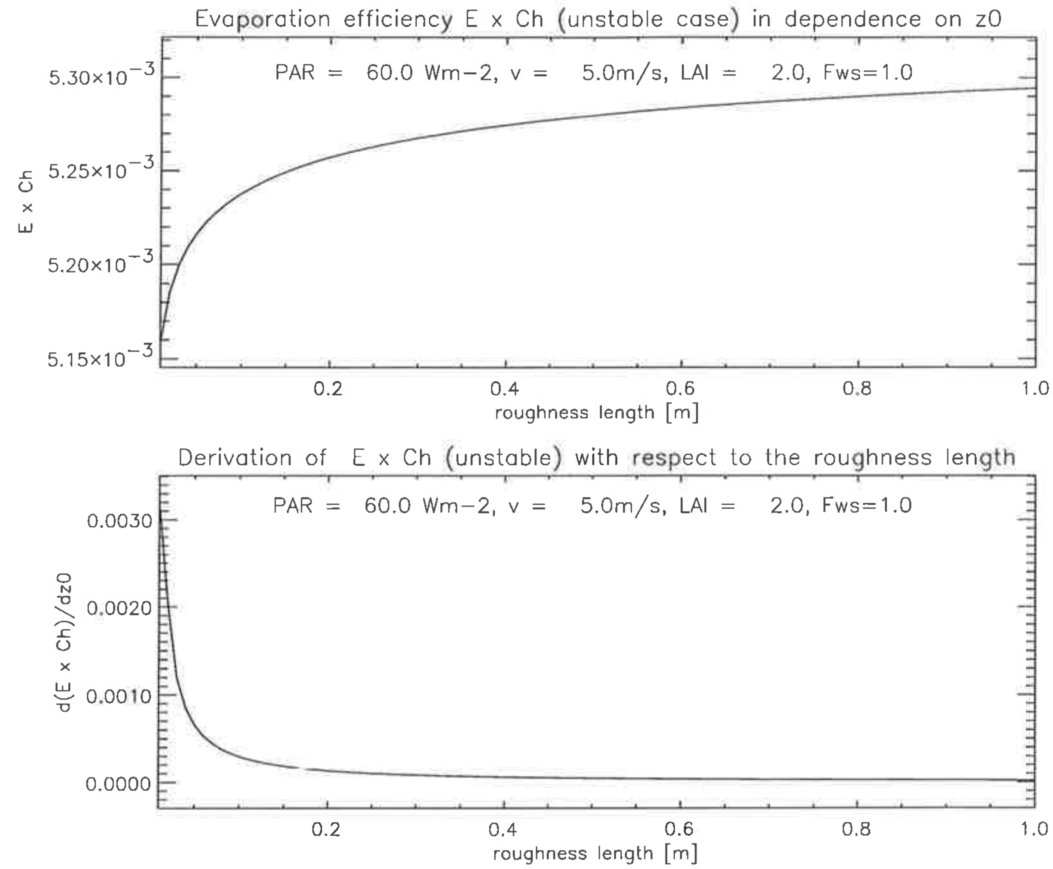

Figure 2.4: *Transfer coefficient multiplied by the evaporation efficiency and the derivative to* z_0 (ECHAM).

is absolutely and relatively much lower in the ECHAM model. The sensitivity of surface runoff decreases much faster for ECHAM.
Snow melt and snow depth produced by the two models respond very differently to roughness length changes. ECHAM shows a much higher sensitivity. While the relative change in snow melt (and depth of the snow pack) in the EM amounts to about 1%, ECHAM has a fourfold larger value. Snow depth and snow melt decrease with rougher surfaces because snow sublimation is significantly increased.
The ground heat fluxes barely change, but have opposite signs in ECHAM and EM. The reason is the prescribed lower boundary condition of temperature for EM. Moreover, the absolute changes are more than ten times higher in EM. The no-flux-condition at the lower boundary in ECHAM provides a better possibility to balance forced changes. The EM looses (or gains) energy by the non-zero ground heat flux through the lowest soil layer.
Figure (2.6) gives an overview over the modeled decrease of sensitivity with increasing roughness length. The figured bars represent the sensitivity for a roughness length z_0=0.15m and z_0=0.45m. The model runs used to compute the first sensitivitiy are z_0=0.10m and z_0=0.20m for the smoother respectively, and z_0=0.40m and z_0=0.50m for the rougher surface respectively.

We recognize the decrease of the sensitivity already mentioned. This corresponds to bar

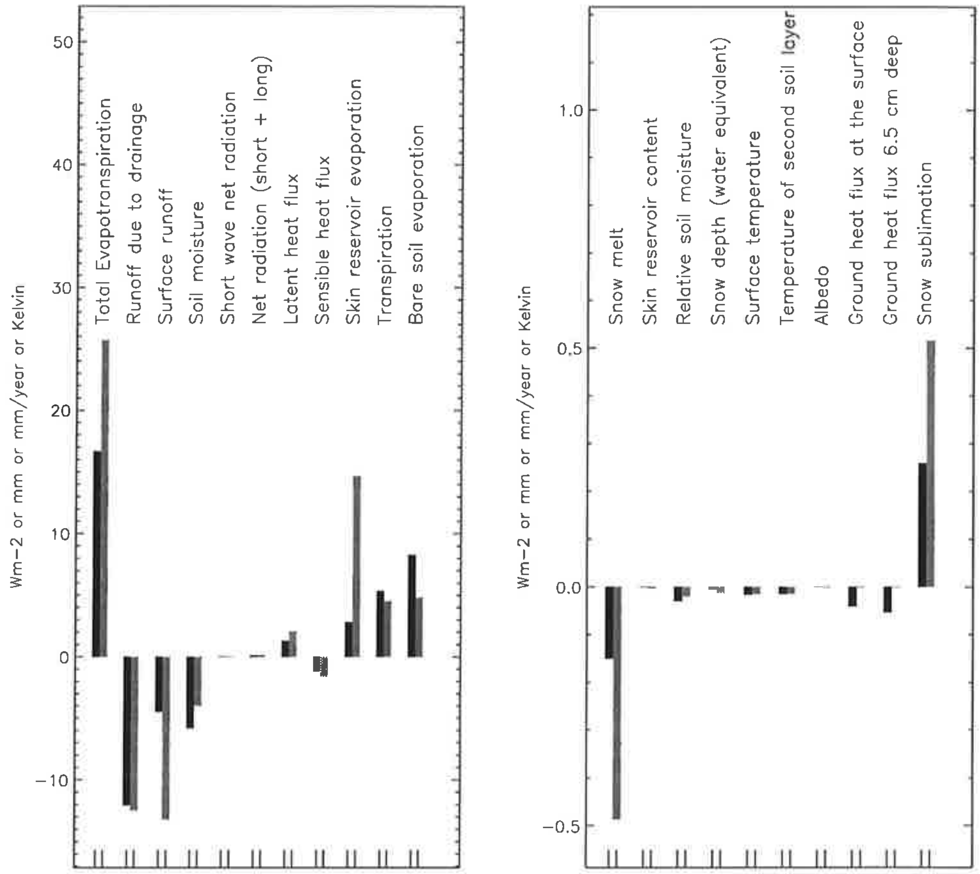

Figure 2.5: *Difference of annual averages (or sums) for the roughness lengths z_0=0.1m and z_0=0.2m. Black bars: EM; Grey bars: ECHAM.*

values in Figure (2.6) of less than 1. For most quantities, the ratio is about 0.5, i.e. the sensitivity is half for the rougher surface. However, there are some exceptions. For shortwave radiation, the ratio is clearly higher for the ECHAM model. Moreover, the sensitivity decreases approximately exponentially in ECHAM for increasing z_0 (not shown) whereas in EM, there is barely any observed dependence. This is due to the distinct dependence of soil moisture on the roughness and the parameterization of albedo including soil moisture. The bare soil evaporation decreases distinctly faster in the ECHAM model. This is caused by the drying of the ground, which is more severe for (too) high z_0-values. Quantities closely related to surface temperatures have positive ratios in EM, but negative in ECHAM. This signifies that the sensitivity changes its sign in the ECHAM simulations. Whereas the changes in surface temperature and upper soil temperature are similar for both models under smooth conditions the sensitivity behaves completely different for rougher surfaces. It has to be mentioned that all absolute changes are very small. The main reason for this different characteristic is the described temperature as a lower boundary condition (EM). For EM, the typical exponential decrease has been found, while ECHAM produces higher surface and ground temperatures with increasing z_0 (valid for

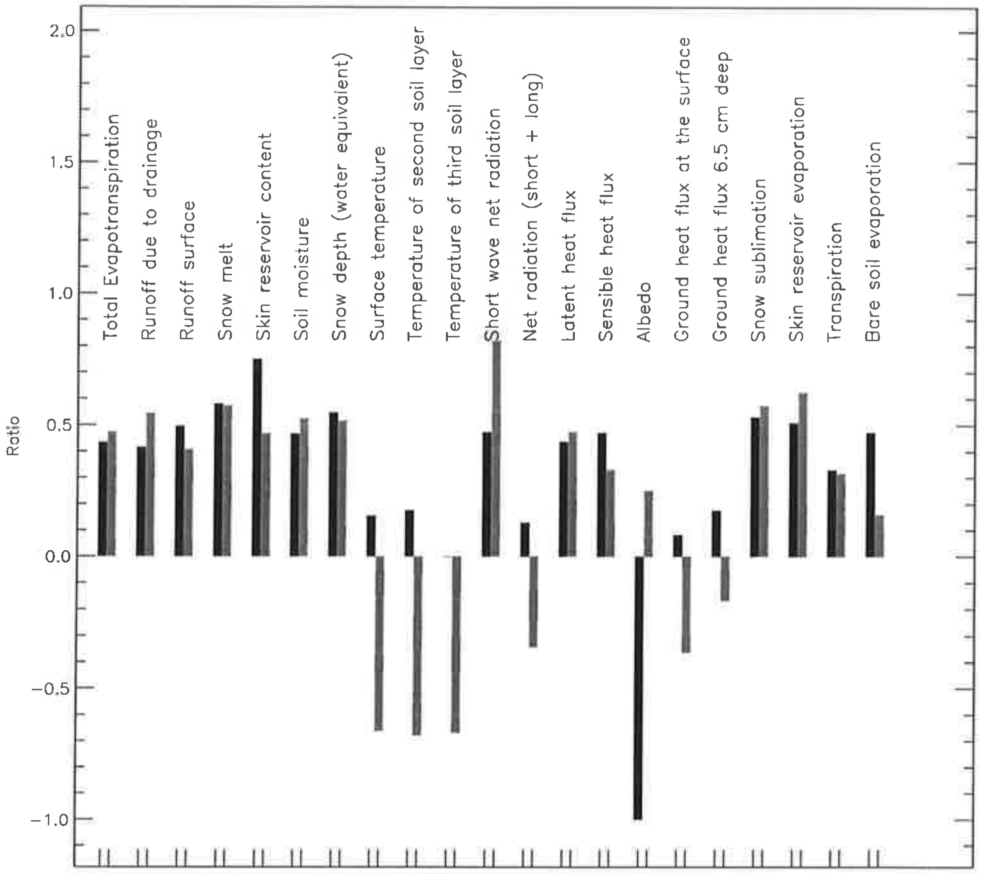

Figure 2.6: *Ratio of sensitivity for a roughness length of 0.15m and 0.45m. Black bars: EM; Grey bars: ECHAM.*

roughness length over 0.25m).

Most of the examined quantities show a more or less distinct annual cycle of the sensitivities. Figures (2.7) and (2.8) give a short overview what can be expected. The plots depict the differences for the model runs with z_0=0.1m and z_0=0.5m (f(z_0=0.5m) - f(z_0=0.1m)).

Runoff due to drainage is nearly independent on the surface roughness during summer (JJA). This is the consequence of an almost zero drainage during summer. During early summer, the ECHAM simulation shows very little sensitivity which is in contrast to the EM. In November and December, ECHAM is more than three times as sensitive as EM. This difference is mainly caused by the indroduction of fast drainage in the ECHAM parameterization. The clear seasonal fluctuation of the skin reservoir content is only observed in ECHAM runs, whereas the EM shows almost no dependence on the roughness length over the year. The annual cycle is mainly caused by the fact that the reservoir is filled more during the colder season. A plot of relative changes (not shown) does not have such a clear annual cycle. The fast infiltration in EM prevents any visible dependence on roughness length. The characteristic of soil moisture

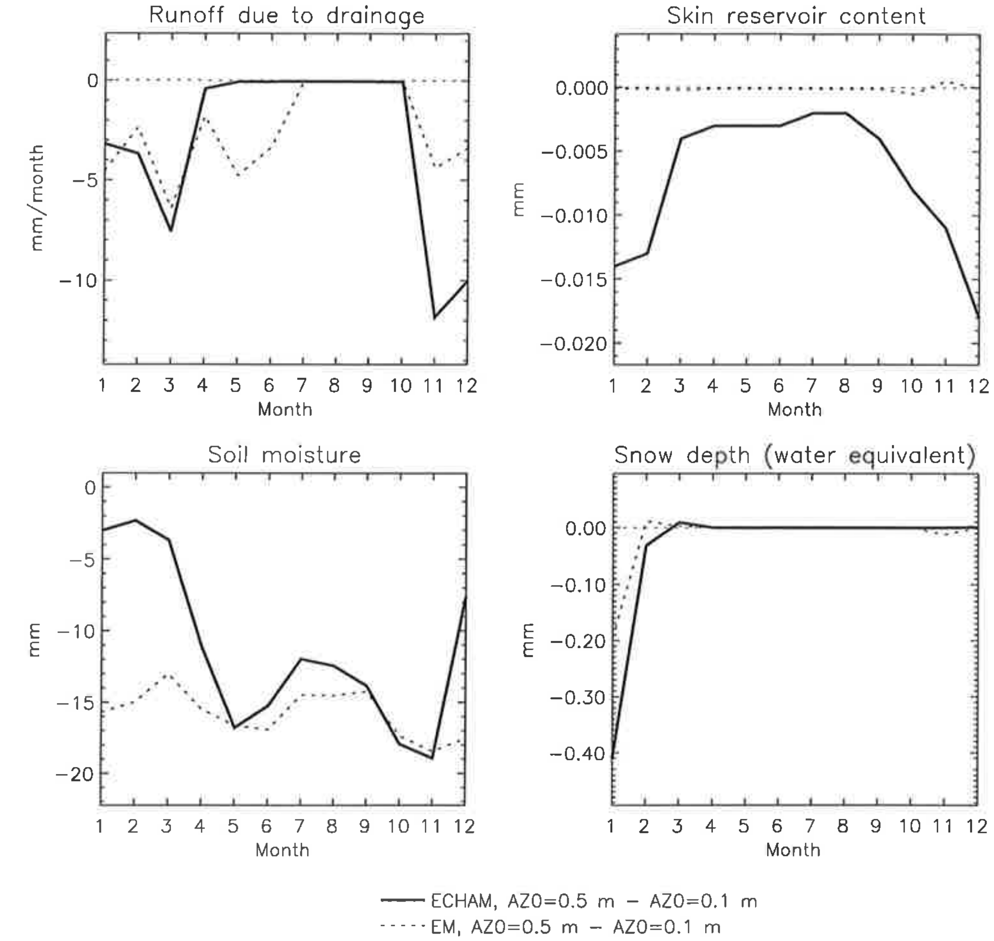

Figure 2.7: *Monthly differences of drainage, skin reservoir content, soil moisture and snow depth for z_0 =0.1m and z_0=0.5m for ECHAM and EM.*

is also very different in both models. The absolute change is rather constant during the year in EM and amounts to about 15mm. ECHAM is much less sensitive during winter (December to April), but shows similar values during the rest of the year. From a relative point of view, ECHAM is more sensitive during summer. ECHAM is obviously not very sensitive if enough water is available. A change in roughness length influences the different water fluxes, but the water content of the reservoir is relatively stable. During summer, when (turbulent) fluxes are mostly higher, the model is not able to compensate the additional loss introduced by rougher surfaces. Snow depth is very low, with the exception to January where more than ten days had a measurable snow pack. In spite of a larger snow depth for the EM control experiment, ECHAM is about twice as sensitive as EM. The is also valid for snow melt and snow sublimation.

The difference in surface temperature for z_0=0.1m and z_0=0.5m depicts a clear annual cycle for both models. Moreover, the values are about the same. During summer, one observes a distinct decrease of temperature for rougher conditions whereas the opposite is true for winter. The amplitude is about 0.4°C. Soil temperatures exhibit a similar evolution for ECHAM but decreases quickly for EM. This is due to the fixed lower boundary condition. The net long- and shortwave radiation exhibit a rather clear annual cycle in both models. This is mainly due to the longwave part which is changed by the surface temperature. Short wave net radiation is very

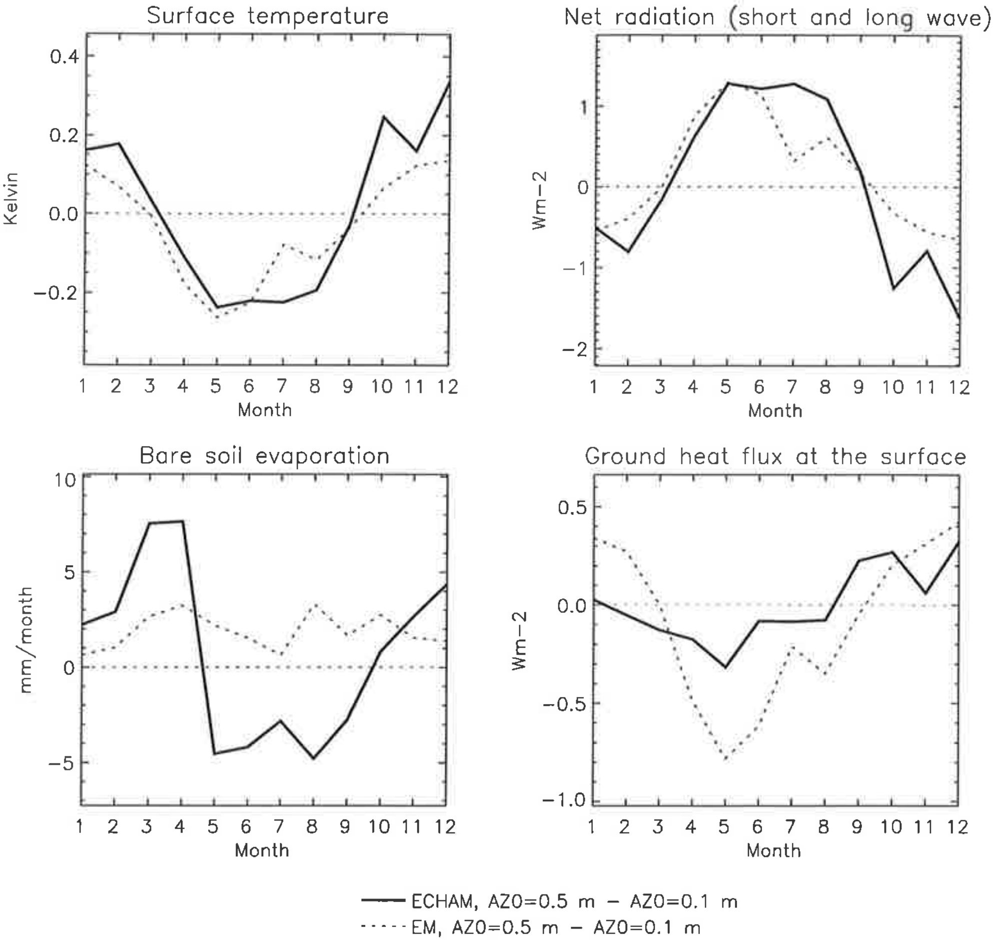

Figure 2.8: *Monthly differences of surface temperature, net radiation, bare soil evaporation and ground heat flux for z_0 =0.1m and z_0=0.5m for ECHAM and EM.*

slightly (of the order of $0.1Wm^{-2}$) reduced in EM because of a drier soil which leads to higher albedos. The ECHAM shortwave net radiation is only changing during winter due to altering snow conditions. The latent and sensible heat flux are typically less sensitive during summer, but the evolution is rather accidental. The sign of the turbulent fluxes' sensitivity is opposite in order to maintain the energy balance. ECHAM shows especially high values during March and April. The same is true for bare soil evaporation. This is due to the still high soil moisture and the already rather high shortwave radiation. During summer, such strong sensitivities are no longer observed because of the dry soil. Sensitivity of bare soil evaporation has an entirely different evolution in both models. EM shows the supposed development. The higher the roughness the higher the bare soil evaporation. Due to the very simple parameterization of bare soil evaporation depending linearly on the soil moisture in EM, sensitivity is mainly influenced by the potential evaporation. The situation is completely different for ECHAM. During summer, rougher surfaces lead to less evaporation whereas the opposite is true during winter. The reason is that rougher surfaces effectively dry the soil during winter and spring due to enhanced evapotranspiration. Therefore, soil water is missing during summer, limiting bare soil evaporation. An interesting detail is that transpiration also increases during summer for rougher surfaces. This is due to the capability of roots to draw water out of deeper soil layers. The parameteriza-

tion of ECHAM is - in spite of the bucket model representation - able to correctly capture this feature.
The behaviour of ground heat flux is the direct result of the evolution of surface and soil temperature. During summer, the land surface is warmed more for smoother surfaces, and as a conclusion, an additional downward heat flux is observed. During winter, the opposite is found. This implies a diminuation of the amplitude of ground heat flux. This is also apparent for surface temperature. For similar surface and soil temperatures, parameterization of both models produce similar ground heat fluxes in spite of totally different parameterization schemes. The temperature T_U in EM that is held constant produces higher differences between soil temperatures and the surface temperature and therefore higher soil heat fluxes.

It is not surprising that, beside the strong seasonal differences of sensitivities, there are clear differences between day and night. 'Day' is defined as the time where shortwave incoming radiation exceeds $2\mathrm{Wm}^{-2}$. Figure (2.9) gives an overview of the day and night sensitivities with respect to z_0. Due to the missing nigthtime shortwave radiation, it is obvious that turbulent fluxes will be smaller. Therefore, the computation of the ratios in Figure (2.9) are based on relative sensitivities. Relative sensitivities are computed as follows:

$$relS = \frac{f(x_2) - f(x_1)}{(x_2 - x_1)f(x_1)} \tag{2.2}$$

where f represents any quantity and x the parameter. In Figure (2.9), x is the roughness length z_0 with x_1=0.1m and x_2=0.2m.

Positive values signify that the relative sensitivity of ECHAM and EM has the same sign, whereas negative values represent a different sign of the models' relative sensitivities. Values approaching 1 show us that the relative sensitivity is about the same in both models. If the bright (day) and dark (night) bars have the same height, this means that relative sensitivities of the two examined models are equal for day and night. Snow melt increases with increasing roughness in ECHAM during the day but decreases at night. For EM, the converse is true. Moreover, relative sensitivity is much larger for ECHAM (the absolute bar height is more than 1, the bar for the situation at night is cut off and would be about -40). This fits the alternate theories of snow melt parameterization in both models. The differences are even more significant at night. The large values for the skin reservoir (cut off, right values are about 25 (day) and 50 (night)) are due to the fact that a large portion of the ECHAM skin reservoir water is evaporated at the potential rate and therefore is very sensitive to z_0 whereas in the EM, most of the water is immediately infiltrated. The different signs for shortwave radiation and albedo during the day are due to the dependence of albedo on the soil moisture of the uppermost soil layer in EM which is not included in ECHAM. The difference concerning bare soil evaporation captures the fact that during the night absolute sensitivity is higher in ECHAM whereas at day EM parameterization is more sensitive. A bar height of less than 1 during the day and more than 1 during night signifies that the same is true for relative sensitivities.

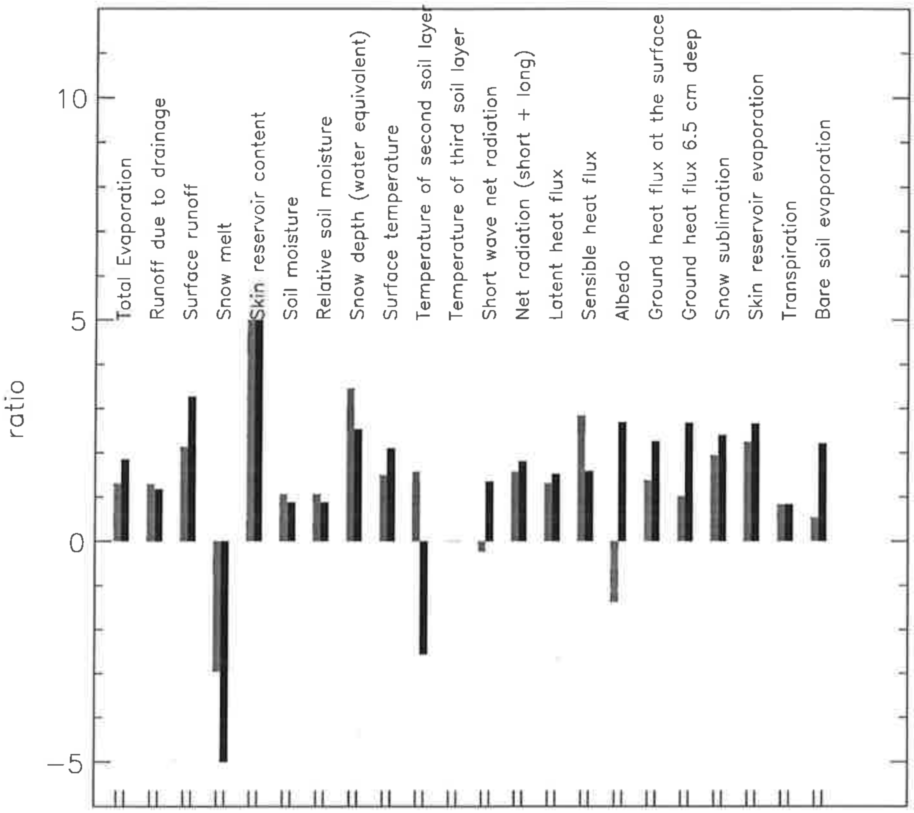

Figure 2.9: *Ratios of the relative sensitivity at day and at night (annual basis) for ECHAM and EM. The calculation is based on the model experiments with* z_0*=0.1m and* z_0*=0.2m. Left bar: ECHAM/EM at day, right bar: ECHAM/EM at night. The bars of snow melt and skin reservoir content are cut off.*

2.3 Sensitivity to the leaf area index (LAI)

The leaf area index is the surface of all leaves projected on a horizontal plane. This parameter is not easy to determine and has a distinct annual cycle in many regions of the earth (e.g. in Europe). Despite this, the LAI is kept constant in time in both the ECHAM3 and ECHAM4 version.
The LAI is not well suited to catch all the characteristics of vegetation. It is a poor parameter to describe certain physical processes (e.g., surface energy balance). Therefore, it may be useful to introduce additional indices to describe the vegetation more completely. A number of such vegetation indices have been proposed in the literature (Verstraete, 1994). Vegetation indices are based on remote sensing data and attempt to exploit the spectral contrast of green vegetation. The most widely used indices are the Simple Ratio (SR) and the Normalized Difference Vegetation Index (NDVI), defined as follows:

$$SR = \frac{\rho_{NIR}}{\rho_{RED}} \tag{2.3}$$

$$NDVI = \frac{\rho_{NIR} - \rho_{RED}}{\rho_{NIR} + \rho_{RED}} = \frac{SR - 1}{SR + 1} \tag{2.4}$$

where ρ_{RED} and ρ_{NIR} are the measured reflectances in the red and near-infrared spectral regions, respectively. The main advantage of these indices is that they may provide useful information at a low cost. They suffer a number of drawbacks, however, including relatively high sensitivity to soils, atmospheric conditions or illumination. Some of these indices have been optimized to reduce these sources of error. A recently proposed index is the Global Environment Monitoring Index (GEMI), which is a rather sophisticated function of two spectral bands (Verstraete, 1994).

This section uses the Dickinson-evaporation for the EM experiments. This is due to the fact that the operationally used parameterization for evaporation is very simple and does not take into account the leaf area index at all (see formulae (1.45) and (1.48)). An advantage is that it is possible to check the parameterization formulae in the model. The LAI was also held constant for EM-runs inspite of the simple possibility to introduce an annual cycle. For sensitivity studies, this is an ingenious assumption which makes interpretation easier.
A short description of the Dickinson parameterization gives a better understanding of the following results. This parameterization takes into account the stomatal resistance as the main element, which is a function of the soil moisture content, the photosynthetically active radiation, the temperature and the humidity. The formula for transpiration is

$$TR = \frac{R_{net} + \rho_a \frac{C_A C_F}{C_A + C_F} B_e \delta q}{1 + \frac{C_A + C_V}{C_A + C_F} \frac{C_F}{C_V} B_e} \tag{2.5}$$

with

B_e	$= \frac{c_p}{L} (\frac{\delta q_{sat}}{\delta T})^{-1}$
C_A	$= C_h v_h$ [ms^{-1}]
C_F	$= LAI {r_{la}}^{-1}$ [ms^{-1}]
C_V	$= r' C_F$ [ms^{-1}]
C'	Constant; 0.05 $(\mathrm{ms}^{-1})^{0.5}$
c_p	Specific heat capacity [$\mathrm{Jkg}^{-1}\mathrm{K}^{-1}$]
L	Specific heat of vaporization [Jkg^{-1}]
LAI	Leaf area index

q	Specific humidity [$\mathrm{kgkg^{-1}}$]
${r_{la}}^{-1}$	$=C'(u_\star)^{0.5}$ [$\mathrm{ms^{-1}}$]
TR	Transpiration [$\mathrm{mms^{-1}}$]
ρ_a	Density of air [$\mathrm{kgm^{-3}}$]

The reduction factor r' contains the stomatal resistance r_{st} and the function r_{la}. The formula can be simply transformed into an equation easier to derive with respect to the leaf area index:

$$TR = \frac{LAI(R_1 + Q_1 C_A) + R_1 C_A r_{la}}{(1+B_e)[LAI + r_{la} C_A] + C_A B_e r_s} \tag{2.6}$$

with

Q_1	$=\rho_a B_e \delta q$ [$\mathrm{kgm^{-3}}$]
R_1	$=R_{net}/L$ [$\mathrm{mms^{-1}}$]

and all other abbreviation as in Equation (2.5).
In the following, the parameterization formulae which are directly dependent on the leaf area index are described.
The maximum content of the skin reservoir W_{lmx} (Equation (1.14)) is parameterized the same way for both models when using the Dickinson parameterization in EM. Another formula for W_{lmx}, which is not dependent on the LAI, is implemented in the operational EM (Equation (1.24)). This equation directly determines the filling grade of the skin reservoir. The higher the leaf area index the more water can be held on leaves after a rainfall event. It is evident that the distribution of rainfall is significant for the water content of the skin reservoir. The derivative of Equation (1.14) with respect to LAI is simply $W_{lmax} C_v$, where W_{lmax} is the maximum amount of water held on one layer of leaf or bare ground and C_v represents the grid fraction covered with vegetation.
The second formula which contains the leaf area index is the transpiration. The parameterizations of the stomatal resistance is the main part of both model formulae. The parameterizations are not the same. In ECHAM the following formula is applied

$${r_{st}}^{-1} = F(W_s) \frac{\frac{b}{dPAR} ln(\frac{de^{-kLAI}+1}{d+1}) - ln(\frac{d+e^{-kLAI}}{d+1})}{kc} \tag{2.7}$$

with

a	$=5000\mathrm{Jm^{-3}}$
b	$=10\mathrm{Wm^{-2}}$
c	$=100\mathrm{sm^{-1}}$
d	$=\frac{a+bc}{cPAR}$
$F(W_s)$	Water stress factor
k	$=0.9$
PAR	Photosynthetically active radiation

One recognizes the exponential function of LAI in the formula above. This parameterization is based on the exponential decrease of shortwave radiation penetrating into a canopy layer. The introduction of LAI is a good method to allow for this exponential decrease of shortwave radiation. With increasing penetration into canopy, the shortwave radiation and therefore transpiration is weakened. In contrast to ECHAM, the Dickinson parameterization of the stomatal resistance does not include the leaf area index (although the whole transpiration formula does), but a dependence on temperature and humidity:

$$r_{st}^{-1} = r_{s,max}^{-1} + (r_{s,min}^{-1} - r_{s,max}^{-1}) F_{WG} F_{ST} F_{TB} F_{DQ} \tag{2.8}$$

$$F_{WG} = \begin{cases} 0 & ;\ WBR \leq PWP \\ \frac{WBR-PWP}{FC_{BR}FC-PWP} & ;\ PWP < WBR < FC_{BR}FC \\ 1 & ;\ WBR \geq FC_{BR}FC \end{cases}$$

$$F_{ST} = \begin{cases} 0 & ;\ PAR = 0 \\ \frac{PAR}{R_C} & ;\ 0 < PAR < R_C \\ 1 & ;\ PAR \geq R_C \end{cases}$$

$$F_{TB} = \begin{cases} 0 & ;\ T_{2m} \leq T_0 \\ 4\frac{(T_{2m}-T_0)(T_{end}-T_{2m})}{(T_{end}-T_0)^2} & ;\ T_0 < T_{2m} < T_{end} \\ 0 & ;\ T_{2m} \geq T_{end} \end{cases}$$

$$F_{DQ} = \begin{cases} 0 & ;\ q_{2m} \leq q_{sat,2m} Q_{BRT} \\ \frac{q_{2m}-Q_{BRT}q_{sat,2m}}{(1-Q_{BRT})q_{sat,2m}} & ;\ q_{sat,2m}Q_{BRT} < q_{2m} < q_{sat,2m} \\ 1 & ;\ q_{2m} \geq q_{sat,2m} \end{cases}$$

with

FC	Field capacity
FC_{BR}	Fraction of field capacity below which water stress begins to work (=0.75)
PWP	Permanent wilting point
q	Specific humidity [$kgkg^{-1}$]
Q_{BRT}	Fraction of saturation humidity below which stomatas are closed (=0.75)
R_C	$=100Wm^{-2}$
T	Temperature [K]
T_{end}	=313.15K
T_0	Freezing point
WBR	Higher value of relative soil moisture of the two upper soil layers
$r_{s,max}$	Maximum stomatal resistance (= $4000sm^{-1}$)
$r_{s,min}$	Minimum stomatal resistance (= $100sm^{-1}$)

These four functions control the dependence of transpiration on soil moisture, radiation, temperature and humidity. The critical point (start of water stress) is set equal to 75% of the field capacity for EM and 50% for ECHAM. This is quite a large difference, however one has to remember that the ECHAM soil can not exceed field capacity while the soil moisture of EM is only saturated at the pore volume. For better understanding, the four functions are represented in Fig. (2.10). All functions except the temperature function are linear and increase with increasing value. The function FTB has a parabolic shape and reaches a maximum at T=20°C. The stomatal resistance is equal to $r_{s,max}$ if the
- temperature is below freezing point or over 40°C,
- at night (no shortwave incoming radiation),
- soil moisture falls below the permanent wilting point, or
- specific humidity falls below 75% of the saturation value.

The last condition is a very strong one. For the Cabauw site, the function F_{DQ} is often close to zero, greatly influencing the transpiration. The original work of Dickinson omits this

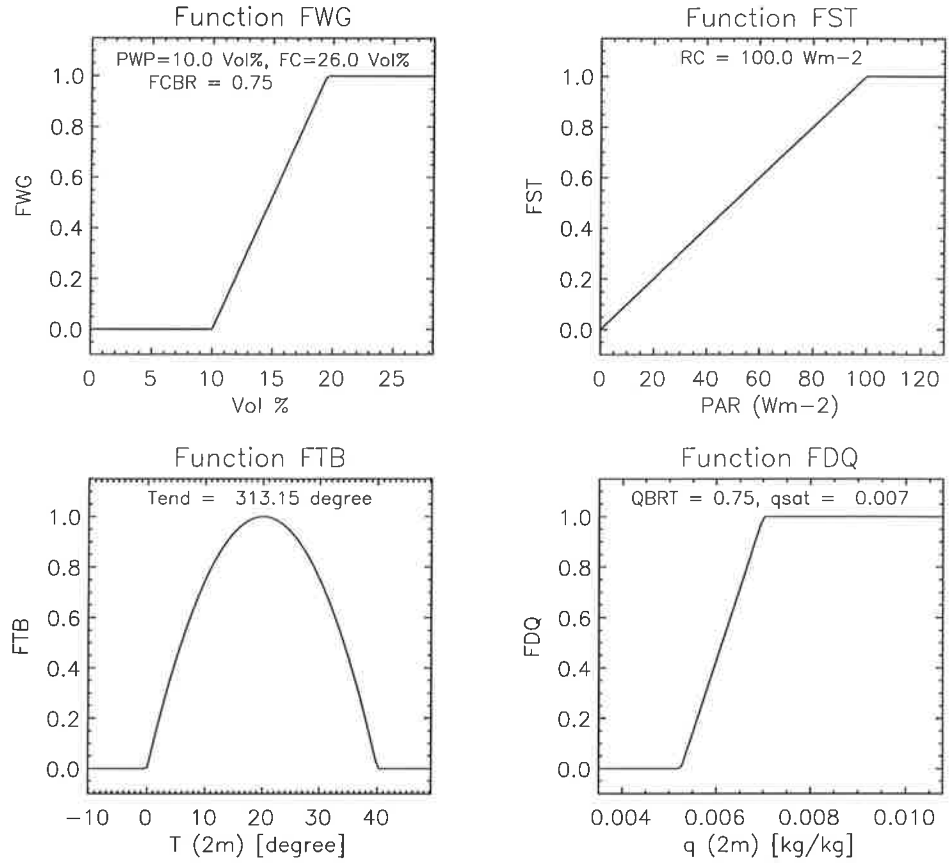

Figure 2.10: *Functions F in the parameterization for the stomatal resistance according to Dickinson. FWG is the function for the dependence on soil moisture, FST for radiation, FTB for temperature and FDQ for specific humidity.*

function because the connection of stomatal restistance and humidity was very uncertain and poorly explored. Therefore, the results presented here are based on the assumption F_{DQ}=1.0.

First we want to look closer at the typical exponential decrease of transpiration (Fig. (2.12)) with increasing LAI which is only observed for ECHAM. As mentioned earlier, from a physical point of view this characteristic is expected. This signifies that the higher the leaf area index the lower the sensitivity. It is clear that the difference of transpiration for high LAIs (e.g. LAI=9 and LAI=10) can not be large because of almost total shading of the lowest leaf layer. This characteristic of sensitivity can be shown by plotting the transpiration and its derivative for both models. Fig. (2.11) indicates that $\Delta Transpiration/\Delta LAI$ decreases faster for the ECHAM parameterization whereas the Dickinson parameterization indicates an almost linear decrease. Moreover, we recognize distinctly higher transpiration rates for the Dickinson parameterization. The absolute values are not as important (and too high) because it is supposed to be windy and sunny during 24 hours. The development of transpiration sensitivity in EM for LAI larger than 3 is surprising. The changes are very small and do not obey the characteristics found in Fig. (2.11), namely the expected distinctly higher sensitivity for EM than for ECHAM for dense vegetation. The reason can be found analysing the evolution of the soil water content. The high

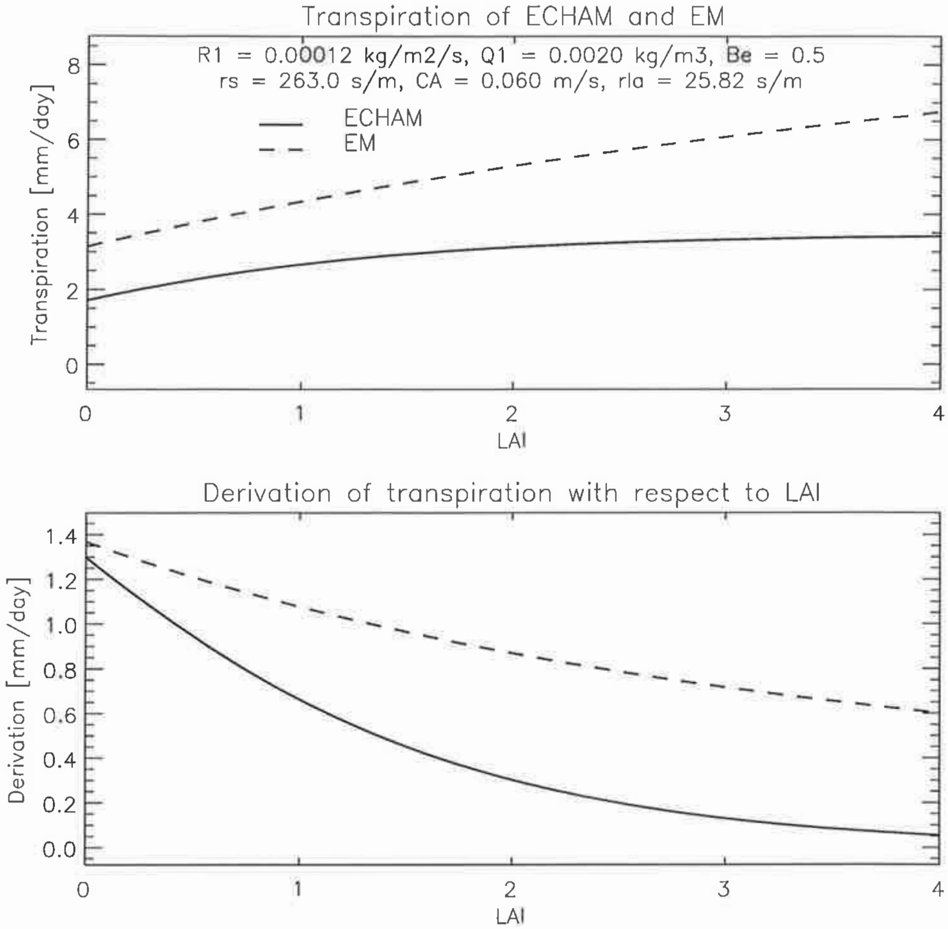

Figure 2.11: *Transpiration of ECHAM and EM (Dickinson version). Typical mean values for a sunny summer day are chosen. The photosynthetically active radiation (PAR) is set to $75 Wm^{-2}$. Abbrevations are the same as in Equation (2.5) and (2.6).*

transpiration of EM strongly dries out the soil. This leads to the fact that transpiration can not further increase in spite of higher leaf area indices: A typical negative feed back.

Because most of the grid element is vegetated (for all experiment: 87% of the area is vegetated) and sensitivity to the LAI is high especially for low leaf area indices, it is not surprising that soil moisture decreases with denser vegetation. The decrease is more than three times stronger for EM (LAI=1.5) than for ECHAM. For dense vegetation the relative soil water content is even smaller for EM than ECHAM. During the late summer period (August till September) the relative soil moisture content reaches the very low value of roughly 0.3. In spite of the low value, the water which is drawn out of the soil by the roots is supposed to be taken from the uppermost soil layer. Only if the soil moisture falls below 1.25 times the wilting point (for the soil of sandy loam, this corresponds to a relative soil moisture content of 27%), it is assumed that water uptake from deeper soil layers is possible. The soil water directly influences the bare soil evaporation, drainage and surface runoff. For ECHAM, all these quantities show the typical characteristic found for transpiration, an exponential decrease of the sensitivity with increasing LAI. All these

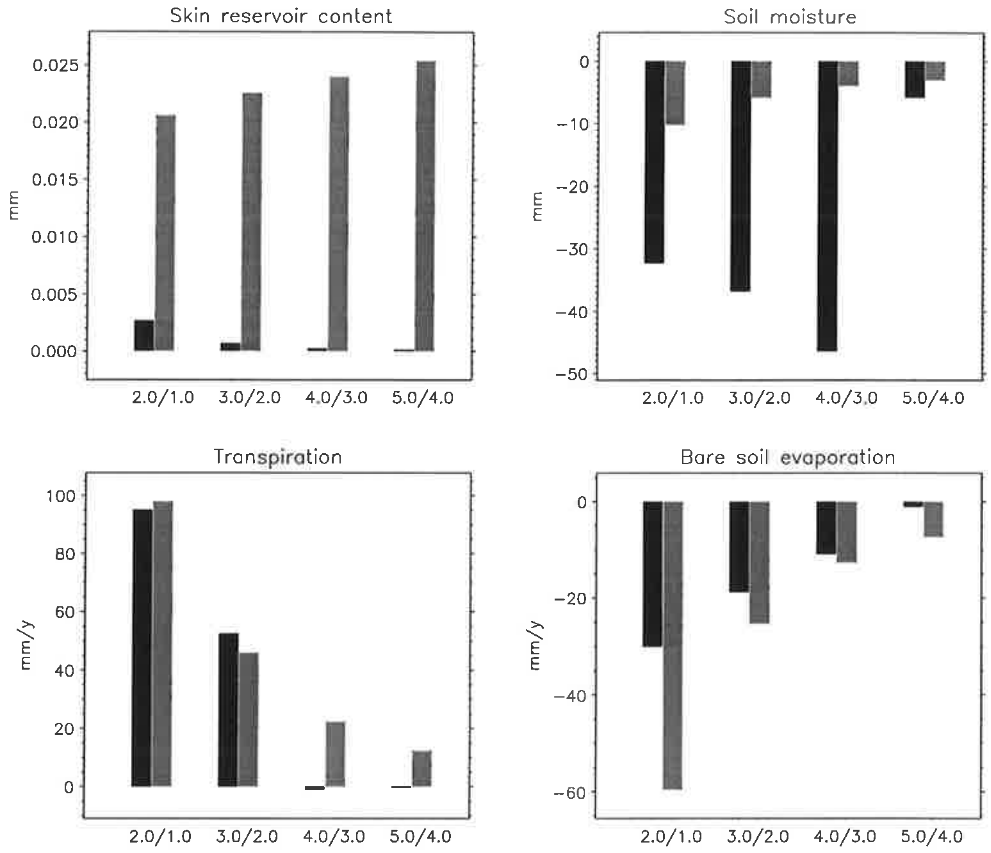

Figure 2.12: *Sensitivity of soil moisture, skin reservoir content, transpiration and bare soil evaporation with respect to the leaf area index for ECHAM and EM. Left bar: EM; right bar: ECHAM.*

quantities decrease with higher leaf area index for both models. However, surface runoff in EM is different. For a LAI greater than 3, the surface runoff clearly increases, whereas the drainage decreases strongly and has values close to 0. We have to remember that most of surface runoff consists of water discharge out of the uppermost soil layers while drainage is computed from the water outflow of lower soil layers. Obviously, the water is not able to reach lower soil layers when the soil moisture content is too low. Skin reservoir content shows a far higher sensitivity for the ECHAM model. This is due to the fact that the calculation of the maximum skin reservoir content is the same for both models, but the water of the whole EM-skin reservoir infiltrates within short time whereas in ECHAM the water on leaves does not and evaporates at the potential rate.

How does the surface temperature respond to changes in the vegetation density? For increasing LAI, the higher transpiration is decisive for higher latent heat fluxes. Since evaporation needs energy for transformation of water to vapour, the surface is cooled, i.e. the surface temperature decreases with higher leaf area indices (Fig. (2.13)). However, the absolute value is very small because of a strong forcing given at the lowest atmospheric model level. In addition, the temperature evolution influenced by an altered latent heat flux will be immediately partially

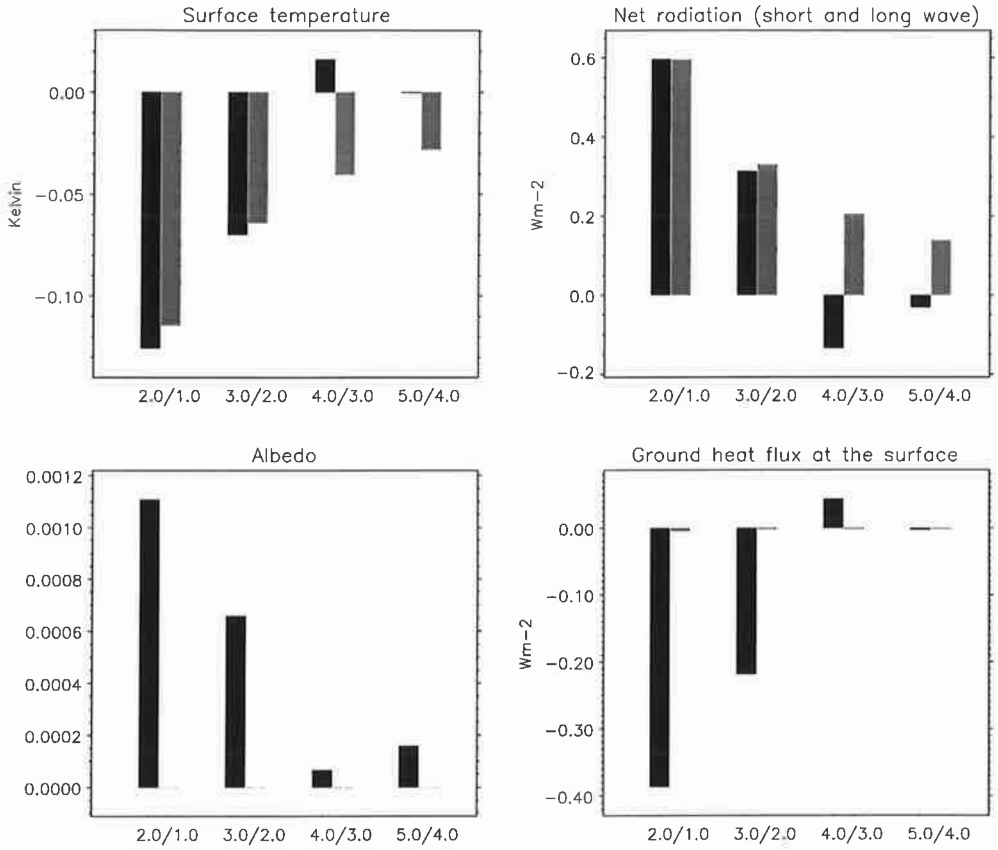

Figure 2.13: *Sensitivity of surface temperature, net radiation, albedo and ground heat flux with respect to the leaf area index for ECHAM and EM.*

compensated by a change of the sensible heat flux. It is striking that for EM, an inversion of the sign is observed. The same is true for net radiation and ground heat flux. The reason is the latent heat flux which also decreases between LAI=3 and LAI=4: Although transpiration stops decreasing, bare soil evaporation still clearly decreases. The values of computed sensitivities are very similar for surface and soil temperatures in ECHAM, but decrease quickly in the EM because of the fixed lower boundary condition. ECHAM shows no change in albedo with different vegetation densities. The EM responds slightly because of changes in the soil moisture of the uppermost soil layer, i.e. higher LAIs lead to higher albedos because a drier soil has a higher albedo than a wet one.

A graphical overview of the sensitivities of some quantities with respect to LAI is given in Figs. (2.14) and (2.15).

Only some interesting results are pointed out. As mentioned above, changes of LAI strongly influence the soil water content in EM. Total runoff consists of the sum of surface runoff and drainage. The change in total runoff is, in a first approximation, the same for both models. However, the partition between drainage and surface runoff differs. While surface runoff is much more sensitive for the ECHAM experiment, drainage is more sensitive for EM. For ECHAM,

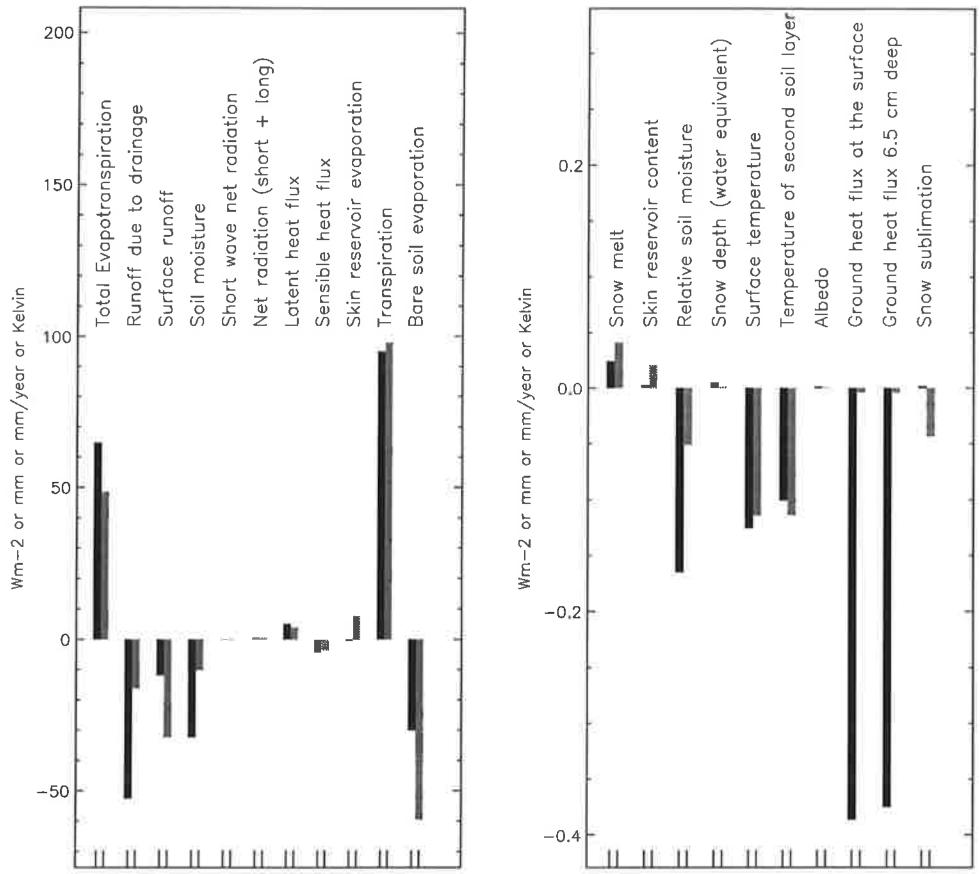

Figure 2.14: *Change of different quantities for an increase in LAI from 1 to 2 (annual basis). Left bar: EM; right bar: ECHAM.*

the decrease of the fractional saturated grid area, which leads to less surface runoff (see (1.19)), is obviously more important than the less frequent occurrence of fast drainage which applies for relative soil moisture contents over 90%. A probable explanation for EM is the following: The water for the higher transpiration is taken during the entire year from the uppermost soil layer because soil water content stays above the threshold of 1.25 times the wilting point. This leads to a depletion of the uppermost soil layer and to a fast decrease of water flowing from the first to the second soil layer. This is a consequence of Darcy's Law, which describes capillaric rise and infiltration. This decreases the lateral water outflow from the second and third soil layer (drainage).

Sensible heat flux has a similar absolute sensitivity but the relative values are quite different. The annual average of sensible heat flux is close to zero (about $6 Wm^{-2}$ for LAI=1 and $3 Wm^{-2}$ for LAI=2). The sensitivities are very similar for the latent heat flux, but with an opposite sign. The turbulent heat fluxes are effective to compensate possible changes in surface temperature. The change in net radiation is very similar for both models. However, the reason is somewhat different. The change in surface temperature is a little larger for EM and leads to less upward

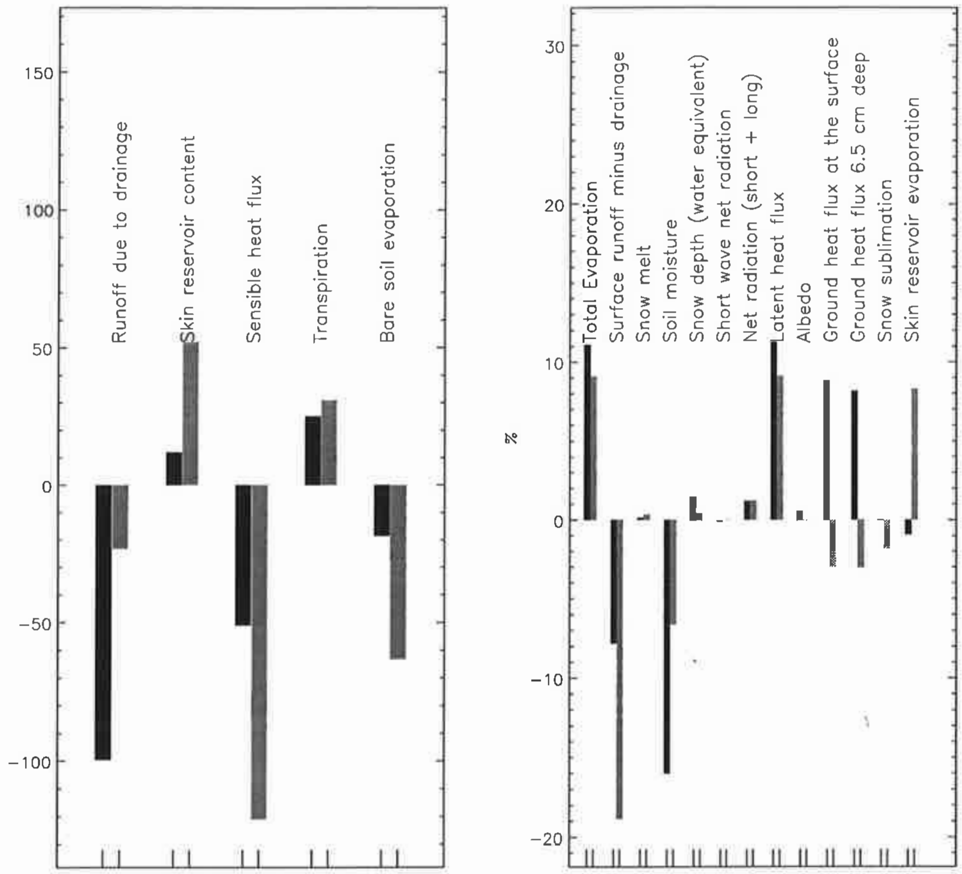

Figure 2.15: *As Fig. (2.14) but relative to the value of LAI=2.*

long-wave radiation. This is compensated by a slightly higher EM-albedo due to a drier soil and results in more reflected shortwave radiation.
Bare soil evaporation is much larger for EM. As is shown later in chapter (5), this is mainly due to the chosen evaporation formula. The Dickinson parameterization for bare soil evaporation is less sensitive to the LAI than the ECHAM formula and consequently, an increasing difference with denser canopy has been found.
Finally, the ratios of the sensitivity for a dense and a transparent canopy are depicted and discussed.

Fig. (2.16) shows that the sensitivity is generally decreasing with increasing LAI (for values are below 1). The other striking feature is the very low values of EM-bars. For transpiration, ground heat fluxes, turbulent heat fluxes, drainage and temperature, the quotient is close to zero. Obviously, EM reaches an equilibrium condition where an increase in the canopy density barely influences the output. From the physical and meteorological point of view, this is reasonable. An optimum of foliage exists for trees, i.e. if the canopy is too dense, no light can penetrate the lower canopy and moreover a too high transpiration draws too much water out of the soil destroying the canopy by lack of water. This equilibrium condition can also be reached

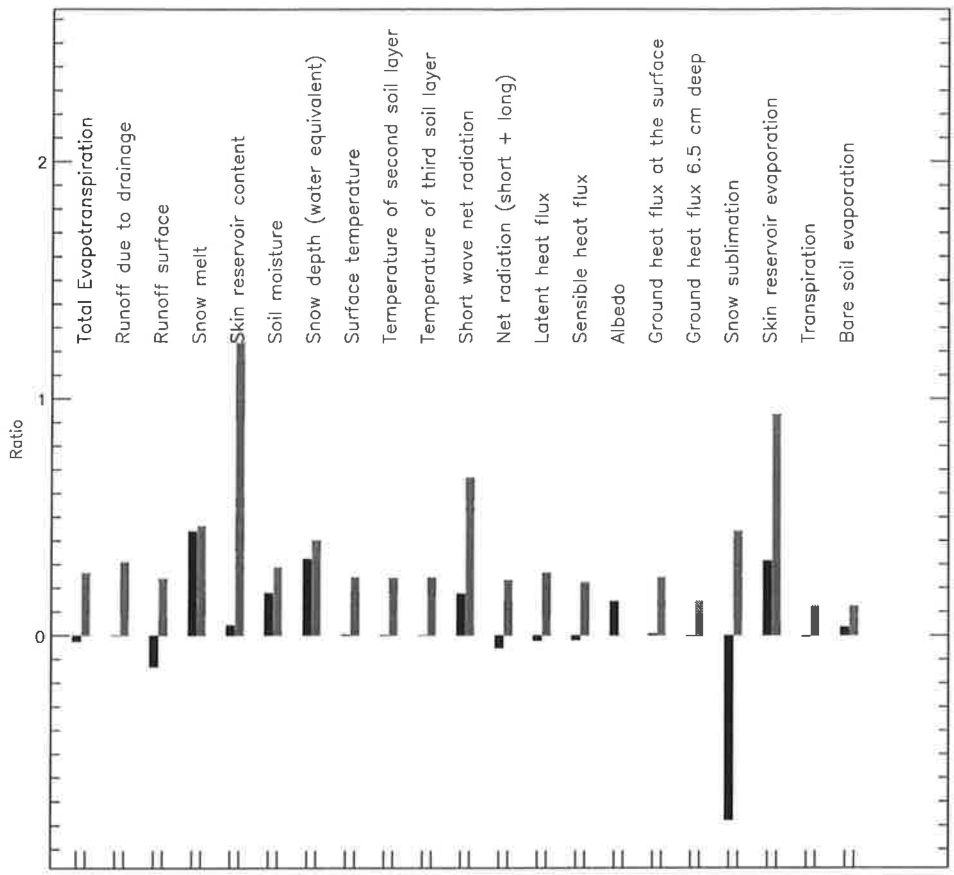

Figure 2.16: *Ratio of sensitivity for LAI=1.5 and LAI=4.5 for ECHAM and EM. Left bar: EM; right bar: ECHAM.*

by ECHAM but higher LAIs are necessary.

Annual evolutions of the sensitivies are very different for the two models. On the basis of monthly averages, only the more interesting quantities are presented (Fig. (2.17)).

The differences of transpiration show a clear annual cycle for ECHAM, but decrease sharply in late summer for EM. This leads to a higher transpiration rate in September for LAI=1 than LAI=5 and to a very strong drying of the EM-soil for very dense vegetation in late summer leading to a collapse of transpiration. However, the period from October to June shows similar differences.

The soil moisture shows very large differences. The relative soil moisture is changed for the two experiments by about 0.5, with a maximum of 0.7 during winter whereas EM shows maximum differences in relative soil moisture of only 0.2 and close to zero in winter. The transpiration in EM can strongly modify the soil moisture over the year, while the ECHAM can fill the soil water reservoir up to saturation each winter. The phase shift of the ground heat flux is striking: EM reaches the maximum in June and ECHAM in April. This shift is also observed for latent and

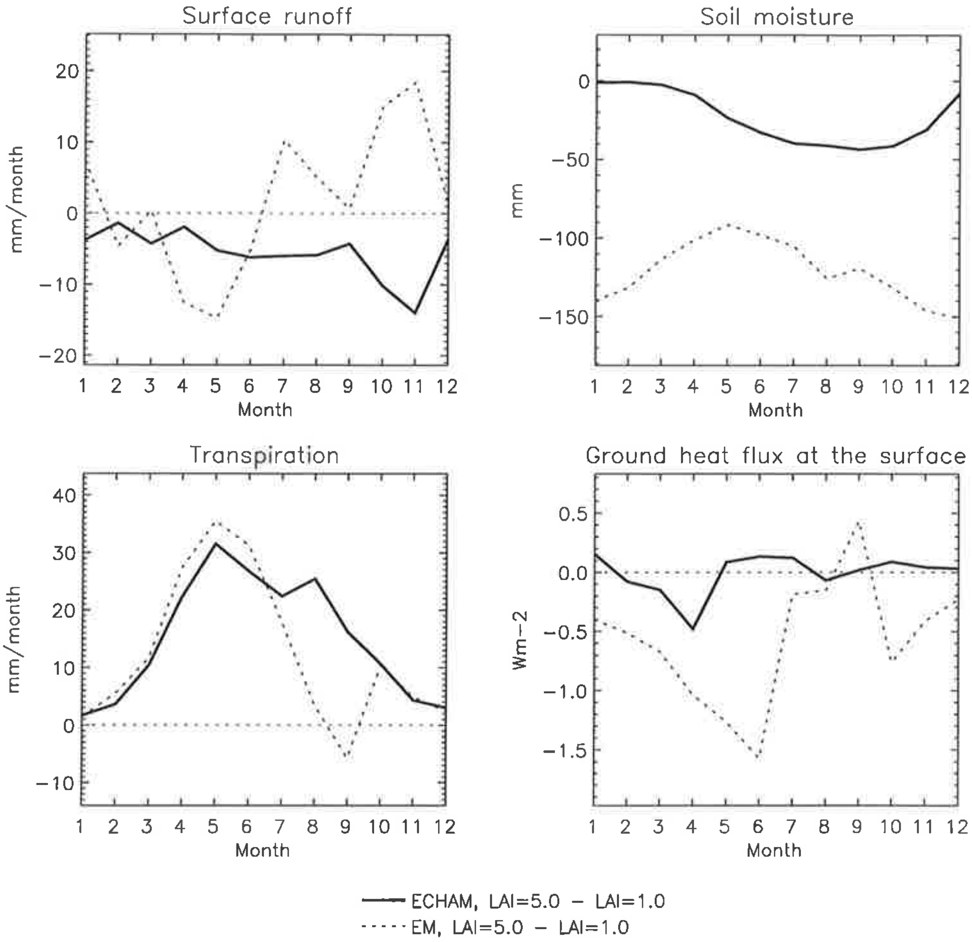

Figure 2.17: *Differences of monthly surface runoff, soil moisture, transpiration and ground heat flux for the experiments with LAI=1 and LAI=5.*

sensible heat flux as well as surface temperature, but the phase shift is about one month shorter.

2.4 Sensitivity to the vegetation ratio

The dependence of various output parameters on the vegetation ratio is very important for climate change. For example, vast regions of rain forests are being cut down, and deserts are spreading. It is therefore essential that the influences of a changing vegetation ratio are well understood, and that the parameterizations are represented in a correct manner. The vegetation ratio and the leaf area index are similar quantitities in the respect that an increase in the density of a forest can lead to a similar increase in the vegetated area of a grid element. Both can occur when the climate is changing. The value of LAI can also be efficiently changed by the air pollution (less leaves and needles).
It should be added that EM includes no forest fraction whereas ECHAM distinguishes forest and non forest but vegetated areas. This means that EM uses no parameterization formulae which incorporate a differentiation between forest and other vegetation (e.g. grass).
Which are the formulae which directly contain the vegetation ratio? The most important effect is the partition of water vapour fluxes from vegetated area and bare soil. The question is which process is more efficient to draw water out of the soil of a specified fixed area. For ECHAM, this depends on different variables such as soil moisture, specific humidity, radiation and leaf area index. Therefore, it is difficult to decide which process is dominant.
For EM, the parameterization of transpiration and bare soil evaporation is much simpler (see Eqs. (1.45) and (1.48)). Figure (2.18) shows the functions β_E and β_B which control bare soil evaporation and transpiration. The graphic shows that for very dry soils (below 41% relative soil moisture) and wet soil (above 84% relative soil moisture) bare soil evaporation is more efficient than transpiration to draw water out of the soil. The difference is larger for relatively wet soils which often occur at Cabauw. The conclusion is that higher vegetation ratios mean lower sums of bare soil evaporation and transpiration. This is confirmed in Fig. (2.19). The same characteristic is shown by the much more sophisticated parameterization of ECHAM.

The formula computing the maximum skin reservoir content contains the vegetation ratio in both models. The derivative with respect to the vegetation ratio is

$$\frac{\delta W_{lmx}}{\delta \sigma_{PLNT}} = \begin{cases} W_{lmax}(LAI-1) & \text{(ECHAM)} \\ 5\ W_{I,MB} & \text{(EM)} \end{cases} \tag{2.9}$$

$W_{I,MB}$	Constant set equal to 0.5mm (EM)
W_{lmax}	Maximum amount of water held on one layer of leaf (ECHAM) [mm]
W_{lmx}	Maximum content of skin reservoir [mm]
σ_{PLNT}	Vegetation ratio

The standard value of W_{lmax} is 0.2mm and the LAI is set to 2. Using these values, the sensitivity of the maximum water content is distinctly higher in the EM. Nevertheless, the skin reservoir content is much more sensitive to vegetation changes in ECHAM. In both models, the water on leaves evaporates at the potential rate. In ECHAM, the water on the leaves remains for a much longer time whereas in EM, the water is infiltrated very quickly into the soil from both vegetation and bare soil. Therefore, there is barely any change in the skin reservoir content. This is also true for skin reservoir evaporation. The annual mean skin reservoir content is more than three times higher for fully vegetated regions than for desert conditions, and evaporation from skin reservoir is nearly doubled (ECHAM).
The EM includes two further direct dependencies on the vegetation ratio. The maximum infiltration rate (Eq. (1.25)) is a function of σ_{PLNT} for the range of $0.5 < \sigma_{PLNT} < 1.0$. The first summation of the formula increases linearly with the vegetation ratio. This means that more water can infiltrate into the soil, raising the soil moisture content and decreasing surface runoff. This concerns only that part which actually runs off at the surface. This process is negligible, however, because over 99% of the total surface runoff consists of lateral flow out of

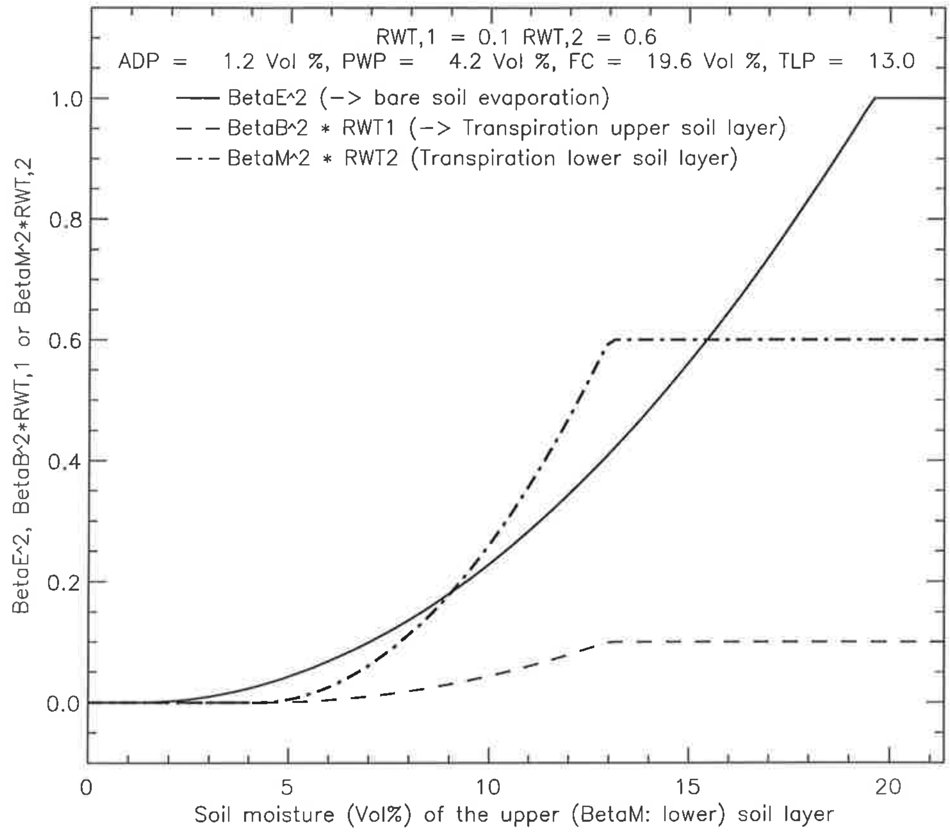

Figure 2.18: *Factor $\beta_B^2 xrWT$ of transpiration formula (1.45) and β_E^2 of bare soil evaporation (Eq. (1.45)). The function $\beta_{B,2}{}^2 r_{WT,2}$ controls transpiration from the lower soil layer whereas $\beta_{B,1}{}^2 r_{WT,1}$ is responsible for upper soil transpiration. Parameters rWT_K are calculated for a root depth equal to 0.7m.*

the uppermost soil layer (which is included in surface runoff). The sensitivity on the vegetation ratio is

$$\frac{\delta N_{max}}{\delta \sigma_{PLNT}} = K_1(PV - W_1)/PV + K2 \tag{2.10}$$

for $0.5 < \sigma_{PLNT} \leq 1.0$ and zero for $0 \leq \sigma_{PLNT} \leq 0.5$. The symbols are as in Equation (1.25). For the soil type 'loamy sand', the range of the derivative is $0.0035 \mathrm{mms}^{-1}$ (very dry) to $0.0055 \mathrm{mms}^{-1}$ (very wet). For low vegetated areas, σ_{PLNT} no longer appears in the formula. However, there is an indirect dependence. If the water content of the uppermost soil layer increases, the maximum infiltration rate is lowered.

The last explicit dependence is the interaction of albedo and vegetation ratio in the EM-parameterization (Eq. (1.36)). EM distinguishes the albedo of vegetated and non vegetated areas. The albedo of snow free vegetation is set to 0.15, but the bare soil albedo depends on soil type and soil water content. In this context, the derivative of total albedo with respect to σ_{PLNT} is of interest:

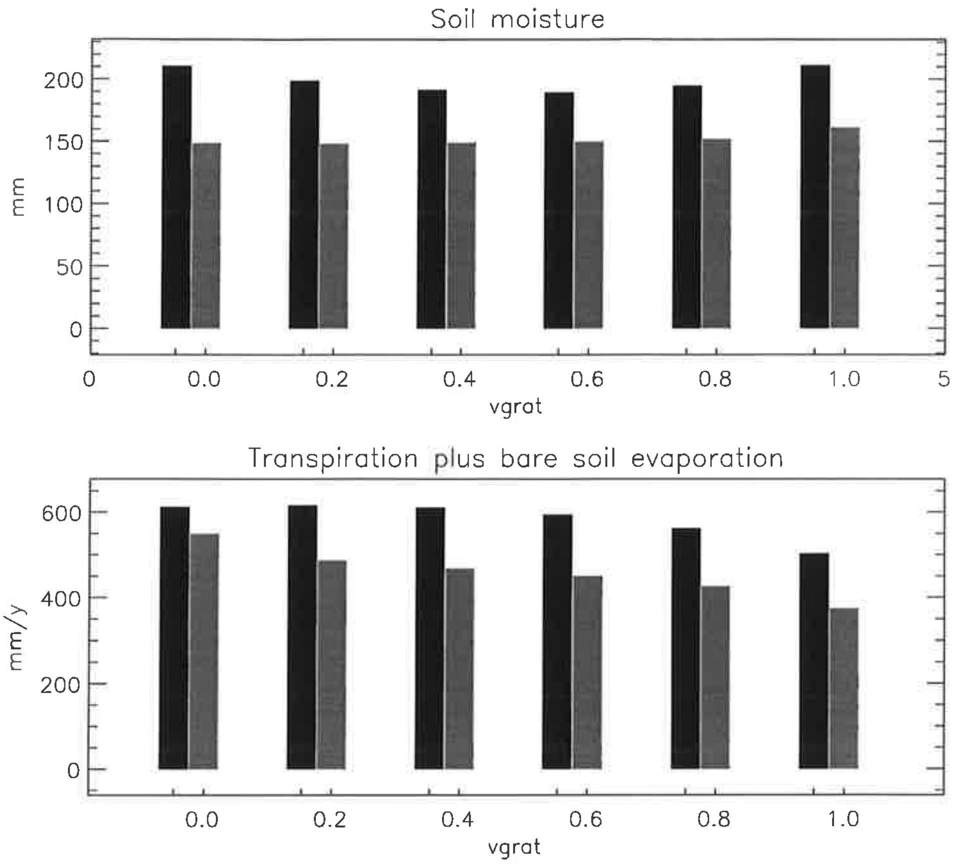

Figure 2.19: *Annual values of soil moisture and the sum of transpiration and bare soil evaporation for different vegetation ratios. Left bar: EM; right bar: ECHAM.*

$$\frac{\delta\alpha_{sf}}{\delta\sigma_{PLNT}} = \alpha_{PLNT} - \left(\alpha_{bas} - \frac{LKW_1}{KR}\right) \tag{2.11}$$

The symbols are as in Equation (1.36). For the soil type of Cabauw, this equation reduces to $\frac{\delta\alpha_{PLNT}}{\delta\sigma_{PLNT}} = 4.25W_1$ - 0.15. With the assumption of a soil close to saturation, this derivative is about -0.06. This means that the albedo of the EM decreases by 0.06 when changing the vegetation ratio from 0.0 to 1.0. This is confirmed by the results from model runs. The influence of the changing soil water content is distinctly less important.

What features of the sensitivities are found for the examined quantities?
The albedo of ECHAM barely changes with changing vegetation ratio. This is a clear deficiency of ECHAM because it is well known that vegetation and bare soil have different albedos. The only slight interaction of albedo and vegetation in ECHAM is found for snow-covered regions, i.e. a vegetation change causes a temperature change, modifying the snow cover and surface albedo. The dependence of snow albedo on fractional forest area is of no importance here because no forest is presumed in ECHAM for all simulations. The sensitivity of total surface albedo in EM is mainly based on different albedos of vegetation and bare soil. The value of -0.06, as calculated in the last paragraph, is only modified slightly by the changing soil moisture content.

The evolution of EM-albedo's sensitivity directly influences the net shortwave radiation. EM experiments show a change of about 1Wm^{-2} for $\Delta\sigma_{PLNT}$=0.1 for low vegetation ratios; for fully vegetated areas this value decreases to about 0.7Wm^{-2}. ECHAM shows a negligible change in net shortwave radiation because of a nearly constant albedo.

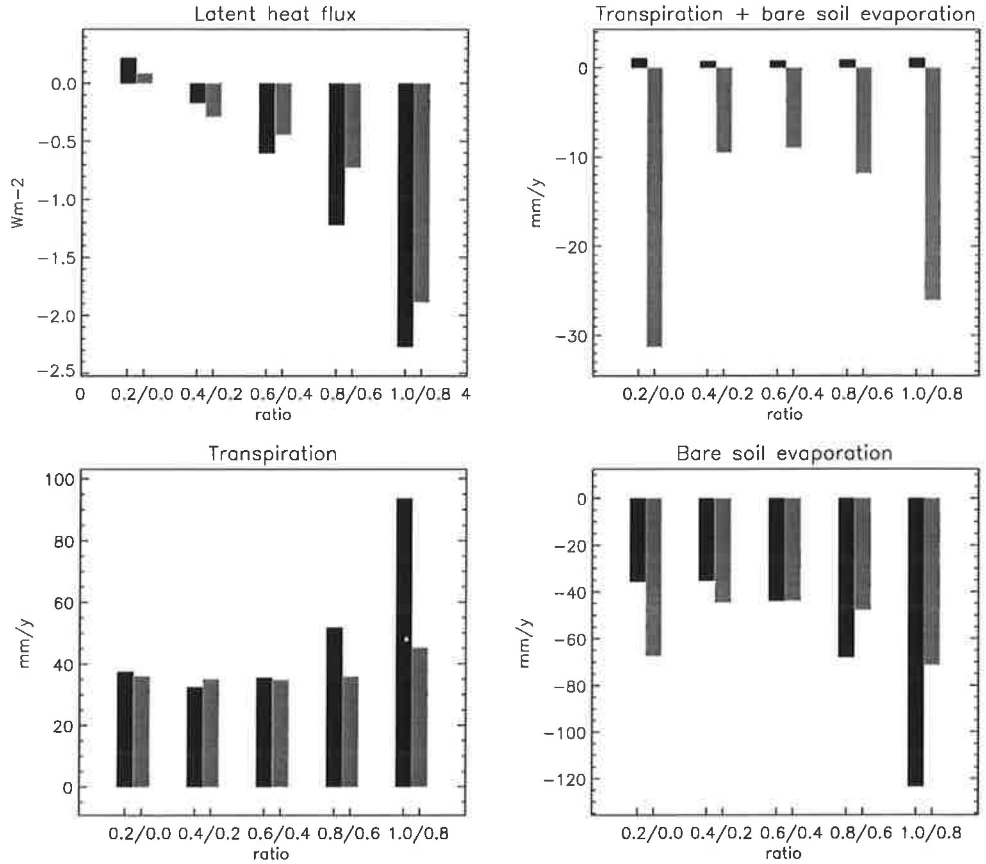

Figure 2.20: *Sensitivity of latent heat flux, transpiration, bare soil evaporation and the sum of transpiration and bare soil evaporation to the vegetation ratio for ECHAM and EM. Values are given for a change in the vegetation ratio equal to 10%.*

The sensitivities of water vapour fluxes are rather different for ECHAM and EM. The sensitivity of transpiration is relatively constant for areas with less than 50% plant cover (35mmy^{-1} for $\Delta\sigma_{PLNT}$=0.1). This increases rather strongly with increasing vegetation ratio for EM, but much slower for ECHAM (Fig. (2.20)). The largest sensitivity is reached for fully vegetated areas for both models (Fig. (2.20)). Bare soil evaporation in EM shows a similar evolution but with opposite signs for transpiration; for ECHAM the sensitivity is largest for the extreme situation (no vegetation and fully vegetated). The sum of transpiration and bare soil evaporation decreases with increasing vegetation ratio. The sensitivity of evapotranspiration minus the skin reservoir evaporation is nearly constant for EM and is largest for ECHAM for the two extremes while reaching a minimum for 50% vegetated grid element (Fig. (2.20)). What could be the reason? The EM parameterization of transpiration and bare soil evaporation (see Fig. (2.18))

suggests a fast decrease of the sum of these two water vapour fluxes, which agrees with the model results. For more than 50% vegetated areas, Equation (2.10) is lowering this tendency, i.e. the higher the vegetation ratio, the higher the maximum infiltration rate which leads to a higher soil moisture. This again should raise transpiration and bare soil evaporation. On the other hand, the maximum skin reservoir content is increasing with increasing vegetation ratio. This has the affect of counteracting the above evolution and leads to more infiltration. This is, because in EM, almost the whole skin reservoir content is very efficiently infiltrated into the soil, and therefore to a wetter soil, more transpiration and bare soil evaporation. A third effect tries to compensate the decreasing latent heat flux, i.e. the higher σ_{PLNT}, the higher the surface temperature. This applies a higher deficit of specific humidity and therefore an increasing potential evaporation which drops in all the formulae calculating water vapour fluxes.
The evaporation from the skin reservoir is clearly increasing with more vegetation in the ECHAM model. The annual sum is about 50mm for σ_{PLNT}=0.1 and double this for the fully vegetated area. For EM, the increase is much slower (of the order of 1mm per 10% increase in vegetation) because most of the water is infiltrated at once into the soil and is therefore lost to evaporation (Fig. (2.21)).
The sum of all water vapour fluxes, the latent heat flux, decreases with more vegetation. Obviously, the increasing canopy evaporation cannot compensate for the decreasing sum of transpiration and bare soil evaporation. The sensitivity of the latent heat flux is small for low vegetation (Fig. (2.20)), but increases faster for grid elements with more than 50% vegetation. The sensible heat flux attempts to compensate this loss and gets higher for more vegetation. The sensitivity for EM is generally more than double than for ECHAM.

The surface temperature is determined by the energy balance. The radiation budget and the turbulent fluxes are the most important quantities determining the energy balance. The model experiments show an increase in surface temperature with more vegetation. This is the consequence of increasing net shortwave radiation (only true for EM) which heats the ground more. The other component is the turbulent fluxes. As the latent heat flux decreases, the cooling of the surface is reduced. The higher temperature leads to an increased sensible heat flux. The sensitivity of the surface temperature is higher for EM than for ECHAM. This is due to the fact that both changes in radiation and turbulent heat flux play a considerable role in EM whereas, for ECHAM, only changes in latent and sensible heat flux are important. The sensitivity is increasing with the vegetation ratio. For a (supposed) desert, the sensitivity of the annual average of surface temperature is about 0.03°C for $\Delta\sigma_{PLNT}$=0.1 and 0.1°C for $\Delta\sigma_{PLNT} = 0.1$ in EM for a fully vegetated grid element (Fig. (2.21)). For ECHAM, these values must be more than halved and are close to zero for low vegetation ratios. It should be added that both models are not able to compute correct surface temperature for vegetation because there is no canopy model calculating radiation fluxes and therefore reasonable temperatures within the plants. This is one reason why snow melt within vegetation is poorly modeled for both models. However, for Cabauw, where only grass is found, this is of less importance.
Sensitivities of snow melt, snow depth and sublimation are rather accidental and very small. It can be said that snow depth decreases slightly with increasing vegetation. In the models, this is mainly due to higher surface temperatures. EM shows an unusual evolution in the sensitivity of snow sublimation and snow melt. Namely that the sign of this sensitivity is arbitrarily changing during the winter months. However, because relative changes are very small, this is probably of little importance, although it may show some deficiencies in the snow parameterization. For ECHAM, the evolution is smoother and sensitivity increases slightly for higher vegetation ratios.
What is the effect on runoff fluxes for changed σ_{PLNT}? Drainage and surface runoff usually increase for higher vegetation ratios (Fig. (2.21)). Only for small (and for Cabauw unrealistic) values of σ_{PLNT} do drainage (EM) and surface runoff (ECHAM) decrease. This is mainly due to the observed decrease in evapotranspiration. The additional water must be transported away by surface runoff and drainage. This is only partly true because soil water content has also changed. For EM, there is a drying of the soil for less than about 50% vegetated areas, but an

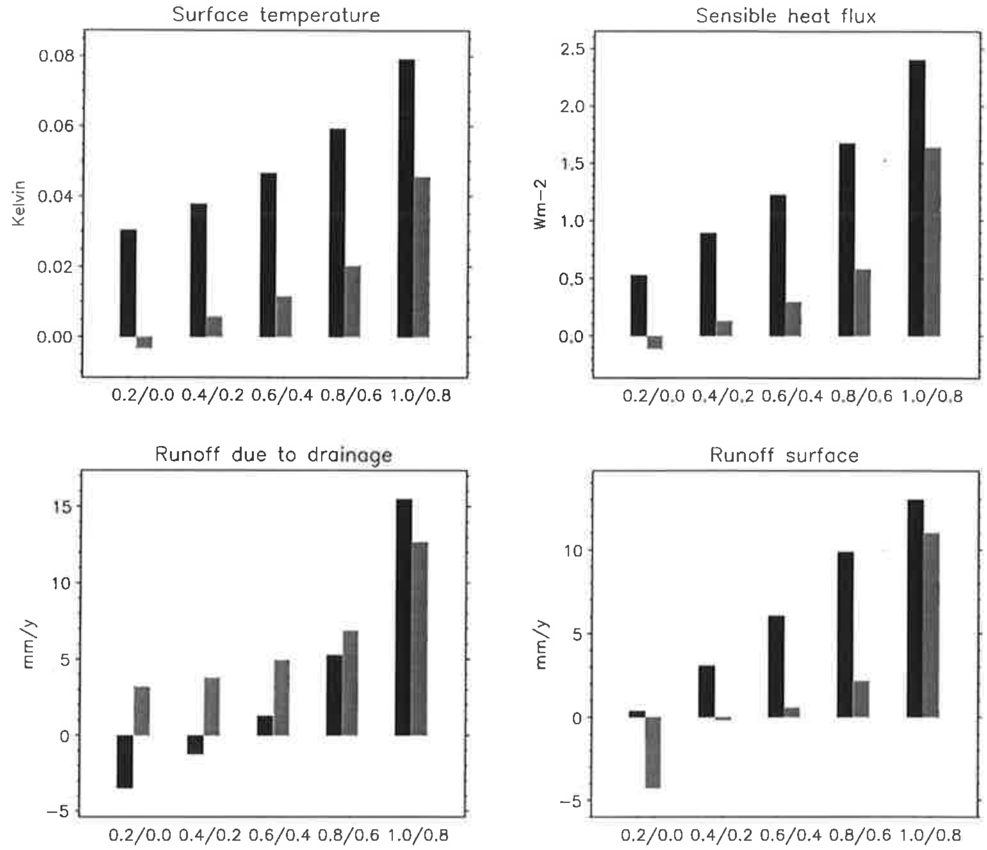

Figure 2.21: *Sensitivity of surface temperature, sensible heat flux, drainage and surface runoff to the vegetation ratio for ECHAM and EM. Values are given for a change of the vegetation ratio equal to 10%.*

increase in soil moisture for higher vegetated areas (Fig. (2.19)). ECHAM barely shows a change in soil moisture for $\sigma_{PLNT} < 0.5$ and a distinct wetting of soil for higher vegetation ratios.
The ground heat flux is slightly influenced by vegetation changes in ECHAM but is rather strongly influenced in EM. This is due to the described temperature T_U at the lower boundary. While ECHAM shows very similar sensitivities for all ground temperatures on an annual basis, the sensitivity in EM is forced to zero for a depth of about 47cm (see Fig. (2.1)). This deficiency leads to a decrease in the absolute value of the ground heat flux between σ_{PLNT}=0 and σ_{PLNT}=1.0.
Fig. (2.22) shows an overview of the sensitivities for a nearly fully vegetated grid element (what is true for Cabauw and formost of Europe). The large change of transpiration and bare soil evaporation is mainly due to the changing fraction covered with plants. It is more reasonable to look at the sum of both water vapour fluxes, which was done in a previous section. We recognize that most quantitities are more sensitive in EM. The main reason is the different parameterization of bare soil evaporation and transpiration. The simple parameterization of EM leads to a larger sensitivity than the more sophisticated one of ECHAM because less feedbacks can reduce a forced change in a land-surface parameter. In addition, the strong sensitivity of the

EM-albedo to vegetation ratio contributes to this result.

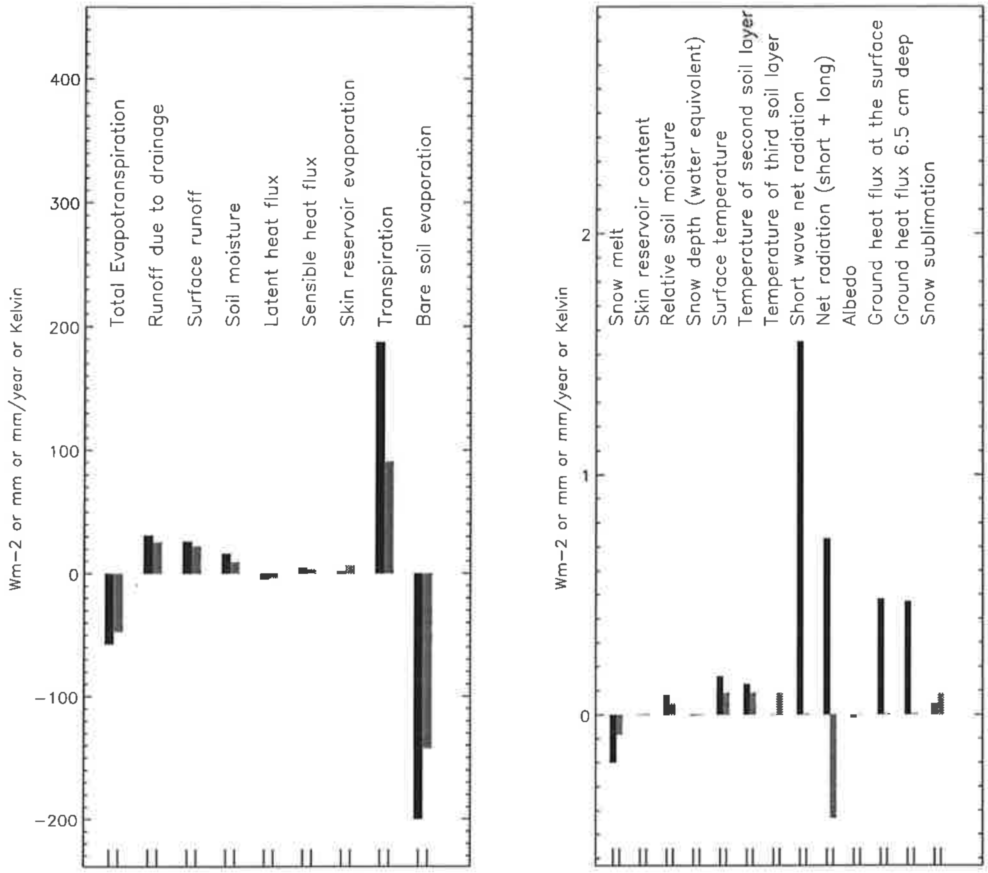

Figure 2.22: *Change of different quantities for an increase in the vegetation ratio from 0.8 to 1.0 (annual basis) for ECHAM and EM. Left bar: EM; right bar: ECHAM.*

Another graphical overview can be given comparing the ratios of sensitivities for a small and a large vegetation ratio (Fig. (2.23)). It is striking that, for most quantities such as turbulent fluxes, runoff, soil moisture or surface temperature, the sensitivity is clearly higher for larger vegetation ratios (absolute values of the bars larger than 1). It is a typical characteristic for both models that sensitivity is often increasing for more vegetated grid elements. For desert situations, the variation for a specified change in σ_{PLNT} is frequently small but there are exceptions, e.g. soil moisture (EM), net shortwave radiation (EM) or canopy evaporation (EM).

The main features of the sensitivities can be captured by annual means as has been done before. However, some interesting examples based on monthly averages are selected and presented. Namely, differences in surface runoff (for (σ_{PLNT}=1.0) - (σ_{PLNT}=0.4)) show a clear annual cycle with an amplitude of about 15mm whereas corresponding differences in ECHAM stay under 5mm during the entire year (Fig. (2.24)). The differences in drainage processes are

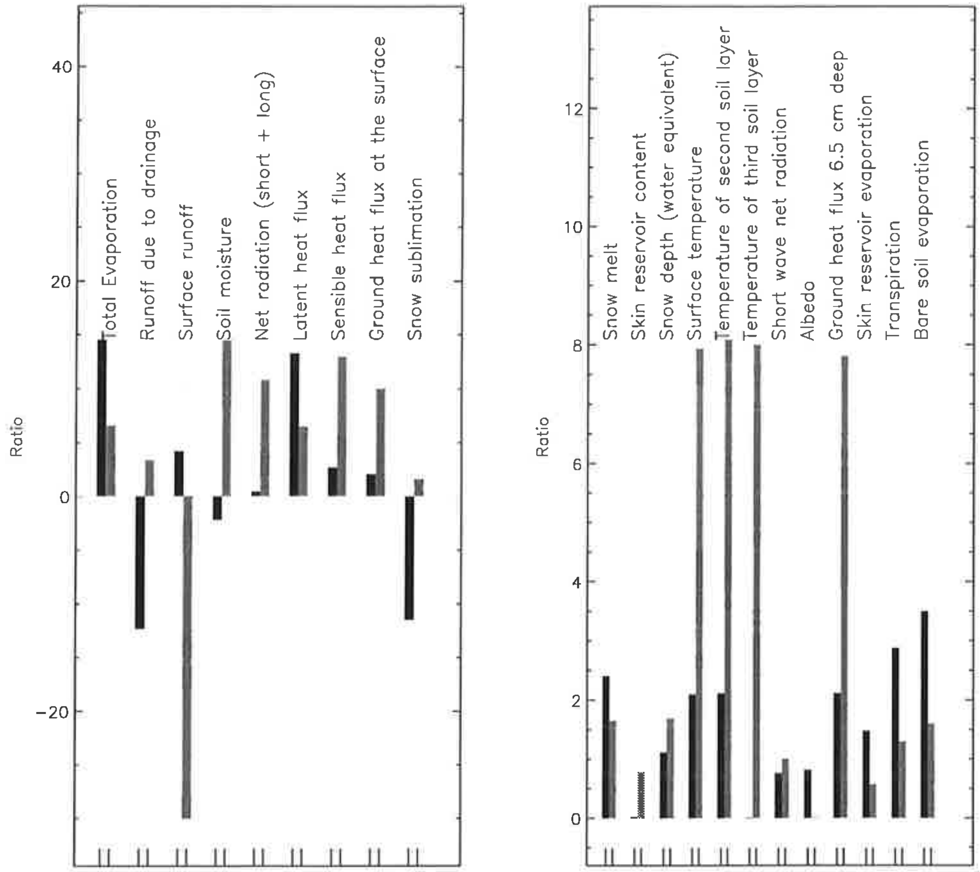

Figure 2.23: *Ratios of sensitivities for a vegetation ratio of 0.1 and 0.9 for the ECHAM and EM (annual basis). Left bar: EM; right bar: ECHAM.*

clearly smaller. This is probably due to the definition of surface runoff in EM that includes the lateral waterflow out of the uppermost soil layer whereas in ECHAM, surface runoff only increases when the soil is almost saturated. The evolution of the sum of evaporation and transpiration is striking in July (ECHAM). For the warm and sunny summer month of July, the fully vegetated grid elements produces a higher water vapour flux. The cause may be the high net shortwave radiation which favours transpiration more than bare soil evaporation. EM does not show this feature because its simple parameterization does not take into account the photosynthetically active radiation (PAR). The same peak is visible for latent heat flux, but is in the opposite direction for sensible heat flux. The albedo of EM shows a clear annual cycle. This is due to the evolution of soil moisture. Its difference between σ_{PLNT}=0.4 and σ_{PLNT}=1.0 is close to zero in winter but approaches 30mm in early summer. Moreover, it is interesting that the plot of the differences of soil moisture shows a phase lag of one to two months (Fig. (2.24)). The EM already reaches the maximum of the difference in April while the ECHAM model is one month later. Moreover, it is evident that the sensitivity of soil moisture during winter, spring and autumn is higher in the weather forecast model. This is a consequence of the evolution of

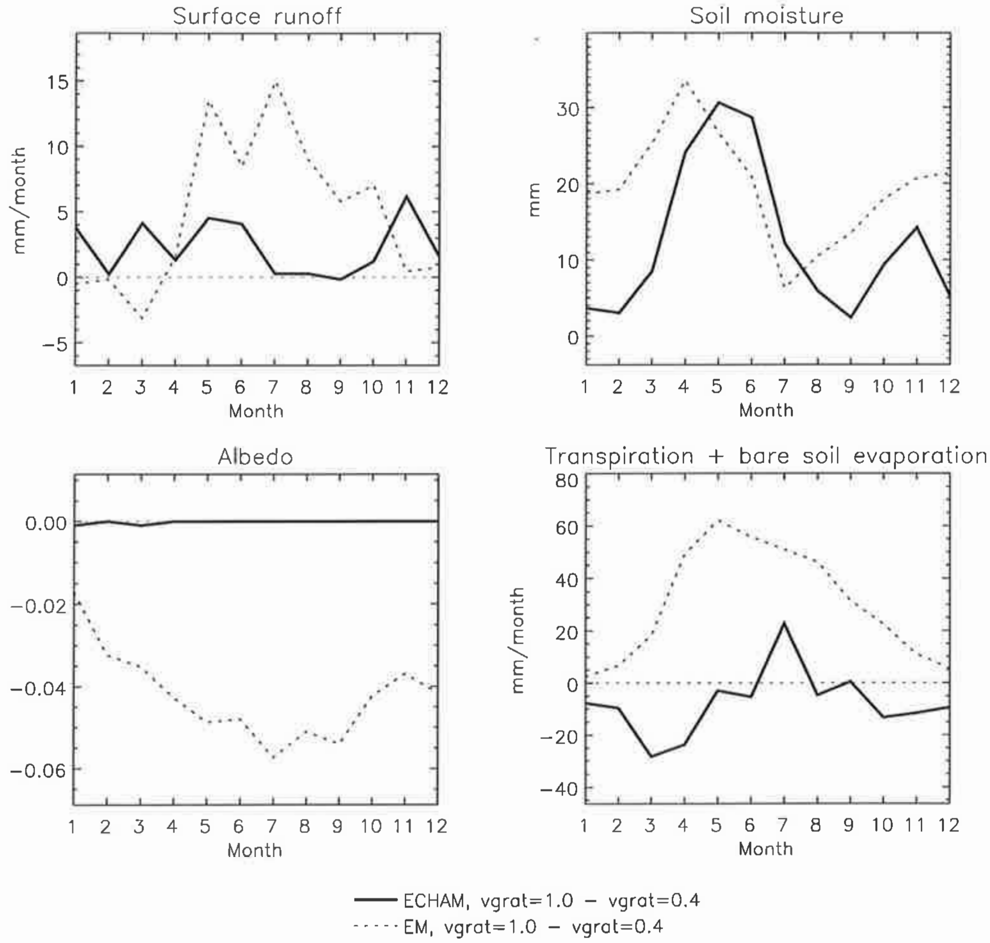

Figure 2.24: *Differences of albedo, soil moisture, surface runoff and the sum of transpiration and bare soil evaporation for the vegetation ratio (vgrat) equal to 0.4 and 1.0 for ECHAM and EM on a monthly basis.*

latent heat flux and runoff.

Naturally, day and nighttime values can be calculated separately. Day is defined as the period where the net shortwave radiation exceeds $2 \mathrm{Wm}^{-2}$. The ratios for the standard case were previously discussed. An overview of how a change in the vegetation ratio changes the annual ratio of day and night values is given in Table (2.3). The first two columns contain the ratio of day and night annual averages for a vegetation ratio of 0.9 in both models. The next two columns depict the quotient computed for a vegetation ratio equal to 0.9 and 0.3, respectively. What do we learn? This ratio shows little change for low and fully vegetated areas (a value equal to 1 in the third and fourth columns indicates no change). Whereas the absolute values change very strongly, the partition in night- and daytime does not significantly change. The only quantity which shows a large change in the day and night distribution for different values of σ_{PLNT} is the sensible heat flux. A more careful examination shows that the annual average of sensible heat flux at day increases rather strongly with higher vegetation ratios. This increase is more distinct for EM since the sensible heat flux is reflected in a higher ratio in the fourth column compared to the third column of Table (2.3). The reason is the increasing temperature caused by lower evapotranspiration, and the fact that sensible heat flux is very sensitive to changes in surface temperature.

Table 2.3: *Ratio of day and nighttime annual means for ECHAM and EM for a vegetation ratio equal to 0.9 and the quotients of the ratios of day and nighttime annual means for* σ_{PLNT}*=0.3 and* σ_{PLNT} *=0.9.*

parameter	**ECHAM vgrat=0.9**	**EM vgrat=0.9**	**ECHAM vgrat=0.9 / vgrat=0.3**	**EM vgrat=0.9/vgrat=0.3**
total evaporation from surface	8.3	10.2	1.13	1.06
latent heat flux	7.4	10.9	1.12	1.04
sensible heat flux	-1.4	-2.1	1.51	2.30
evaporation (skin reservoir)	3.13	1.80	0.97	1.03
transpiration	15.2	12.7	0.99	0.99
bare soil evaporation	6.9	14.5	0.87	1.29
skin reservoir content	0.78	0.86	1.02	0.99
soil moisture	0.93	0.99	1.01	1.00
ground heat flux at the surface	-0.91	-0.60	1.00	1.13
snow melt	2.47	1.48	1.08	1.04
snow sublimation	1.01	1.60	1.00	0.99
snow depth	0.51	0.51	1.00	1.00
net radiation	-3.1	-3.4	0.99	1.04
runoff due to drainage	0.88	0.86	1.03	1.12
surface runoff	0.84	0.77	0.98	1.15
albedo	0.96	0.92	1.00	0.96

Interesting features can be detected by plotting the mean diurnal cycles of each month. Most quantities show rather smooth curves and the typical diurnal cycle expected for radiation and soil temperature, transpiration, bare soil evaporation, latent and sensible heat flux and ground heat fluxes. Figure (2.25) shows an example of the canopy evaporation which depicts a totally different characteristic in both models. In addition to the large difference in the averages, there is a different evolution during day. Neither the corresponding curves of net shortwave radiation nor wind speed or precipitation can explain the fluctuating curves of ECHAM. Actually, high values are expected for a period with high net shortwave radiation and wind speed after rainfall. Values at night are usually smaller than at day which fits with higher wind speed and net radiation during the day.

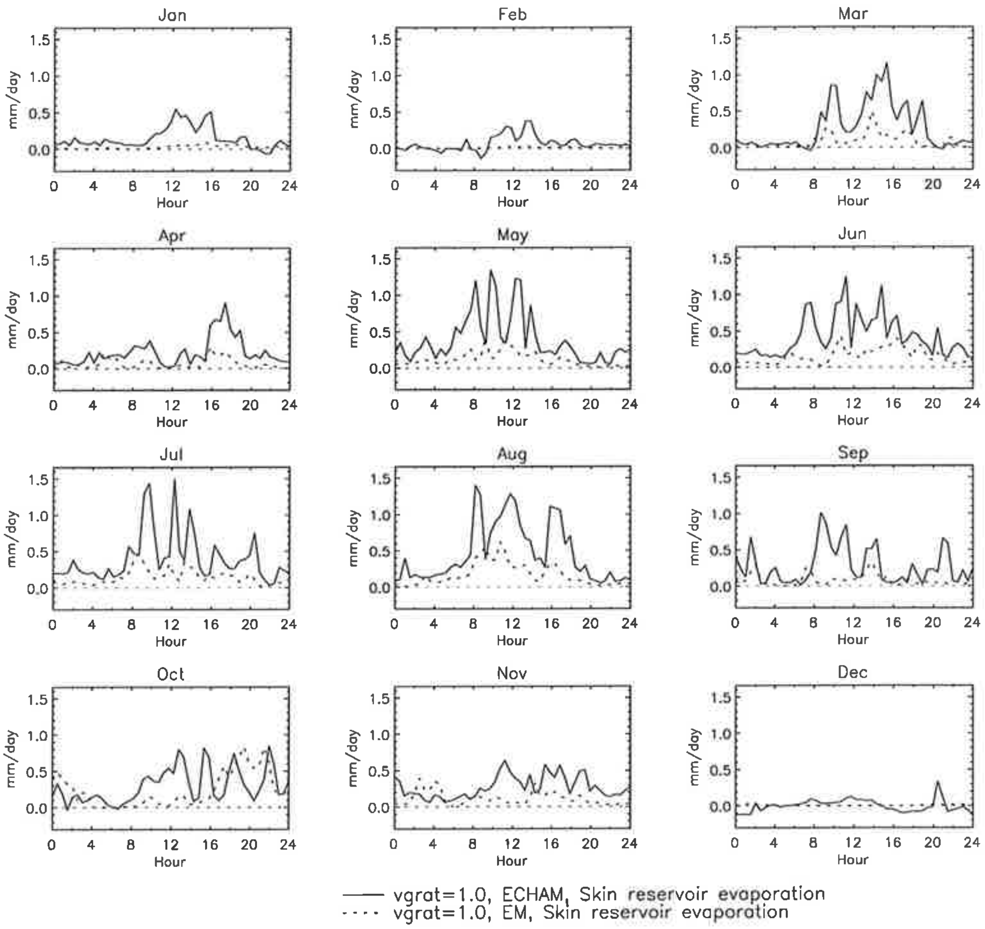

Figure 2.25: *Monthly averages of diurnal cycles of skin reservoir evaporation for a fully vegetated grid element for ECHAM and EM.*

2.5 Sensitivity to the albedo

The albedo is one of the most important parameters in climate models. It gives the ratio of reflected and incoming shortwave radiation. The albedo of ground surfaces is dependent on wave length. Some models fix different albedo values for wave lengths larger and smaller than 0.7 micrometers because green vegetation exhibits a strong increase in reflectance between the visible range and the near-infrared region. For example in BATS (Dickinson et al., 1993), the canopy albedo is about 0.10 for $\lambda < 0.7$ micrometer, but is taken as 0.30 for higher wavelengths. For freshly fallen snow, the corresponding values are 0.85 and 0.65. However, in both models there is no distinction in the value of the albedo for different wave lengths and therefore, an average albedo must be assumed. In spite of many measurements of albedo, the technique of remote sensing is currently not able to determine exact values for a whole grid element. Satellite measurements require radiation models to obtain surface albedos. Tower measurements of shortwave radiation fluxes determine the albedo only for a small limited area, but aeroplane measurements are rather expensive. While aircraft measuremnets have been applied during different experiments, the interpretation of data is not simple.
The sensitivity of net shortwave radiation to albedo is simple; the higher the albedo, the lower the net shortwave radiation. For both models, the derivative is ΔS_{net}=11Wm^{-2} for $\Delta\alpha_{surf}$=0.1 (Fig. (2.26)) and the sensitivity is constant for any albedo. The sensitivity of the net long and shortwave radiation is somewhat smaller. The reason is a negative feedback, i.e. the higher the albedo, the lower the absorbed radiation and the heating of the surface. This again leads to a lower upward directed longwave radiation according to the Stefan Boltzmann-Law

$$\frac{\delta LW_{\uparrow}}{\delta T_S} = 4\sigma {T_S}^3 \tag{2.12}$$

with

$LW_{\uparrow}$	Upward directed longwave radiation [Wm^{-2}]
T_S	Surface temperature [K]
σ	5.669 x 10^{-8} Wm^{-2} K^{-4}

which yields approximately 3.1Wm^{-2}K^{-1} for T_S=240K and 6.8Wm^{-2}K^{-1} for T_S=310K. For temperatures usually measured at Cabauw, this amounts to about 1Wm^{-2} for ΔT_S=0.2°C. The sensitivity of surface temperature to albedo is very strong and is more than -0.2°C for $\Delta\alpha_{surf}$=0.1. The sensitivities are very similar in ECHAM and EM. ECHAM shows a slight increase in the sensitivity whereas EM has an almost constant sensitivity. ECHAM shows no change in sensitivity for the ground temperature (annual basis) whereas for EM, the sensitivity of soil temperature rapidly decreases with depth because of the described lower boundary condition for the temperature T_U.

All turbulent heat fluxes contain the heat transfer coefficient C_h, which is dependent on stability. Since the temperature of the first (atmospheric) layer is held constant, the sensitivity of C_h with respect to temperature is only dependent on the surface temperature. The derivative is depicted (for a typical wind speed of 2ms^{-1} and a temperature of 15°C) in Fig. (2.27). The lower the temperature difference dT between the first atmospheric layer (supposed to be at a height of 30m) and the surface, the more unstable the conditions. The bend of the curve at the value of roughly dT=-0.3K is due to the change from unstable to stable conditions. This value is not equal to zero due to the not vanishing wind shear. We recognize that the derivative is negative and on average of the order of -0.01/K. The sensitivity decreases for both increasing stable and unstable conditions. The largest sensitivity is found near neutrality. Since higher albedos lead to lower temperatures and more stable conditions, the factor C_h decreases with higher albedo. The lower two pictures in Fig. (2.27) present the derivative of potential evaporation with respect to the surface temperature T_S. The derivative of potential evaporation (Eq. (1.42)) is

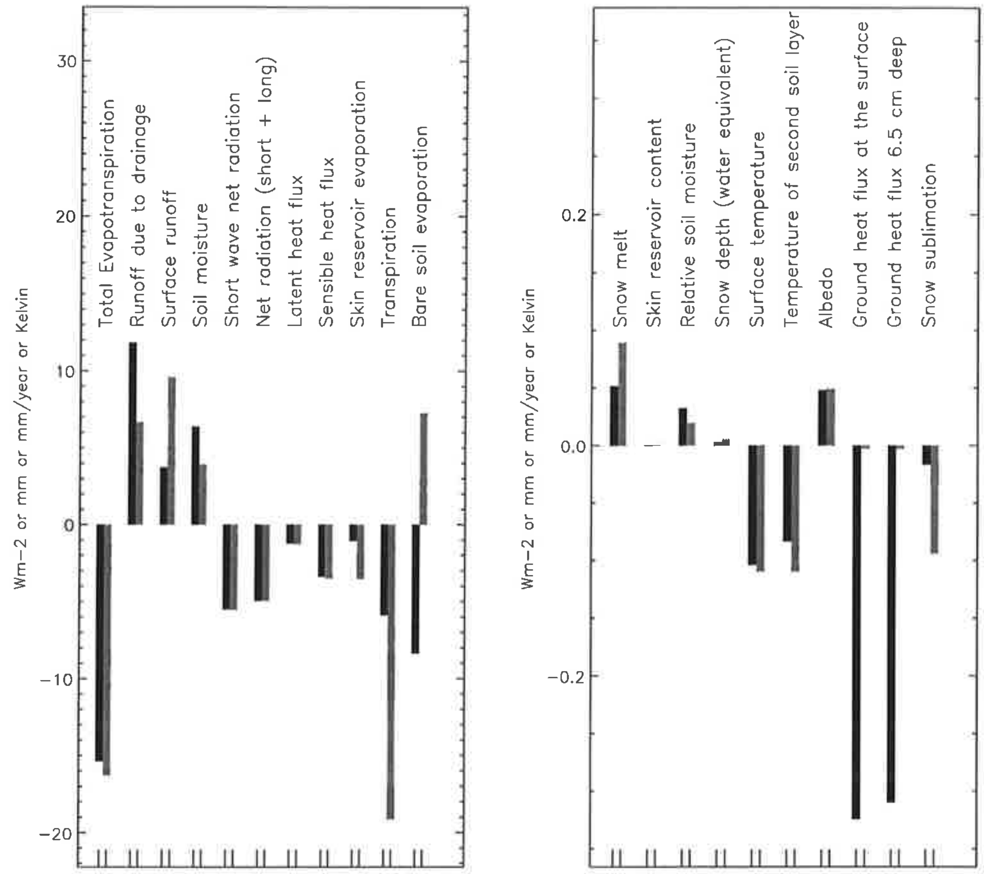

Figure 2.26: *Change of different quantities for an increase in the albedo from 0.15 to 0.2 (snow free conditions, annual basis) for ECHAM and EM.*

$$\frac{J_{q_v}}{dT_S} = \rho|v_h| \left[\frac{dC_h}{dT_S}(q_v - q_{sat}) + C_h \frac{dq_{sat}}{q_v}\right] \tag{2.13}$$

with all symbols as in Equation (1.42).

It can be seen that the potential evaporation decrease is of the order of $5\mathrm{Wm}^{-2}\mathrm{K}^{-1}$. If one remembers that an albedo change of 0.1 leads to dT_S =0.2°C, a corresponding variation of $1\mathrm{Wm}^{-2}\mathrm{K}^{-1}$ is expected. The model simulations, however, give a value of roughly the double, although this is in the possible range. This value is of course strongly dependent on stability conditions. The same value is calculated neglecting the temperature dependence of C_h and setting C_h=0.004 and T_S=280K. For EM, where transpiration and bare soil evaporation is parameterized by a factor times the potential evaporation, a decrease of transpiration and bare soil evaporation with raising albedo is expected. This is confirmed with model simulation (Fig. (2.28)). A crude estimation of the sensitivity of sensible heat flux gives the same value. However, the value can fluctuate over a wide range for different transfer coefficients and stability.

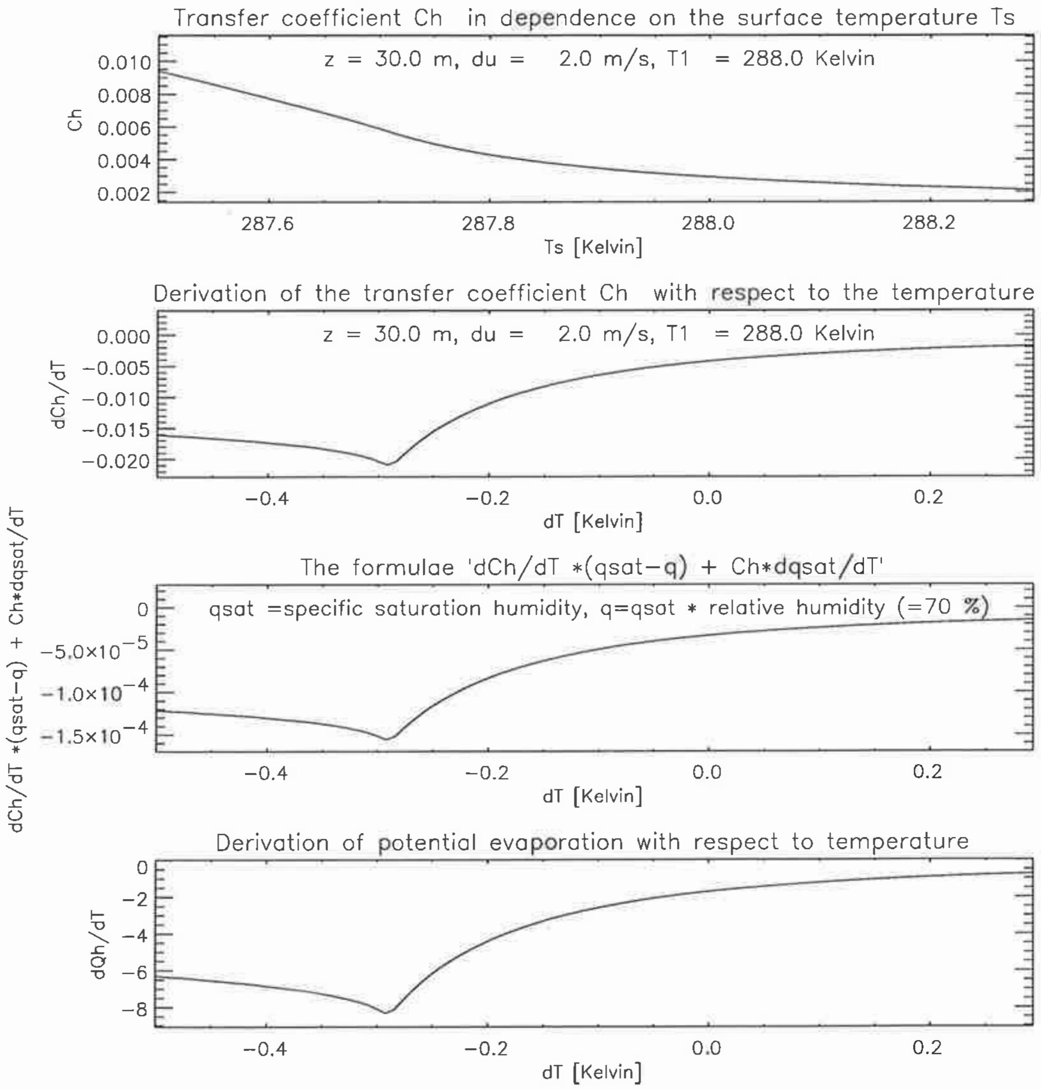

Figure 2.27: *Transfer coefficient C_h and derivative of C_h and potential evporation with respect to temperature (Louis parameterization was applied). Derivation of potential evaporation in $Wm^{-2}K^{-1}$. The temperature T1 at the lowest atmospheric model level at a height of z=30m above the ground is held constant whereas the surface temperature Ts has been varied. For all calculation the windspeed at z=30m is set equal to $2ms^{-1}$. For computation of the specific saturation humidity the Magnus formula has been applied.*

The ground heat flux in ECHAM shows a minimal change because temperature changes in the soil closely follow the variation of surface temperature. The EM produces a higher mean annual downward ground heat flux with higher albedos because of lower temperatures. The higher the temperature gradient, the higher the heat transport trying to compensate for the temperature difference. The simplified equation of the ground heat flux (Eq. (1.13)) can be applied to calculate an approximate derivative of the ground heat flux G_{MB} with respect to the surface temperature T_S. This yields

$$\frac{dG_{MB}}{dT_S} = -8.8 \ \mathrm{Wm^{-2}K^{-1}} \tag{2.14}$$

with the symbols as in Equation (1.13). Since an albedo change of 0.1 leads to a temperature change of about 0.2°C, a change of G_{MB} of about $2\mathrm{Wm^{-2}}$ is expected. The model experiments only produce a change of $0.6\mathrm{Wm^{-2}}$. This is because the surface temperature and the temperature at the boundaries of the upper and lower soil layer is changed.

What are the results of the model simulations? Some quantities have already been discussed. However, some other specialities are worth mentioning. For example, the latent and sensible heat flux decrease with increasing albedo. The sensitivity of the latent heat flux raises rather distinctly with higher albedos whereas the opposite is true for sensible heat flux (Fig. (2.28)). The reason is the lower surface temperature and so the decreased turbulence.

Transpiration strongly decreases with increasing reflection of shortwave radiation because a lower surface temperatures induces a lower transfer coefficient C_h and so a lower potential evaporation. In addition less radiation is left for photosynthesis of leaves. For low albedos, the sensitivity is more than three times larger in ECHAM than in EM (Fig. (2.28)). The decrease of transpiration with increasing albedo is due to the decrease of the transfer coefficient C_h and the potential evaporation. The larger sensitivity of transpiration in ECHAM is probably due to the more sophisticated parametererization of transpiration, i.e. the photosynthetically active radiation which is included in the definition of the stomatal resistance becomes lower with increasing albedo. Moreover, the evaporation efficiency E contains the transfer coefficient and intensifies the decrease of transpiration.

An unusual characteristic is found for bare soil evaporation (Fig. (2.28)). While the EM shows the expected characteristic, namely a decrease with higher albedo values, ECHAM produces an increase. The weaker turbulence due to enhanced reflection is more than compensated by the higher soil moisture caused by the smaller transpiration rates. Further, higher soil moistures lead to higher bare soil evaporation due to an increase in the relative humidity h (Eq. (1.44)).

Runoff at the surface and drainage try to compensate the higher soil moisture which is caused by diminished latent heat flux. It is worth mentioning that the EM transports the additional water away by increasing drainage while for ECHAM surface runoff is more efficient. This is surprising, because the EM surface runoff also includes runoff out of the uppermost soil layer. A reason may be a too fast infiltration of water by gravity. ECHAM, on the other hand, has a rather efficient parameterization to produce surface runoff for soil moisture near saturation. Namely the fractional saturated area, which is defined in Equation (1.19), rapidly increases for nearly saturated soils. This is shown in section (2.7).

In ECHAM, the skin reservoir becomes fuller for higher albedo values. This is due to reduced turbulence, and therefore a smaller potential evaporation. The skin reservoir of EM is barely influenced because all available water infiltrates rapidly into the soil. Snow depth and snow melt slightly increase with more reflection from snow free areas because lower temperature reduces snow melt. The sensitivity is higher for ECHAM. This is probably due to the possibility to redistribute heat in the snow pack and the upper soil layer in the EM representation of snow and snow melt. This mechanism is able to slow down changes forced by a changed net shortwave radiation.

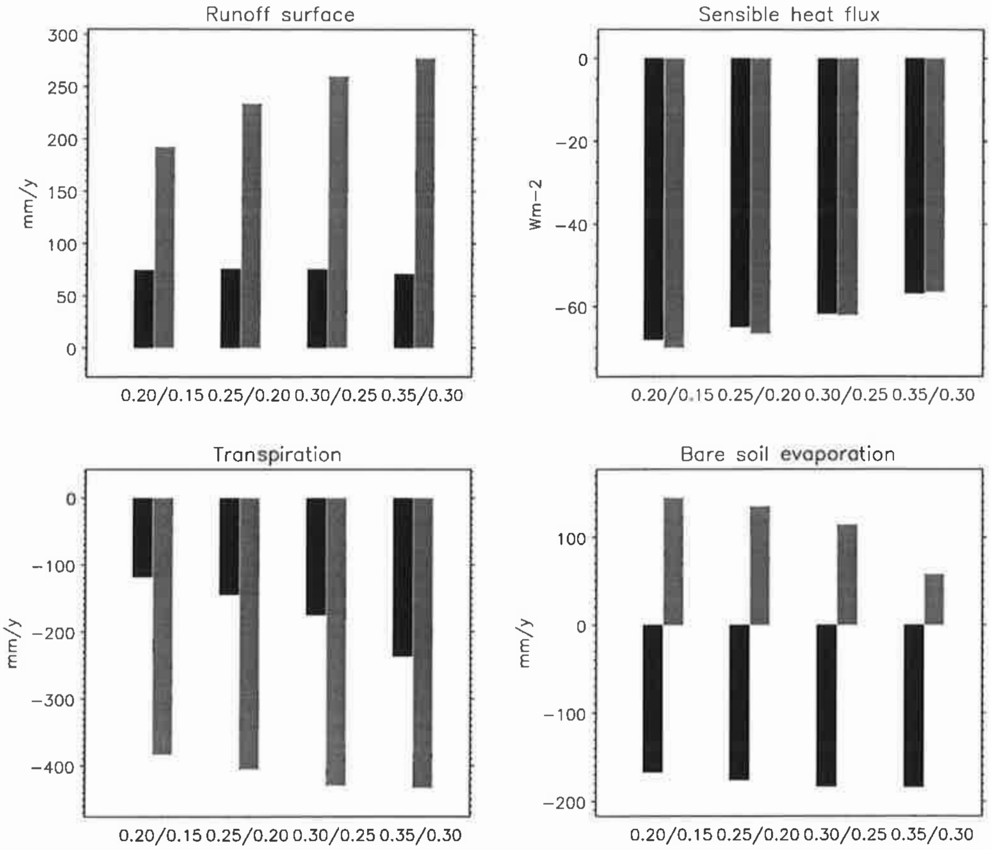

Figure 2.28: *Sensitivity of annual means for different values of albedo (comparison of ECHAM and EM). The x-axis labels indicate the albedos used in the model runs to calculate the height of the presented bars. Left bar: EM; right bar: ECHAM.*

The sensitivity to albedo is dependent on the month. Both models respond very differently on changes of the reflectivity. This is shown in Fig. (2.29) where some differences for albedo values α_{surf}=0.15 and α_{surf}=0.35 are shown. The evolution of bare soil evaporation is striking. Whereas during winter, with near saturated soils, the difference is small and similar for both models, during summer and autumn, the sensitivity has an opposite sign and is distinctly larger for ECHAM. EM produces less bare soil evaporation for higher albedos because of lower turbulence. Soil moisture is of minor importance in EM because the soil is well saturated over the year. ECHAM however shows an opposite characteristic. The increasing soil moisture is obviously more important than the decrease in turbulence.

In both models, transpiration shows a similar evolution during the period from November to June. However, for late summer, EM is much less sensitive to albedo changes than ECHAM. The reason is probably the incapacity of the EM-parameterization to profit on high net shortwave radiation while ECHAM includes a strong dependence on the photosynthetically active radiation (PAR).

The separation of runoff into surface runoff and drainage is also different in the models. While (albedo) sensitivity of drainage is larger in EM during the first half of the year, ECHAM shows a

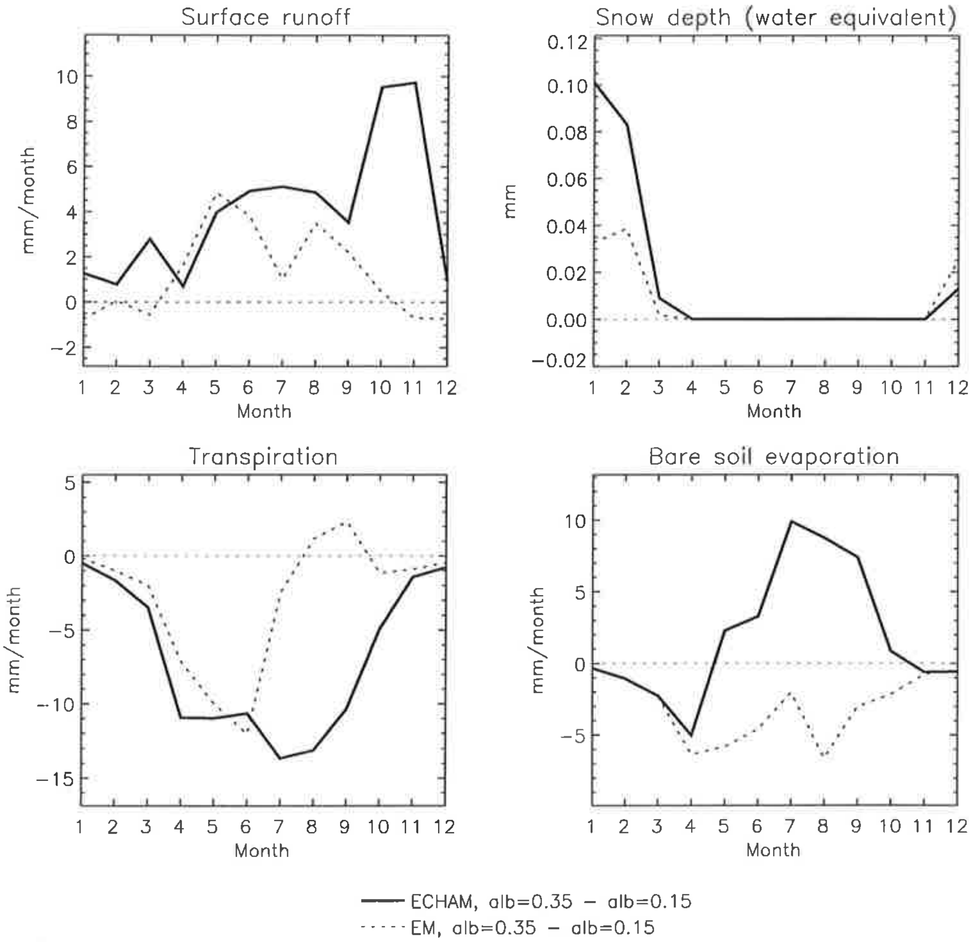

Figure 2.29: *Differences in surface runoff, snow depth, transpiration and bare soil evaporation for albedo equal to 0.15 and 0.35 for ECHAM and EM (monthly basis).*

higher sensitivity of surface runoff from June to March. The especially high sensitivity for October and November is due to the occurence of 'fast drainage', i.e. whereas the soil moisture for an albedo of 0.15 is clearly lower than 90% (the threshold value for slow/fast drainage in ECHAM), this value increases above this threshold in autumn. The higher sensitivity of drainage to albedo in EM is due to the well saturated soil which forces the model to produce lateral outflow. The EM-parameterization generates a flow out of soil layers which linearly increases from the field capacity up to the volume of pores. Further, during the period January to May, soil moisture lies above field capacity for all tested values of albedo. The absolute sensitivity of soil moisture is relatively constant in EM whereas ECHAM barely shows any sensitivity during the period with almost saturated soils (November to March). During summer and autumn, sensitivities of both models are similar.

Snow depth, and therefore snow melt, and snow sublimation changes are about 1% for a change of α_{surf}=0.15 and α_{surf}=0.35. However, sensitivity in both models differs by a factor of about three in January, although ECHAM is more sensitive. This is probably due to the capability of EM to redistribute heat in the snow pack and the uppermost soil layer. This algorithm is able to better compensate forced changes of climatological input. It is interesting that the total grid element albedo is forced to respond more in EM inspite of smaller snow changes. The reason is

the much higher change of snow covered fraction for the same change in snow water equivalent in EM for small snow depth (see Fig. (1.3)).
Ground heat fluxes show a higher sensitivity during the warmer season. This can be explained with a larger absolute change of net shortwave radiation and therefore surface temperature. As mentioned several times before, the ECHAM model has very similar sensitivity for the surface temperature and the upper three soil layers (also on a monthly basis) and therefore ground heat fluxes barely change with modified albedos.
The rather similar sensitivities of latent and sensible heat fluxes are surprising. The largest difference is observed in early summer (May and June). This can be attributed to the characteristic of transpiration. Changes in sensible heat flux are similar in both models in accordance to similar sensitivities of surface temperatures.
An overview of the ratio of the sensitivities on an annual basis is given in Figure (2.30). It can be recognized that most bars have lengths over 1. This means that the sensitivity is increasing with higher albedos. However, most quantities do not change their sensitivities by more than a factor of 1.2. Therefore, it can be stated that in a first approximation, sensitivities are reasonably constant for most quantities on an annual basis. The analysis of the sensitivities on a monthly basis shows distinctly different features.

Table (2.4) shows the distribution of day and night averages for different surface reflectances. Since albedo modifications induce net shortwave radiation changes only during the day, albedo induced changes concern only daytime values. This statement is especially true for fast responding quantities such as water vapour fluxes and sensible heat flux. Ground heat fluxes also show a certain sensitivity during night. Runoff processes (and soil moisture) show similar sensitivities for day and night because they are inert and do not significantly follow the diurnal cycle of incoming shortwave radiation.

Table 2.4: *Daytime annual means divided by the nighttime annual mean. The first two columns presents this ratio for an albedo of 0.15. The last two columns depict the quotients of the ratios of day and nighttime annual means for model simulation with* α_{surf}*=0.15 and* α_{surf}*=0.35.*

parameter	**ECHAM** α**=0.35**	**EM** α**=0.35**	**ECHAM** α**=0.35 /** α**=0.15**	**EM** α**=0.35/**α**=0.15**
total evaporation from surface	7.7	10.1	0.94	0.91
latent heat flux	6.9	11.4	0.94	0.94
sensible heat flux	0.3	-0.8	-0.24	0.31
evaporation (skin reservoir)	3.1	1.6	1.00	0.88
transpiration	14.0	15.9	0.92	0.98
bare soil evaporation	7.3	11.8	1.06	0.84
skin reservoir content	0.8	0.86	1.04	1.00
soil moisture	0.95	0.97	1.03	1.01
ground heat flux at the surface	-0.91	-0.54	1.00	0.84
snow melt	2.0	1.1	0.76	0.78
snow sublimation	0.9	1.6	0.84	0.96
snow depth	0.5	0.5	1.01	1.00
net radiation	288.1	240.0	0.72	0.71
runoff due to drainage	0.84	1.00	0.96	1.02
surface runoff	0.84	0.88	1.00	1.07

Strong changes in the day and night distribution of sensible and latent heat fluxes are linked with the influence of shortwave radiation on surface temperatures and stability. During the night, hardly any change is established because turbulent fluxes are fast responding quantities, and are typically very low during night. Figures in the third column of Table (2.4) are less than 1 for all turbulent fluxes with exception of the bare soil evaporation in ECHAM because turbulence is weaker for higher albedos. The value for the sensible heat flux in the third and fourth column should be analysed because they are low compared to the other listed figures.

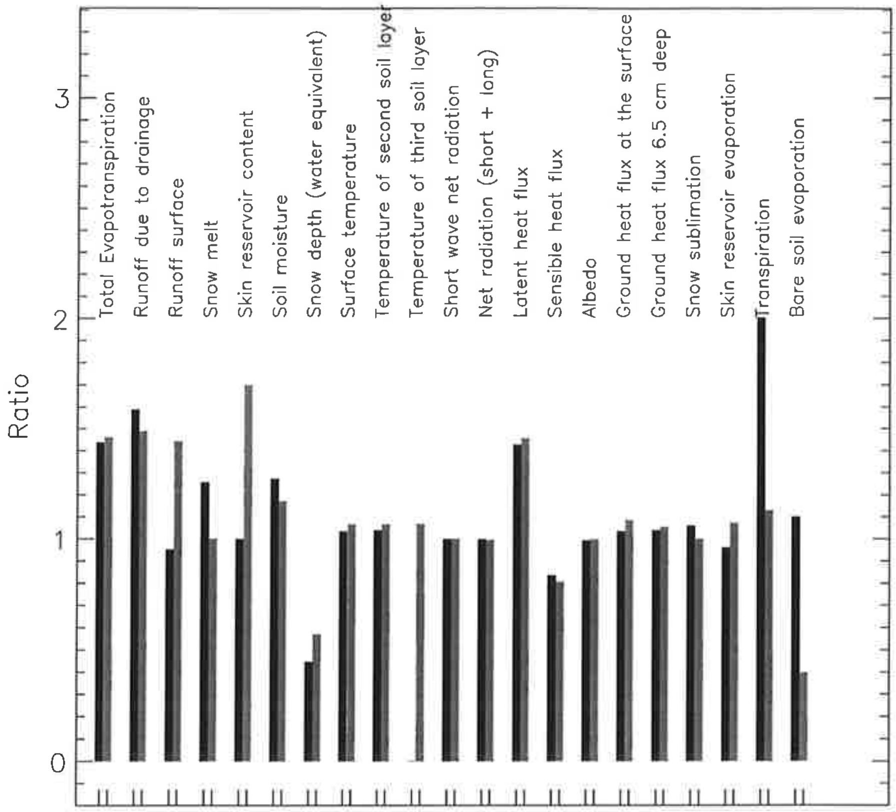

Figure 2.30: *Ratio of sensitivity for a surface albedo of 0.18 and 0.32. Black bars: EM; Grey bars: ECHAM.*

This is caused by the strong decrease of the sensible heat flux during the day with increasing albedo. In EM, the annual daytime sensible heat flux amounts to about 35Wm^{-2} for α_{surf}=0.15 and decreases to little more than 10Wm^{-2} for α_{surf}=0.35. ECHAM even produces a negative flux during the day for albedos above 0.3. For EM, this threshold is only reached for $\alpha_{surf} > 0.42$.

2.6 Sensitivity to the albedo of snow

Snow cover in Cabauw occurs infrequently. By far the most frequent snow cover occured in January (9 days 1-2cm closed snow cover and 6 days with a patchy snow cover). Therefore, the following results are limited to January. Since the first snowfall occurs on January 7 and the last on January 21, the snow water balance must only be correct for January. This means that snow fall is balanced by the sum of snow melt and snow sublimation because the snow pack of the last snow fall on January 21 has melted on the following day.

Although there is only a thin snow cover, interesting conclusions can be drawn. It should be emphasised that this January represents a typical winter month for a large part of Western Europe, including the Swiss midland.

The equations for snow albedo have been discussed in Chapter (1.3). The dependence on the fractional forest area a_f in ECHAM has no influence in this study because a_f=0 for all experiments. The temperature dependence of snow albedo in ECHAM is for non forested grid elements 0.04/Kelvin in the range of 263.15K $< T_s <$ 273.15K. However, the temperature dependence of snow albedo has been switched off for the experiments with varied snow albedo. Therefore, all the observed changes must originate from the calculation of total surface albedo (Formulae (1.34) and (1.37)). A key position has the computation of the snow covered fraction of the grid element which is very different in both models. However, the influence is large only for thin snow packs and decreases for thick snow packs over the critical snow water equivalents of 10 - 15mm.

The two models show large differences in the sensitivities of most quantities with respect to the snow albedo (Figure (2.31)). The figure shows the relative changes of 15 quantities for a change in snow albedo (α_s) from 0.6 to 0.7. Relative sensitivities are presented because in January, absolute values of radiation, and therefore turbulent heat fluxes, are small. The bar of sensible heat flux for ECHAM is cut off and should be close to 100%. However, the absolute change is minor because the annual mean of sensible heat flux for α_s=0.7 is close to zero.

The total surface albedo α_{surf} increases from about 0.21 (α_s=0.5) to 0.29 (α_s=0.9) in ECHAM. The corresponding values for EM are 0.31 and 0.52. Thus, the sensitivity of EM is about three times higher than in ECHAM. This characteristic can be illustrated by plotting the derivatives of α_{surf} with respect to the snow albedo. In Fig. (2.32), the ratio of the sensitivities of both models is presented. The thicker the snow pack, the closer the sensitivities of both models. The typical snow depth at Cabauw of 1cm corresponding to roughly 2-3mm water equivalent. The graphic gives a ratio of about one third, i.e. the EM has an about three times higher sensitivity than ECHAM. This is in reasonable agreement with the results from model simulations, and proves the supposition that the calculation of the snow covered fraction is the main difference in snow parameterization (for a location with only thin snow decks). A model experiment where the parameterization of the snow covered fraction of ECHAM is built in EM gives similar results, i.e. the sensitivity of α_s is reduced by a factor of 2.5. The sensitivity is rather constant for the entire examined range of snow albedo.

The following conclusions are similar as in Section (2.5). The sensitivity of the surface albedo directly influences the net shortwave radiation. The higher the albedo, the lower the net shortwave radiation. The change is close to 0.5Wm^{-2} for $\Delta\alpha_s = 0.1$ in ECHAM and slightly more than 1.5Wm^{-2} for $\Delta\alpha_s = 0.1$ in EM. The lower the net shortwave radiation, the less energy is available for heating the soil. This leads to a cooler surface temperature. However, whereas the sensitivity of the ECHAM surface temperature is almost constant and only slightly more than 0.01K for $\Delta\alpha_s$=0.1, the EM shows a rather strong increase of up to almost 0.1K per $\Delta\alpha_s$=0.1 for α_s=0.9. In a three dimensional run differences may be higher because of the positive feedback, i.e. more snow implies a lower surface temperature which induces more precipitation falling as snow. This feedback is not taken into account using the models in an off-line mode with prescribed forcing.

The parameterization of turbulent heat fluxes is also important. The more sophisticated pa-

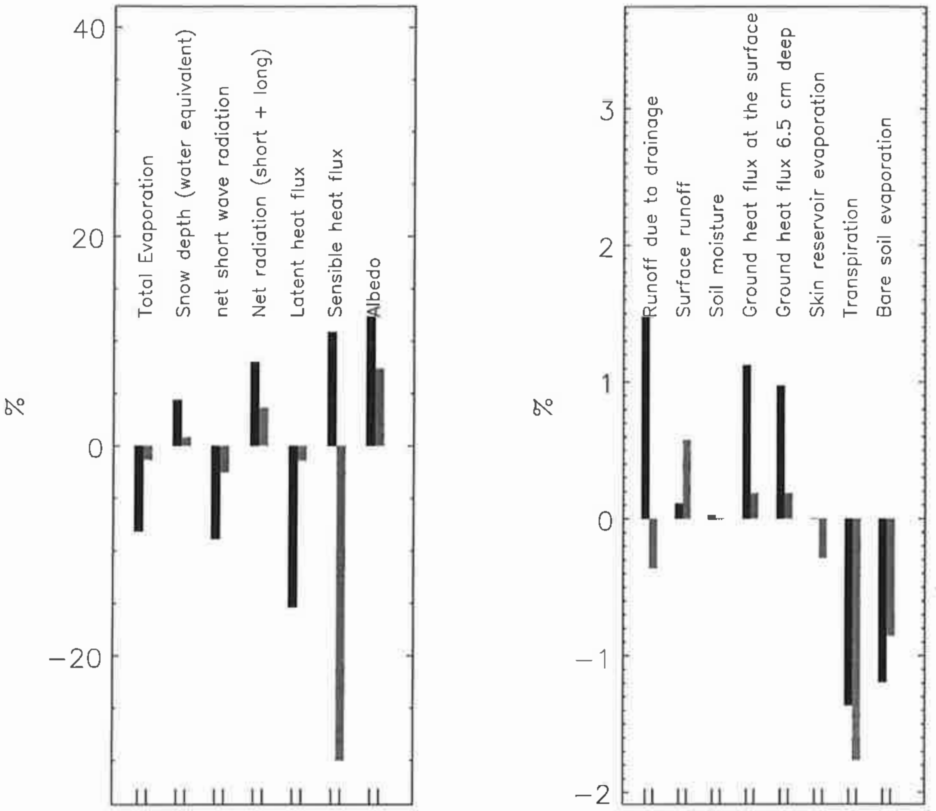

Figure 2.31: *Change of January averages for a change of surface albedo from 0.6 to 0.7 for ECHAM and EM. The %-specification relate to the values for a snow albedo equal to 0.7. The bar for the sensible heat flux (ECHAM) has been cut off and is close to 100%. Black bars: EM; Grey bars: ECHAM.*

rameterization of water vapour fluxes in ECHAM could be the reason that changes in surface temperature are faster and more efficiently balanced. Transpiration, for example, includes a dependence on radiation and so a lower net shortwave radiation leads to a reduced transpiration and therefore, a reduced cooling of the surface.
The soil heat flux at the surface and at a depth of 6.5cm shows a constant and small sensitivity in ECHAM whereas EM has a clearly higher sensitivity for higher values of α_s. The ratio of the sensitivities at the lower and upper range of α_s is greater than 2 (see Fig. (2.33)). This characteristic is due to the described temperature T_U in EM.
Transpiration is more sensitive in ECHAM than in EM. This is due to the dependence on the shortwave radiation in the ECHAM parameterization of transpiration. Model simulation for different values of the photosynthetically active radiation (PAR) (not shown) give a change in the transpiration rate of the order of 10% for Δ PAR=5Wm^{-2}. The soil moisture is not a limiting factor for tranpiration in January. Changes in transpiration can also be caused by

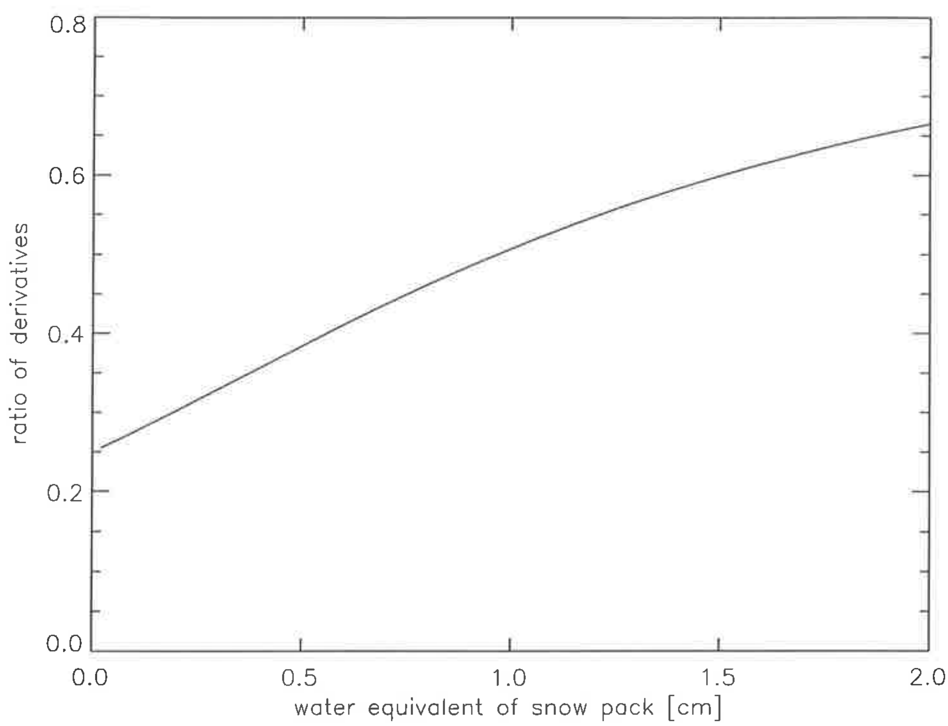

Figure 2.32: *Ratio of derivatives of total surface albedo with respect to snow albedo of ECHAM and EM.*

changed surface temperature, i.e. the cooler the surface, the lower the turbulence and therefore, the water vapour fluxes. This explains the decrease in transpiration, bare soil evaporation and snow sublimation with increasing snow albedo. It is straightforward that the lower surface temperature leads to a larger downward directed sensible heat flux because more stable situations will be found.

Since no snow is observed in the beginning and end of January, the increasing snow depth with increasing snow albedo must be balanced by a higher melting rate. In addition, less snow is transported away by sublimation due to weaker turbulence.

The lower evaporation for higher snow albedos applies a higher soil moisture content. Therefore, a higher runoff can be expected. This is true for both models but the distribution of the additional runoff into surface runoff and drainage is totally different. Whereas the sensitivity of surface runoff is much larger in ECHAM, the opposite is true for drainage. The reason for the high sensitivity of surface runoff in ECHAM is that, for nearly saturated soils, almost all precipation goes into surface runoff. The soil is near saturation in January. EM allows rapid infiltration of water in the lower soil layer. Therefore, changes in drainage are distinctly higher in EM.

An overview of the ratio of sensitivities for a high and a low snow albedo is given in Fig. (2.33). We detect that in most cases, the bar heights are close to 1 for ECHAM whereas EM shows a large scattering. The EM shows an increasing sensitivity for albedo, net shortwave radiation, surface and soil temperature and ground heat fluxes. These quantities are closely

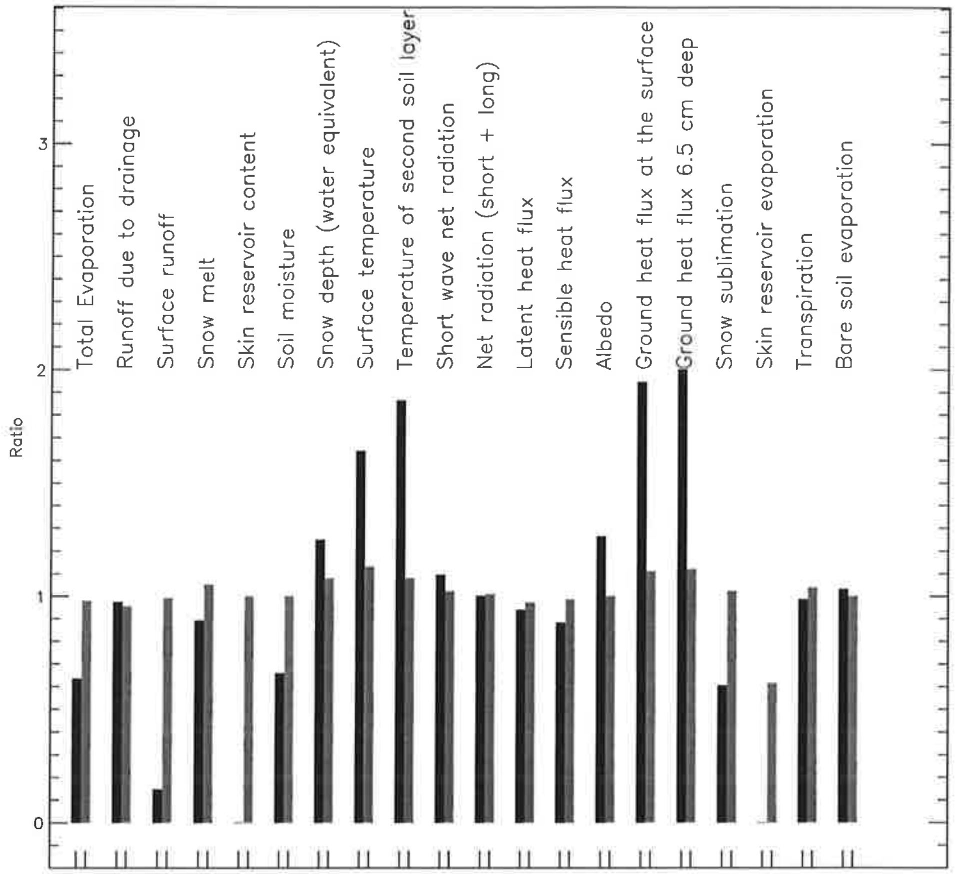

Figure 2.33: *Ratio of sensitivity (January) for a snow albedo of 0.5 and 0.8 for ECHAM and EM. Left bar: EM; right bar: ECHAM.*

physically related. Decreasing sensitivities are observed for surface runoff, soil moisture and turbulent heat fluxes.
Finally, we want to show how α_s modifies the monthly average of diurnal cycles for January (Fig. (2.34)). The two thicker curves, representing the ECHAM model, are almost identical. This shows that the sensitivities are nearly independent on snow albedo. The only striking exception is the snow melt where a phase shift of the maximum by two hours is found in the late evening. The reason remains an unsolved problem and could be a hint to a deficiency in the snow parameterization. In EM, a higher α_s leads to more snow melt between 23 UT and 9 UT whereas during the day, a decrease is found. The reason may be that during the day, a stronger cooling occurs for higher reflectivities whereas at night, temperatures are barely influenced.
The sensitivity of the ground heat flux in EM shows a phase shift which is due to a phase shift in the soil temperatures. This again is mainly because of the described temperature T_U which incorporates no diurnal cycle.
The sensitivities at noon are often an order of magnitude larger than monthly averages, i.e. the latent heat flux changes by $6\mathrm{Wm}^{-2}$ (EM) and net shortwave radiation by about $15\mathrm{Wm}^{-2}$ for

$\Delta\alpha_s$=0.2 .

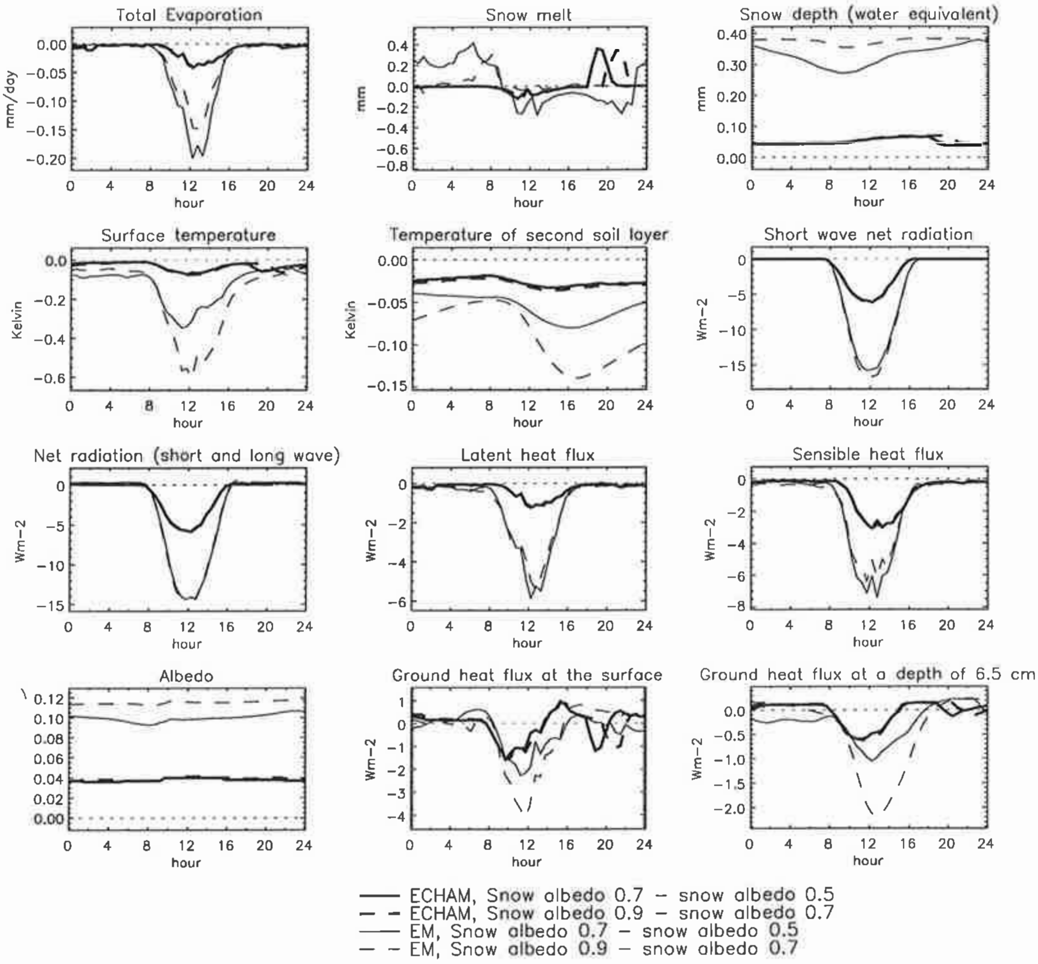

Figure 2.34: *Differences of mean diurnal cycles for January of ECHAM and EM. Differences are presented for α_s=0.5 and α_s=0.7 resp. α_s=0.7 and α_s=0.9.*

2.7 Sensitivity to the maximum soil water content

The soil moisture content is very important concerning the climate of a region. It determines to a large extent the development of vegetation and the surface temperature. Bare soil evaporation, surface runoff and transpiration are mainly controlled by the soil moisture. The partition between latent and sensible heat fluxes is also influenced by the soil moisture. Moreover, the soil moisture strongly changes the heat capacity of the soil because of the high heat capacity of water. The parameterization formulae take this into account by including the soil moisture as a key variable. Whereas the ECHAM includes only one layer for water (bucket model), the EM incorporates two or more different layers for water. This implies that in ECHAM, all of the evaporation and runoff processes have to be parameterized using one single soil moisture. This is physically not correct because the above mentioned processes originate at different depths in the soil. For bare soil evaporation, the soil moisture near the surface is most important while drainage processes originate from lower soil layers. The transpiration rate, on the other hand, depends on the root depth of plants which draw water out of the soil. Therefore, a more physically based description of these processes is possible by introducing several soil layers for water which is implemented in the EM.
In ECHAM, it is obvious to equate the maximum soil water content with W_{smax}. However, the EM leaves two possibilities open to define the maximum soil water content: The field capacity (FC) or the volume of pores (PV). It was decided to take the volume of pores as the maximum water content because the field capacity can be exceeded during longer periods. This is confirmed by both field and model experiments. However, the relative soil moisture is computed relative to the field capacities since most authors use this approach. Therefore, relative soil moistures larger than 1 are possible. Measured monthly means of relative soil moisture in West Europe in winter are of the order of 1.1. The other parameters describing the soil (field capacity, permanent wilting point and air dryness point) are determined to obtain the same quotients between the four parameters as in the soil type 'loamy sand', which is applicable for the Cabauw site.
It is of interest to explicitely investigate the formulae which include soil moisture (or the maximum soil water content). The formulae often contain the relative soil moisture content W_{srel} rather than the absolute amount of water W_s. For example, the second summation of fast drainage is easily transformed into $c\ (W_{srel}\ \text{-}0.9)^d$ where c is a constant; the water stress factor $F(W_s)$ is $F(W_s)$=10/3 W_{srel} - 2/3 for the standard land-surface parameters. The evaporation efficiency E, which is equal to the ratio of transpiration and potential evaporation, and the relative humidity h at the surface (Eq. (1.44)) can also be written as a function of W_{srel}.
Runoff of ECHAM increases strongly when approaching the field capacity. The magnitudes are shown in Figures (2.35) and (2.36). We observe the rapid increase of drainage and surface runoff with relative soil moisture content. Drainage increases by about a factor of 25 for an increase in relative soil moisture from 90% to 100% whereas the corrresponding ratio for surface runoff is only 2. This means that the partition between total runoff into drainage and surface runoff changes strongly for different soil moisture contents. While the derivative of drainage with respect to the water content W_s increases only by a factor 3 for the shown range the corresponding derivative for surface runoff amounts to 7. Moreover, the derivative curve for drainage flattens while the sensitivity for runoff shows a nearly exponential increase.

The relative humidity h at the surface is represented by a cosine function of the relative soil water content. This leads to the highest sensitivity of bare soil evaporation for W_{srel}=50% and a decreasing sensitivity for drier or wetter soils. This statement is only true when neglecting the water vapour gradient in the boundary layer.
The evaporation efficiency E contains the water stress function $F(W_s)$ which linearly increases from the permanent wilting point to the critical value. Figure (2.37) shows that the evaporation efficiency increases between 20% (permanent wilting point) and 50% (critical value). The sensitivity of E with respect to W_s decreases with increasing soil moisture content for

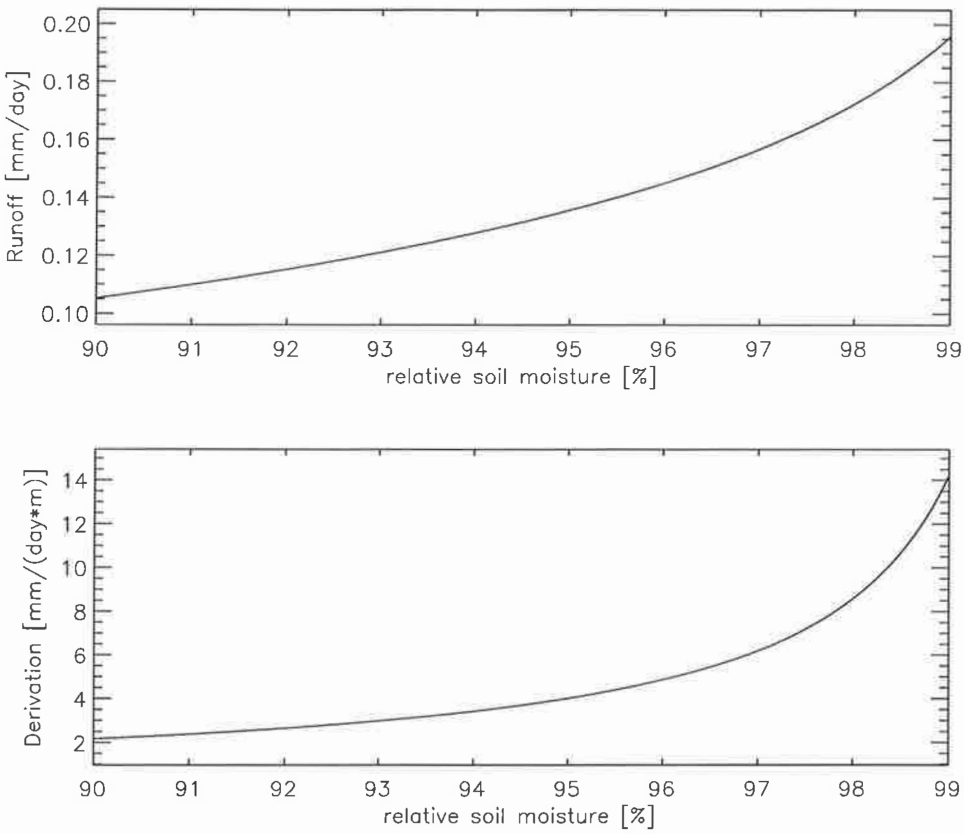

Figure 2.35: *Surface runoff and the derivative with respect to Ws (soil moisture content) in ECHAM. The quantities refer to a period of one day. The parameter Q comprises the total water input which is available for runoff and infiltration and is set equal to 0.002m/day. The maximum soil water content is 0.2m.*

W_{srel}=[20%,50%] and is zero outside this range.

The EM formulae containing the soil water content refer to either the soil moisture content of the upper or the lower layer. The bare soil evaporation increases as a quadratic function of soil water content in the uppermost soil layer. This means that the sensitivity increases linearly with the soil water content between the air dryness point and the field capacity. The transpiration rate is also represented by a quadratic function of soil water. This is true for the transpiration from each soil layer. However, the range for non-zero transpiration and non-zero bare soil evaporation are different: Below the permanent wilting point, transpiration stops and above the turgor loss point, transpiration should work optimally.
The sensitivities of runoff processes in the EM are not easy to assess because of the differential Darcy equation (1.30) which describes the transport of water between the soil layers. Moreover, the coefficients in this equation are dependent on the soil moisture. The lateral runoff out of the layers increases linearly with the soil moisture content between the field capacity and the volume of pores, which is synonymous with a constant sensitivity with respect to W_s. As outlined in

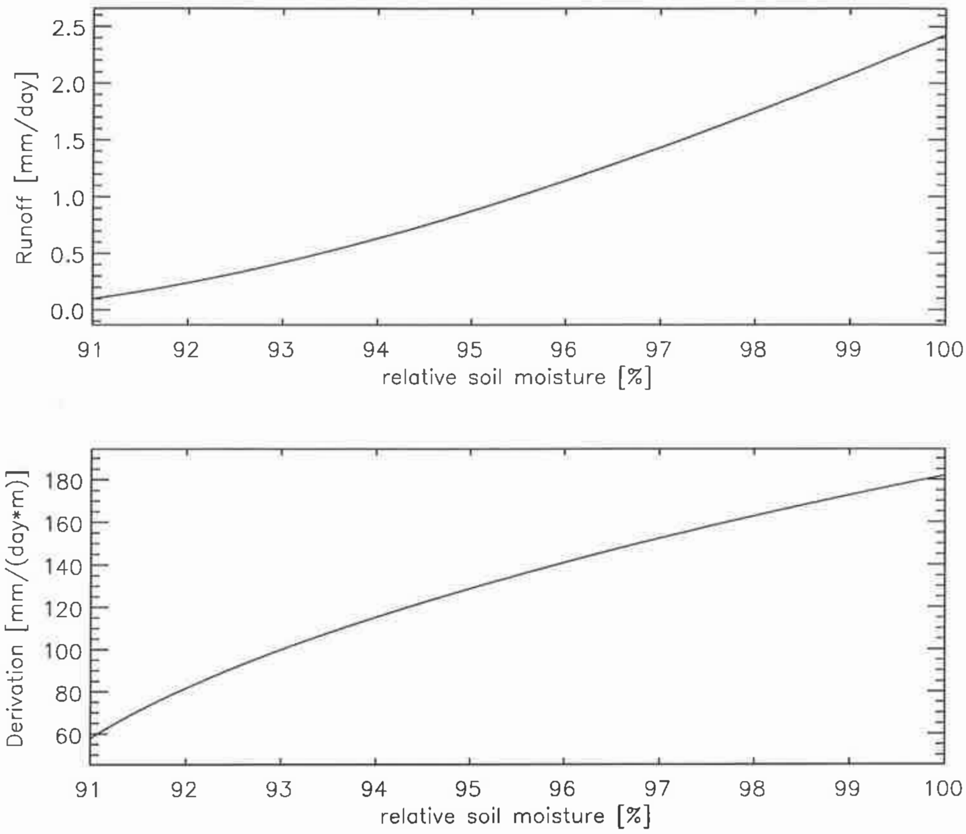

Figure 2.36: *Drainage and the derivative with respect to Ws (soil moisture content). The quantities refer to a period of one day. All other parameters are set as in the ECHAM control experiment.*

Chapter (1.2), the most important contribution to the surface runoff consists of lateral flow out of the uppermost soil layer. Therefore, the partition of total runoff in drainage and surface runoff is mainly determined by the speed of water exchange between both soil layers.
In both models, the (annual) soil water content clearly increases with increasing maximum soil water content W_{smax}. The sensitivity is almost constant for the whole examined range of maximum soil water content and amounts to about 6mm (ECHAM) or 8mm (EM) for W_{smax}=1cm. It is interesting that the relative soil moisture remains nearly constant (Fig. (2.39)). The sensitivity amounts to slightly positive values of the order of 1 pars pro mille for ΔW_{smax}=1cm. The importance of the key variable W_{srel} suggests constant transpiration, bare soil evaporation, surface runoff and drainage. This is especially true for transpiration and surface runoff (Fig. (2.39)). Transpiration can additionally be influenced by a change in turbulence: A lower surface temperature (summer) leads to less turbulence and a smaller specific humidity deficit. However, this mechanism is of little importance here. Drainage distinctly decreases and bare soil evaporation increases with increasing maximum soil water content. The annual cycle on a monthly base shows that for both models the relative soil moisture is higher for lower W_{smax} during winter and spring. The opposite is true during summer and autumn. Lower values of

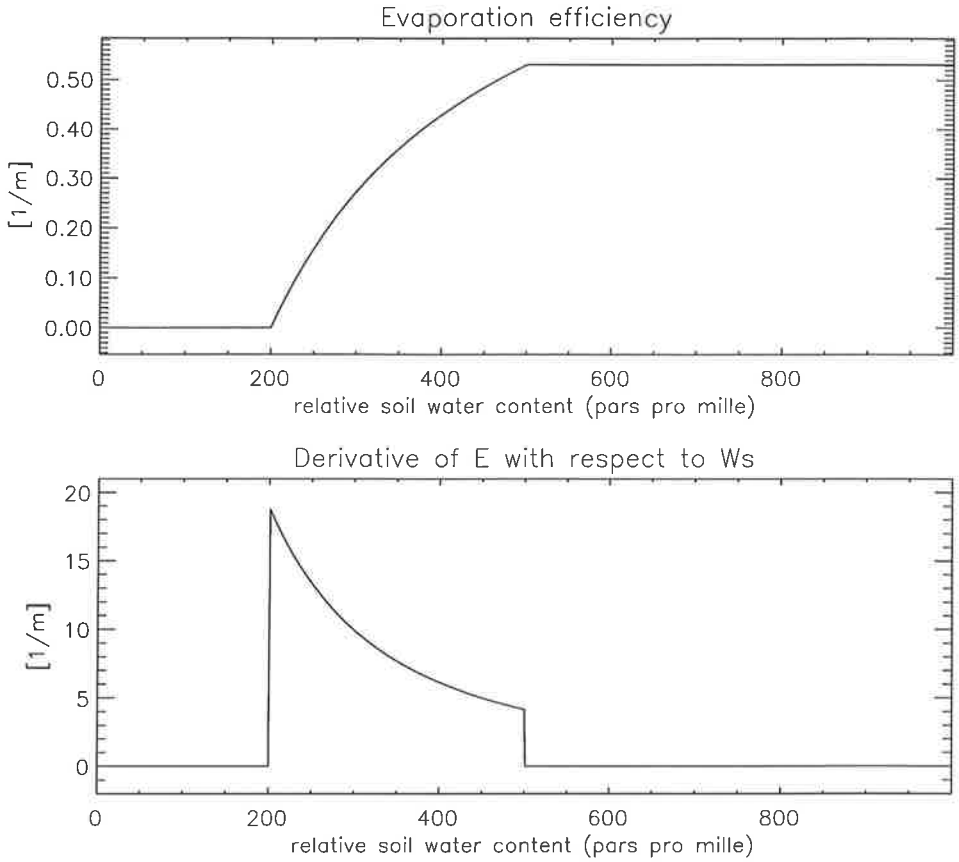

Figure 2.37: *Evaporation efficiency E and the derivative with respect to the soil moisture content. The photosyntetically active radiation (PAR) is equal to the average value of Cabauw in June. The transfer coefficient C_h is equal to 0.005 and wind speed v at a height of 30m is equal to $5ms^{-1}$.* All other parameters are set as in the ECHAM control experiment.

W_{smax} lead to a higher annual amplitude of relative soil moisture. This increases the number of days with a greater than 90% saturated soil and therefore, for more rapid drainage events. The parameterization of surface runoff, on the other hand, does not distinguish between a slow and fast process. Annual bare soil evaporation typically depends on the soil moisture situation during the period with high net shortwave radiation. Therefore, the higher relative soil moisture during summer and autumn for higher values of W_{smax} leads to higher bare soil evaporation. During winter and spring, where the soil is already close to saturation, the influence of changing soil moisture plays a minor role for the total annual bare soil evaporation. This is also partly true for EM.

Drainage decreases slower in the EM than in the GCM for higher maximum water contents, but runoff at the surface decreases in EM whereas ECHAM shows a negligible sensitivity. The reason is that the water exchange between the two layers is often not determined by the Darcy equation but by the empirical constraint that only 10% of the volumes of pores can flow from the upper to the lower one (per time step). This signifies that a higher volume of pores brings the water faster to the lower layer, and therefore, more lateral flow from the lower soil layer is

possible. Thus, the reduction of drainage in EM is smaller than in ECHAM and surface runoff clearly decreases with increasing field capacity.
Evaporation from plants is more sensitive in EM than in ECHAM. The only reason can be the characteristic of the factor $\beta_{B,K}$ in Equation (1.48). The key parameter of this formula is the turgor loss point. Its value lies between 70% and 75% (in the model experiments) during night and winter with low incoming shortwave radiation. During the warmer season and at daytime, values often lie above 95% of field capacity, representing the time when transpiration is high. This is the reason why transpiration decreases when the relative soil water content falls below the field capacity during summer, and the drying of the soil is more significant for low maximum values of the pores volume (see Fig. (2.38)). This leads to a stronger decrease of $\beta_{B,K}$ and thus transpiration. Another interesting fact can be seen in Figure (2.38). The annual amplitude of the relative water content of the upper soil layer is higher than that of the lower layer. For W_{smax}=0.2, this ratio is about 3. The modeled W_{srel} of the lower soil layer partly exceeds 1.5. This is not in agreement with observations which measure monthly averages of about 1.1 in Western Europe during winter. However, it should be emphasized that the soil parameters for the experiments used in this Chapter do not correspond to any real soil type. Another striking feature is that the relative soil moisture of the second layer increases with lower maximum soil water content for the period from December to March, whereas summer and autumn show an opposite characteristic. The uppermost soil layer, on the other hand, has an increasing relative soil moisture for higher volume of pores during the first half of the year. Since the lower soil layer is much deeper, the characteristic of the entire soil is dominated by this layer.

The latent heat flux increases in both models with increasing maximum soil water content, although the increase is faster for EM (see Fig. (2.39)). The sensitivity is a direct result of the corresponding sensitivities of transpiration and bare soil evaporation because the sensitivity of the skin reservoir is of little importance. Skin reservoir evaporation slightly decreases for increasing values of W_{smax}, but the sensitivity gets smaller. The decrease is faster for EM (see Fig. (2.40)). This characteristic can be explained with Formula (1.25). If the volume of pores becomes larger, the maximum infiltration rate increases. This signifies that the precipitation water infiltrates faster and so less water is available for evaporation.

Sensible heat fluxes decrease with increasing values of maximum soil water content. This is mainly due to the opposite characteristic of latent heat flux and is in accordance with surface temperature. The higher evaporation of water needs more energy and therefore cools the surface. The cooling effect is very similar for both models for low values of W_{smax}, but sensitivity decreases faster for increasing W_{smax} in EM. This fits to the faster decrease of the sensitivity of latent heat flux. The absolute changes in the turbulent heat fluxes are similar in both models but the changes in the sensible heat flux are relatively larger.
The ECHAM albedo remains the same for different amounts of soil water. The EM albedo, on the other hand, is influenced by the soil moisture of the upper soil layer and becomes lower with larger volume of pores because of the low albedo of water (see Fig. (1.1)). However, the change is small and amounts to about 0.01 for ΔW_{smax}=0.2m for the complete examined range of W_{smax}. The albedo directly influences net shortwave radiation. The sensitivity is about 0.3Wm^{-2} for ΔW_{smax}=0.1m and shows a slight increase with a higher volume of pores. Since ECHAM shows no sensitivity the change in the total net radiation is more marked in EM. EM shows a small decrease with increasing W_{smax}. For lower values of W_{smax} the sensitivity of net shortwave radiation and net longwave radiation has the same order (EM). For a higher volume of pores, the changes in shortwave radiation become increasingly important because temperature change in EM nearly vanishes for W_{smax}=0.4m. This small sensitivity is caused by the two counteracting processes for increasing W_{smax}: The lower albedo increases the surface temperature whereas more evaporation reduces it.
The snow conditions of both models are only slightly influenced by changing soil moisture. The sensitivity of EM concerning snow melt, snow sublimation and snow depth is more than an

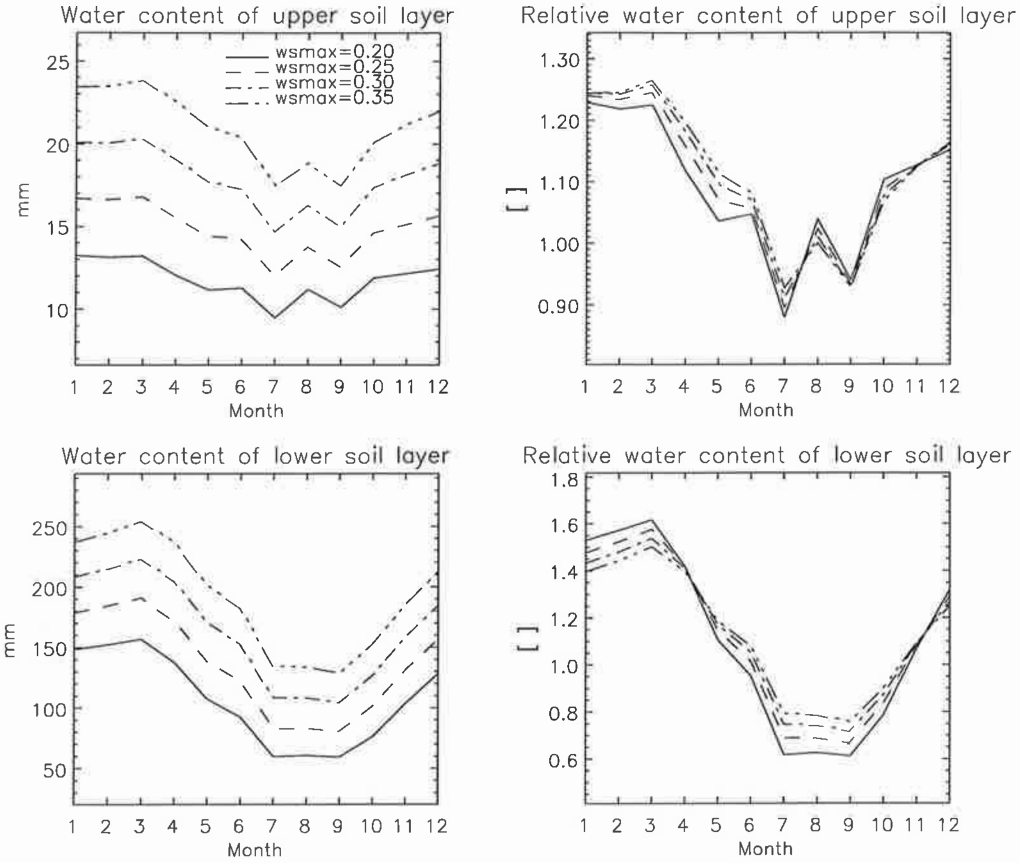

Figure 2.38: *Relative and absolute soil water content of upper and lower soil layer for different maximum soil water contents (EM, monthly averages).*

order of magnitude larger than in ECHAM. The sensitivities are rather constant for the entire examined range of W_{smax}. In both models, snow sublimation is calculated as potential evaporation. However, snow melt is parameterized differently. The only plausible reason for the larger sensitivity of snow variables in EM is the larger sensitivity of surface temperature, soil temperature and ground heat flux in EM mainly due to the described temperature T_U. Model experiments have proved that if the EM soil is forced to have the same temperature regime as ECHAM, sensitivities of snow variables become similar in both models.
An overview of how sensitivities behave for the chosen range of maximum soil water content is given in Figure (2.40). A rather inhomogeneous distribution has been found. Soil moisture, snow parameters (only EM), drainage and bare soil evaporation (ECHAM) have bar lengths close to 1. This means that the sensitivity is approximately constant for the whole range of W_{smax}. Total evaporation reduces by about one half for the change from W_{smax}=0.2m to W_{smax}=0.4m. The sensitivities of temperatures (ECHAM), net radiation, ground heat fluxes (EM) and skin reservoir evaporation (ECHAM) show a similar decrease. The high bars for the ECHAM ground heat fluxes are not of great importance because absolute changes are negligible and results rather accidentally. Sensitivity of transpiration is very small in ECHAM and changes its sign. Albedo and net shortwave radiation are the only two quantities in EM with clearly increasing sensitivity.

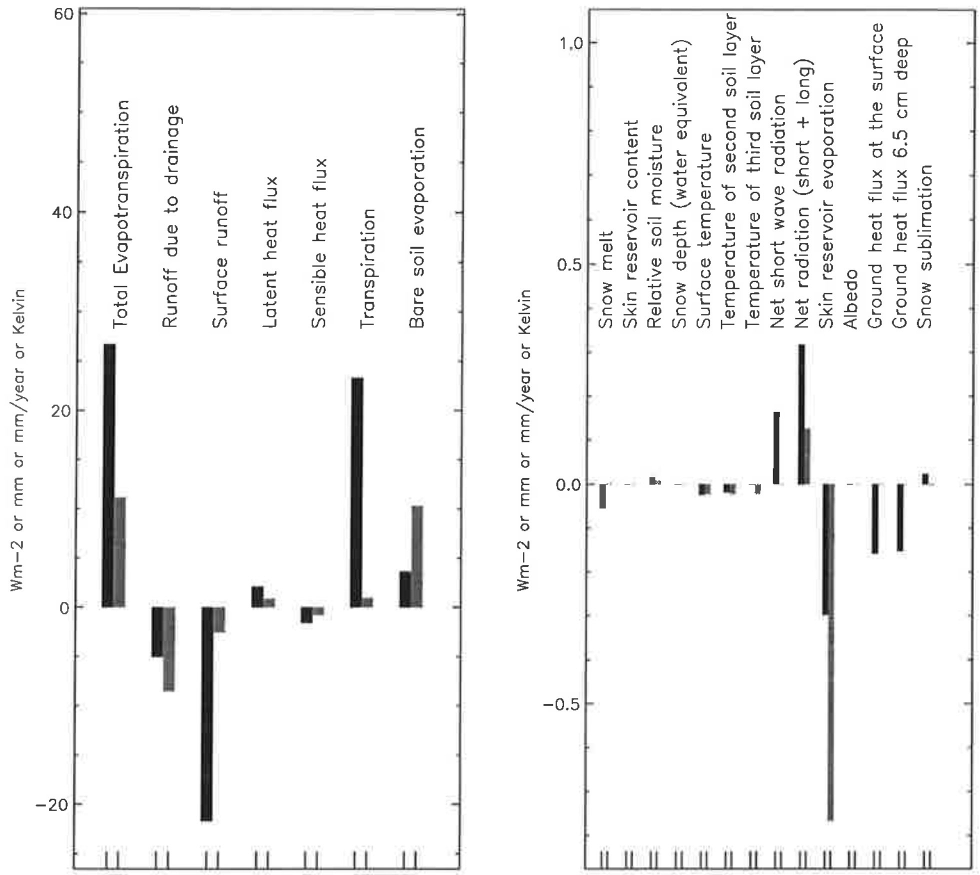

Figure 2.39: *Change of different quantities for a change of the field capacity from 0.20m to 0.25m. Left bar: EM; right bar: ECHAM.*

This result is closely related to the water content of the uppermost soil layer.
The closer investigation of day- and nighttime sensitivities shows some interesting results. In spite of the inert soil moisture content, a roughly 10% higher soil moisture during night is observed in both models. The reason is the diurnal cycle of latent heat flux (mainly transpiration) which draws more water out of the soil during the day. Only two quantities are described here which show a clear change in the ratio of annual day and nighttime sensitivity: Drainage and surface temperature (only EM). Surface temperature decreases with increasing maximum soil moisture content. Whereas in ECHAM both day and night contribute to this result, EM shows a clear decrease in surface temperature only during the night. The opposite is true during day and moreover, the sensitivity slightly increases with increasing W_{smax} during the day whereas nighttime sensitivities decrease in a roughly exponential way. This leads to a strong change in the ratio of day and night sensitivity. The higher absolute values of daytime sensitivities are caused by the stronger change in water vapour fluxes.
In EM, annual averages of drainage at daytime remain rather constant for the chosen range of W_{smax} whereas the nighttime values clearly decrease. The values for day and night are nearly

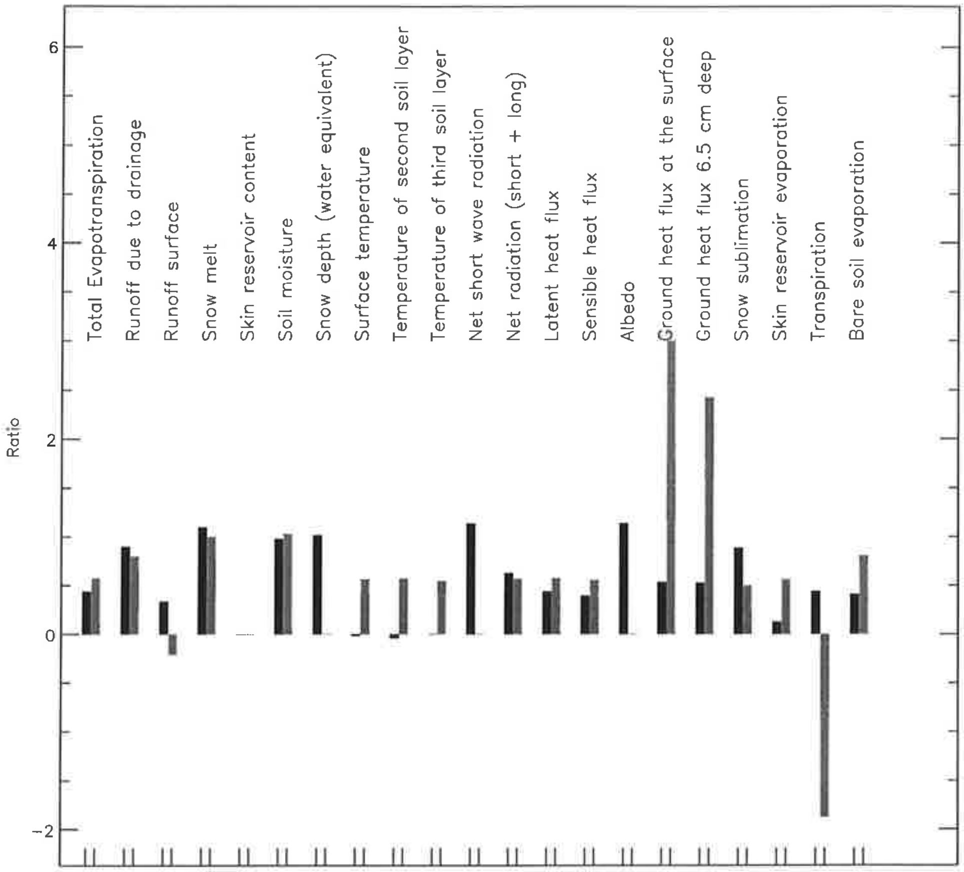

Figure 2.40: *Ratios of sensitivities for a value of the maximum soil water content of 0.225m and 0.375m for the ECHAM and EM (annual basis). Calculation of the sensitivities are based on W_{smax}=0.20m and 0.25m rsp. W_{smax}=0.35m and 0.40m. Left bar: EM; right bar: ECHAM.*

the same for W_{smax}=0.4m, while for W_{smax}=0.2m, the nighttime value is about one quarter higher than the corresponding value measured during day. In ECHAM, drainage during the night yields a higher contribution to total drainage for $W_{smax} > 0.28$m. This may be explained by the fact that a higher pore volume leads to a smaller filling grade of the soil during winter (when most of drainage occurs) and therefore the night is better for drainage because only a small amount of water is lost by evaporation.

Chapter 3

Comparison of annual and monthly mean values for the control experiments of ECHAM and EM

This section compares the annual and monthly means for the control experiments (see Section (2.1)) of both models. In spite of the rather difficult definition of the parameters' values of the control simulations, interesting results could be found.
The annual values of 23 output values are compared in Table (3.1). It can easily be observed that even on the basis of annual averages, quite large differences exist between the ECHAM and EM.
First we want to look closer to water vapour fluxes. The total evaporation in EM is about 44mm or 8% higher than in ECHAM. However, the partition between the different water vapour fluxes (from bare soil, the skin reservoir and plants) shows much larger differences. The most significant deviations can be observed in the skin reservoir evaporation, where the ECHAM computes a value greater than 2.5 times higher than the other model. This is very surprising when looking closer at the maximum skin reservoir content: Formula (1.24) gives a value of 3mm for the EM (independently of LAI) whereas the ECHAM calculates a corresponding value of about 0.04mm (LAI=2, fully vegetated grid element). However, ECHAM has on average about 1.7 times more water in that reservoir. The reason is the very efficient infiltration into the soil (see Equation (1.26)) of the EM. It should be mentioned that EM makes no difference in the infiltration rate from the skin reservoir of vegetated area (leaves) and bare soil. For bare soil, Equation (1.26) may describe the water input into soil correctly but incorrectly for plants and trees. The skin reservoir of plants will only be emptied by potential evaporation. As a result, ECHAM evaporates 58mm/year more from the skin reservoir than EM. This large difference is more than compensated by the transpiration and bare soil evaporation, which are distinctively higher in EM. Transpiration is slightly higher in the EM during September to March whereas during spring (April - June), the difference is clearly higher (about 20mm per month for this period). The reason is that the soil moisture does not fall below the critical value where water stress begins to act. Therefore, the factor β in formula (1.48) is equal to 1. During summer (July to September), the ECHAM parameterization for transpiration gives slightly higher transpiration values. The main reason is the rapid decrease of the factor β^2 in Equation (1.48) when the soil moisture falls below the turgor loss point (critical point), and the turgor loss point is close to field capacity during summer at daytime with high potential evaporation.

Table 3.1: *List of annual values of ECHAM and EM for standard configuration*

parameter	ECHAM	EM	ratio (ECHAM/EM)	difference (ECHAM-EM)
total evapotranspiration from surface	534mm	578mm	0.92	-44mm
latent heat flux	$42.2Wm^{-2}$	$44.8Wm^{-2}$	0.94	$-2.6Wm^{-2}$
sensible heat flux	$2.9Wm^{-2}$	$8.8Wm^{-2}$	0.33	$-5.9Wm^{-2}$
evaporation (skin reservoir)	93mm	35mm	2.68	58mm
transpiration	317mm	381mm	0.83	-64mm
bare soil evaporation	94mm	160mm	0.59	-66mm
skin reservoir content	0.04mm	0.02mm	1.70	0.02mm
soil moisture content	154mm	200mm	0.77	-46mm
relative soil moisture	0.77	1.02	0.75	-0.25
surface temperature	281.91K	281.75K	-	0.16K
soil temperature, second layer	281.9K	282.1K	-	-0.20K
soil temperature, third layer	281.7K	283.4K	-	-1.5K
ground heat flux at the surface	$0.14Wm^{-2}$	$-4.5Wm^{-2}$	-0.03	$4.6Wm^{-2}$
ground heat flux, depth 6.5cm	$0.13Wm^{-2}$	$-4.7Wm^{-2}$	-0.03	$4.9Wm^{-2}$
snow melt	12.2mm	17.1mm	0.71	-4.9mm
snow sublimation	2.43mm	2.45mm	0.99	-0.02mm
snow depth	0.28mm	0.34mm	0.83	-0.06mm
net shortwave radiation	$93.3Wm^{-2}$	$94.0Wm^{-2}$	1.001	$0.7Wm^{-2}$
net radiation	$49.3Wm^{-2}$	$48.5Wm^{-2}$	0.98	$-0.76Wm^{-2}$
runoff due to drainage	70.0mm	54.2mm	1.29	15.7mm
surface runoff	171.8mm	153.8mm	1.12	17.9mm
albedo	0.17	0.18	0.91	-0.02

The bare soil evaporation is not very important for the Cabauw site because, for the control simulation, only slightly more than 10% of the grid element should to be free of vegetation. Nevertheless, the behaviour of the bare soil evaporation should be investigated because different characteristics of the two models can be seen. During winter (November - April), when both model soils are more or less saturated, the water vapour fluxes from bare soil are similar. However, in May, the ECHAM evaporation suddenly breaks down and in late summer, evaporation is similar as in winter. The curve of the EM, on the other hand, shows a clear annual evolution with a maximum during the summer, which is expected (see Fig. (3.1)). This results in an annual ratio of bare soil evaporation between EM and ECHAM of 0.59; during late summer, the ratio is about 0.2.

The annual mean of the sensible heat flux in EM is equal to $8.8Wm^{-2}$, distinctly higher than in ECHAM ($2.9Wm^{-2}$). The largest differences are observed during late summer and from February to April (see Figure (3.1)). Model experiments show that sensible heat fluxes in ECHAM and EM are rather similar when applying the same surface temperatures to both models (Figure (3.2)). The different computation of the heat transfer coefficients (see Eqs. (1.51) - (1.57) and Fig. (1.4)) leads to a larger amplitude in ECHAM than EM. Figure (3.2) shows that the lower boundary condition for temperature plays a significant role for the values of the sensible heat flux in EM.

The ground heat fluxes show a very different feature in both models except during winter. Whereas the ECHAM has the expected evolution (directed to the surface during summer and opposite during winter), EM results are less encouraging. The monthly mean fluxes are directed upward for almost the entire year, in contradiction to the ECHAM results and observations (Figure (3.3)). This can be easily explained. The too high described temperature T_U in EM during summer produces an upward directed heat flux. Although the formulae for calculating the ground heat fluxes are totally different in ECHAM and EM (Eq. (1.7) and (1.8)), the results are similar when forcing the two models to have the same soil temperatures. This is shown in Figure (3.3).

The similarity of the annual evolution of surface runoff and drainage in both models is rather

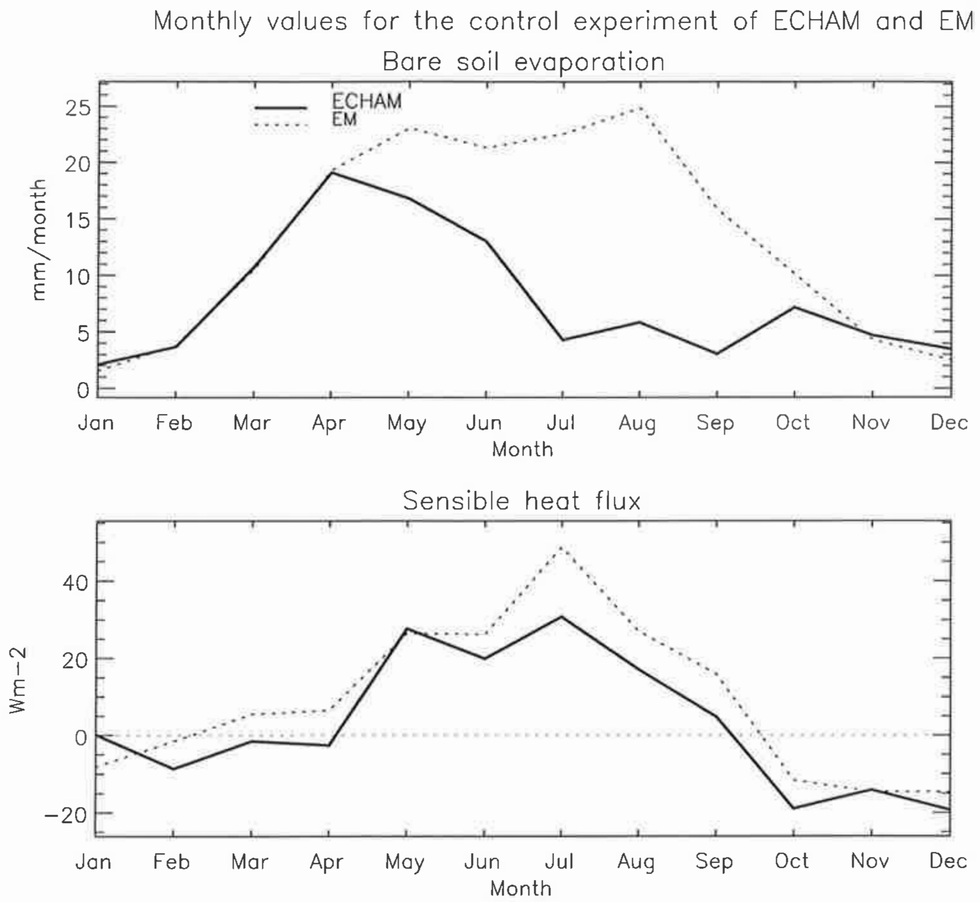

Figure 3.1: *Monthly means of bare soil evaporation and sensible heat flux of the ECHAM and EM.*

striking when taking into account the complicated processes and different parameterizations. Both the surface drainage and runoff due to drainage are about 20mm lower for the EM-control experiment. Since the annual total of surface runoff is more than double the drainage sum, the relative difference is more significant for drainage processes. The higher annual drainage in EM is mostly caused by higher values during winter. The explanation can be found analysing the parameterization formula (1.24). The bucket is more than 90% filled in ECHAM during winter. Therefore, the fast drainage, which is very efficient, is applied. During the warmer season (May to October), the drainage is close to zero in both models.
The surface runoff of the EM includes the runoff out of the uppermost soil layer (see Chapter (1.2)). A model experiment shows that this is the main contribution (more than 99%) for total surface runoff. All other components are negligible. This is due to the very efficient infiltration of rain water into the soil. During winter, ECHAM produces mostly more surface runoff than EM. This can be explained by regarding Equation (1.19), which defines the fractional saturated area by taking the subgrid orography into account. Although the structure parameter b is small for the Cabauw site (b=0.2, which corresponds to a rather flat terrain), the fraction of the grid element from which rain and snow melt runs off is increasing rapidly for an almost saturated soil. For a relative soil moisture of 95%, the saturated fraction amounts to about 7%, for 99%

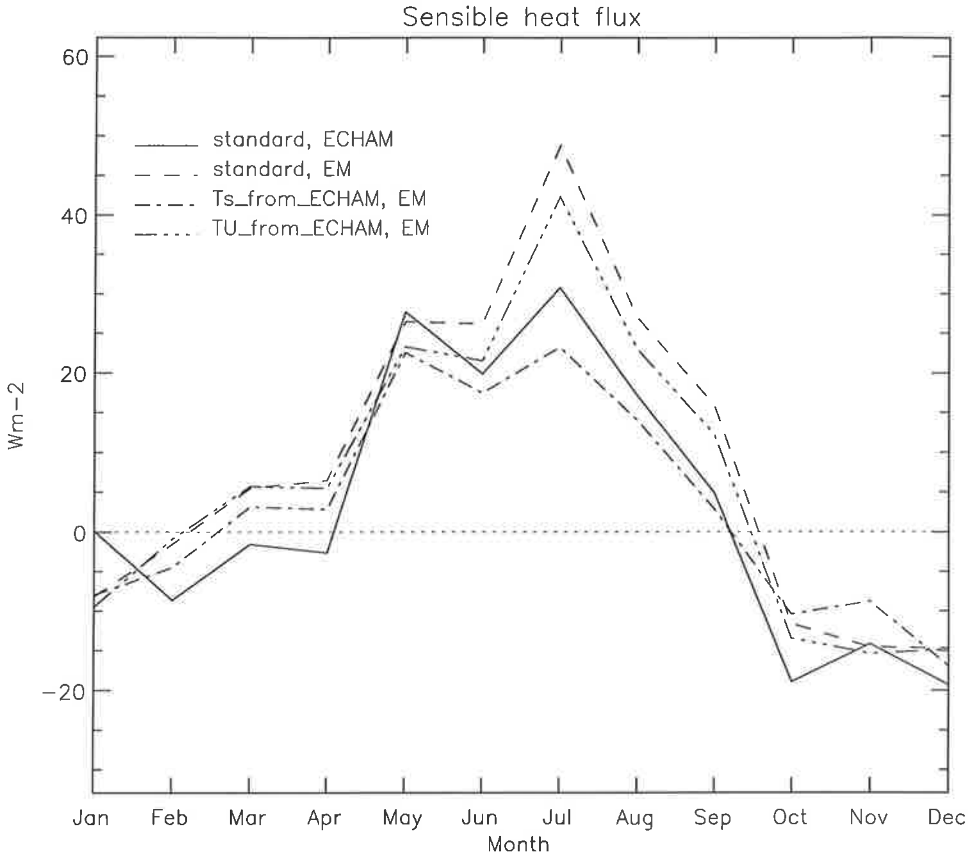

Figure 3.2: *Monthly means of sensible heat flux for different assumptions of surface temperature. The legend's abbreviation 'Ts_from_ECHAM, EM' means that the EM was forced to have the same surface temperatures as ECHAM. The curve 'TU_from_ECHAM' was computed by forcing the EM to have the same temperatures at the lower boundary of the soil as ECHAM in the same soil depth.*

saturation the corresponding value is 11%.
The soil moisture contents is difficult to compare because of different definitions. The relative soil moisture is defined as the ratio of the soil moisture content and field capacity. Since the EM allows (for relatively short periods) values above the field capacity, the relative soil moisture is often more than 1 for the standard EM run, especially in winter. During summer, the monthly relative soil moisture reaches values of about 0.8, and 0.6 in ECHAM. The ECHAM performs a stronger drying of the soil than EM. Further, the annual mean of the absolute soil water content is more than 40mm higher in EM. However, the two curves for the monthly means of the modeled soil moisture run parallel (not shown).
The radiation fluxes show only slight differences between the climate and weather forecast model. This is due to the forcing. Namely, the same downward directed short- and longwave radiation is used in both models. Concerning the longwave radiation radiated from the surface, the Stefan-Boltzmann-Law determines the observed differences. An increase of the surface temperature by one degree leads to a $4Wm^{-2}$ (-10°C) to $6Wm^{-2}$ (30°C) higher upward longwave radiation.

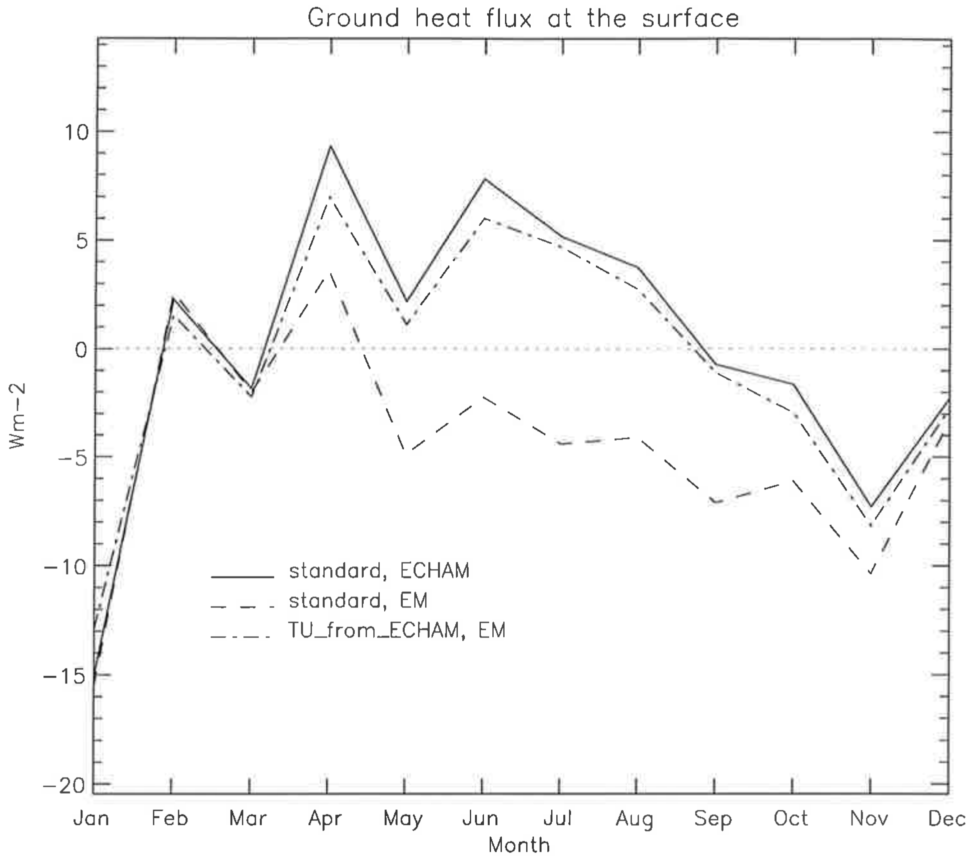

Figure 3.3: *Monthly means of ground heat flux at the surface for Cabauw ('Observation'), ECHAM and EM (control experiment and forcing of EM with the ECHAM soil temperature (lower boundary condition)).*

In the annual average the upward longwave radiation is about 1.5Wm^{-2} higher for the EM run. During summer, the difference is clearly higher whereas during winter, the reverse occurs because of the lower surface temperature (about 0.5°C).
Net shortwave radiation is only influenced by the albedo. During the snow free period (March to December), the computed albedo of both models are very similar and close to 0.15. During winter, large differences between the models' albedo values are found. In January, the mean albedo in ECHAM is about 0.27 whereas for EM, a value of more than 0.4 results for the standard experiment. Two reasons can be given. Firstly, the snow covered fraction of the grid element much larger for EM than for ECHAM (see Figure (1.3)). The less important influence is the slightly higher snow depth in EM during January and February. This is due to the slightly lower surface temperature. This difference in albedo leads to a deviation in the net shortwave radiation of 5Wm^{-2} or about 20% in January.

A comparison of how the model results fit the observations can be made for the following quantities:

- surface temperature
- latent heat flux
- sensible heat flux
- ground heat flux at the surface
- ground heat flux at a depth of 6.5cm
- net shortwave radiation
- net longwave radiation.

At first, it should be mentioned that this comparison has no eminent importance in this report. The main aim of this study is the comparison of the two models and the investigation of the characteristics and deficiencies of the applied parameterization formulae. Moreover, the height where the forcing data at Cabauw were measured and the lowest atmospheric model level do not correspond. The level where the observation were made is 20m above ground whereas the lowest model level of the ECHAM and EM is about 30m. This makes a not negligible difference (Figure (3.4)). Nevertheless, some results of the comparison are shortly discussed.

The comparison of surface temperatures is not trivial. The ECHAM model computes the same temperature for the surface and the uppermost soil layer of 6.5cm depth (under snow free conditions). Therefore, it is not straightforward to define this temperature as surface temperature. Other authors suggest a very thin uppermost soil layer to compute a more realistic skin temperature (e.g. Betts et al., 1993; Viterbo and Beljaars, 1995). The EM incorporates a computation of the surface temperature which is usually different to the modeled soil temperatures near the surface. Another problem is the measurement of the surface temperature. Most papers which deal with Cabauw data suppose the temperature measured at a depth of 2cm to be the surface temperature. However, the possibility exists to compute the (effective) surface temperature by the Stefan-Boltzmann-Law. A comparison of the modeled temperatures of ECHAM and EM with the observed 2-cm-temperature and temperature derived from the upward longwave radiation (effective skin temperature) is shown in Figure (3.5).

We recognize large differences between the two possibilities to determine the observed surface temperatures. The model results lie in between the 2-cm-temperature and the effective skin temperature and show relatively little difference. This fact suggests that model results could be close to reality but does not prove it. Another point sustains the hypothesis modeled surface temperature are reasonable. During summer, the modeled (ECHAM) surface temperatures are about 0.3°C higher than the temperature at a height of 20m whereas in winter the reverse is true (the difference is about half a degree). These are reasonable values and is consistent with the frequent stable boundary layers during winter (inversion) and unstable conditions during the warmer season (convection).

The comparison of monthly means of sensible and latent heat flux, net shortwave radiation and ground heat flux of both models with observations (Figure (3.6)) gives a clear impression. The ECHAM results of latent and sensible heat flux are in better agreement with the observations than the EM results. The sensible heat flux is overestimated by both models although ECHAM better fits the observation. The main reason for the bad result of EM is the incorrect lower boundary condition for temperature T_U. When replacing these values by a better estimate calculated from ECHAM results, the agreement is strongly improved and the EM generally fits the observation better (mainly during summer time) than ECHAM. Ground heat flux is strongly underestimated in EM whereas ECHAM follows the observation quite well. The reason for the upward directed ground heat flux (monthly averages) in the EM during summer is the too high prescribed temperature T_U. When forcing the EM to have the same surface temperature as ECHAM, the different methods to calculate ground heat fluxes give similar results.

Latent heat flux is slightly overestimated in both models. The EM results show a striking difference between model and observation for the period from April to June. This difference

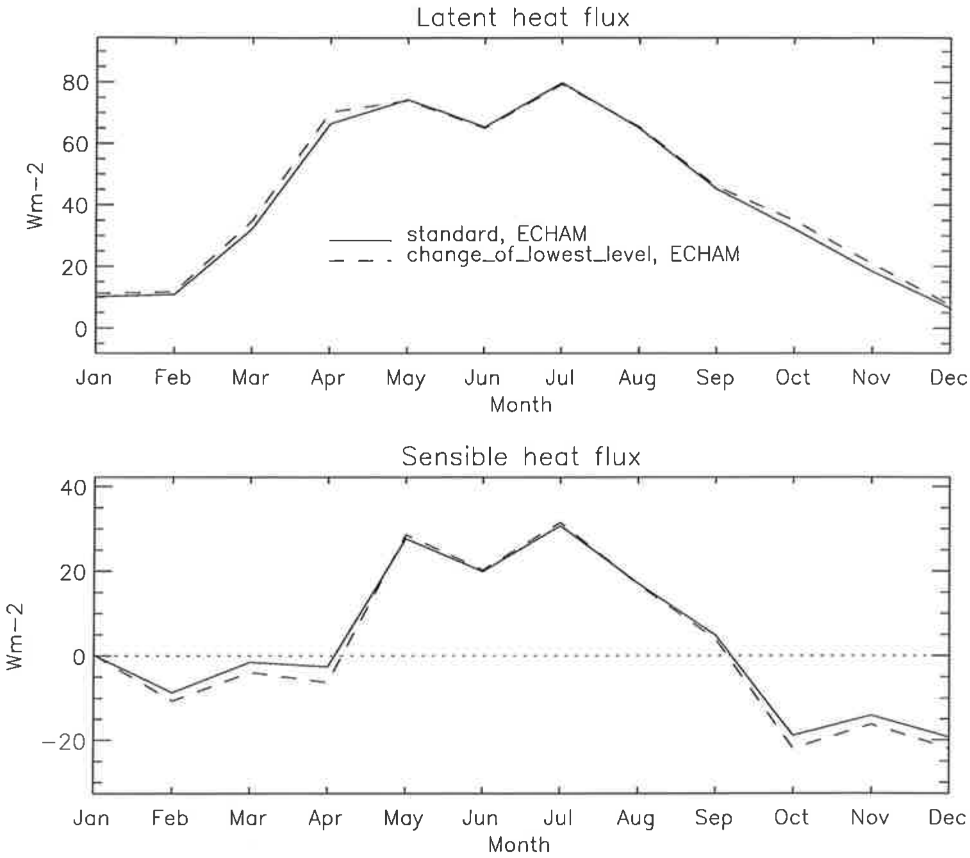

Figure 3.4: *Comparison of latent and sensible heat flux for different height of lowest model level. The lowest model level of the standard version is taken to be 30m above surface. The dashed curve labeled with 'change_of_lowest_level' represents the model simulation with the lowest model level at a height of 20m.*

is mainly caused by a too high transpiration rate during these three months. The too simple parameterization of transpiration is obviously not able to compute realistic transpiration values. Both models show a very similar evolution of monthly shortwave radiation but net radiation is clearly overestimated. The reason is the assumption of an obviously too low albedo for the Cabauw site (set to 0.15). The data from the Cabauw site suggests an albedo of about 0.3 which appears to be very high.

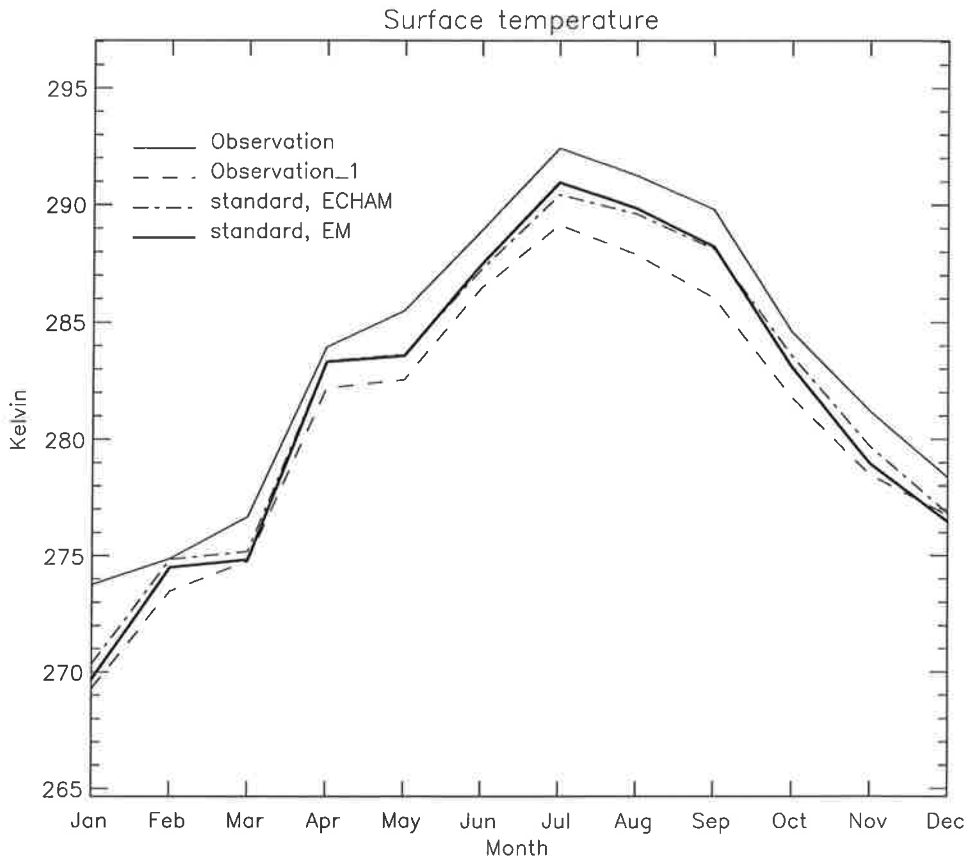

Figure 3.5: *Monthly means of observed and modeled surface temperature. The line 'Observation' represents the 2-cm-temperature; 'Observation_1' has been calculated with the Stefan-Boltzmann-Law.*

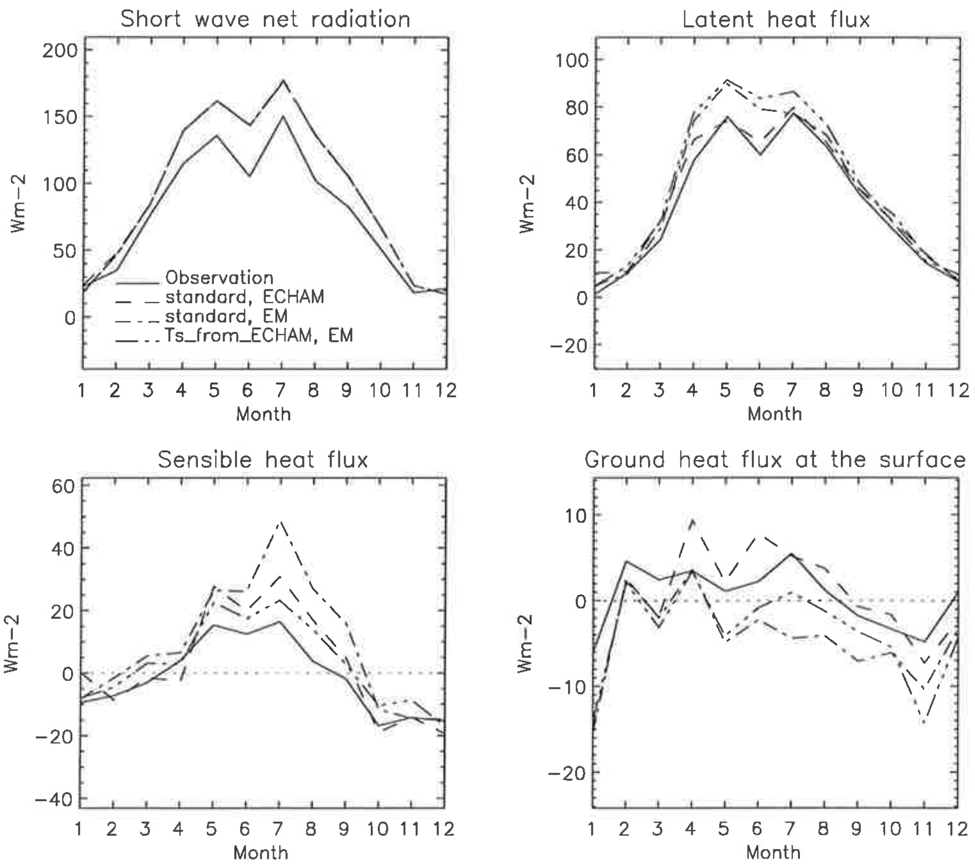

Figure 3.6: *Monthly means of latent and sensible heat flux, net shortwave radiation and ground heat flux.*

Chapter 4

Comparison of diurnal cycles and day/night annual mean values for the control experiments of ECHAM and EM

For calculating day and nighttime values, the incoming shortwave radiation was used to distinguish 'day' and 'night'. If the shortwave radiation falls below $2\mathrm{Wm}^{-2}$, it was assumed to be night. The annual ratios of 17 output values are compared in Table (4.1). It should be emphasized that the computation does not take the various lengths of day and night during winter and summer into consideration. However, because these are annual averages, this is of little importance for most quantities (an exception is e.g. snow melt). A figure equal to 1 in Table (4.1) states that the annual means for day and night are identical. Negative values indicate a change in the direction for day and nighttime. This is valid for ground heat flux, sensible heat and net radiation.
What are the main characteristics of day and nighttime values? Concerning evaporation, it can be noticed that daytime fluxes are much higher (Figure (4.1)). During the night roughly 10% of the total evaporation takes place. The reason is the diurnal cycle of potential evaporation. This again is due to the diurnal cycle of wind speed and, more important, net radiation and surface temperature (not shown). This directly influences the saturated specific humidity. The observed specific humidity at a height of 20m above ground shows only a slight diurnal cycle. Therefore, the difference $q_v - q_{sat}$ in Equation (1.42) also shows a clear diurnal cycle.

The ratio 'day/night' of bare soil evaporation is distinctly larger in EM than in ECHAM: 7.8 in ECHAM and 14.0 in EM. This indicates that daytime bare soil evaporation is more efficient in EM. In ECHAM, bare soil evaporation breaks down in late summer/autumn during the day. However, wintertime values are higher for ECHAM. This is due to the higher transfer coefficient C_h in this model and the fact that the soil is nearly saturated in both models in winter. This implies that soil moisture is no limiting factor for evaporation. For transpiration, the difference for day and night is even larger. The factor 16 shows that there is barely any transpiration during the night. Additionally, there is no annual cycle for nighttime values whereas during the day transpiration is much higher in summer than in winter. The highest value is reached in July for ECHAM because of the highest net shortwave radiation, and therefore photosynthetically active radiation PAR, which is taken as 55% of net shortwave radiation. The EM parameterization does not take into account this quantity and so does not show this feature. In spite of the small absolute values, it is striking that during the night, the EM transpirates more in winter. The

Table 4.1: *List of ratios of day- and nighttime annual values of ECHAM and EM*

parameter	ratio day/ night (ECHAM)	ratio day/ night (EM)
total evaporation from surface	9.0	11.1
latent heat flux	8.0	12.1
sensible heat flux	-1.6	-2.6
evaporation (skin reservoir)	3.4	1.8
transpiration	15.8	16.3
bare soil evaporation	7.8	14.0
skin reservoir content	0.77	0.86
soil moisture	0.93	0.96
ground heat flux at the surface	-0.90	-0.64
ground heat flux, depth 6.5cm	-0.91	-0.47
snow melt	2.2	1.5
snow sublimation	1.1	1.6
net shortwave radiation	288	240
net radiation	-3.1	-3.4
runoff due to drainage	0.88	0.97
surface runoff	0.84	0.82
albedo	0.96	0.92

reason is again due to the missing dependence of transpiration on shortwave radiation.

Concerning skin reservoir evaporation, ECHAM shows a larger difference between day and night. This can be explained by reminding the reader that in EM, the whole skin reservoir content infiltrates very efficiently and rapidly into the soil while the ECHAM parameterization allows a substantial part of the water to remain on leaves from where it evaporates at the potential rate which is much larger during the day. October is the only month where EM-evaporation is much larger during the night than during day. This is due to very high precipitation in October during the night (80mm fell during the night, 15mm during the day). This rain distribution leads to a soil which is not able to allow all the water to infiltrate and therefore to uncommonly large evaporation during night.
Are there any differences in soil water content? The whole soil water reservoir shows no difference between day and night because the water reservoir is too inert to change quickly. Experiments have shown that a disturbance of soil moisture needs several months to attain the old undisturbed conditions (not shown). A slight difference between day and night can be observed for the uppermost soil layer in the EM which is 10cm deep. However, the amplitude of the diurnal cycle is not more than 1mm or 5% of mean water content. Another feature shows the skin reservoir content which has an average content of only some tenths of a millimeter. For ECHAM, the skin reservoir has usually a higher content during night than day. The reason is the lower potential evaporation at night, i.e. after a precipitation event, water remains longer in the reservoir. The EM shows a less clear distinction between day and night.
The monthly means of the sensible heat flux for both models is directed upward during the day and reversed during the night. This is physically correct because at daytime, a strong downward net shortwave radiation leads to a heating of the ground and therefore a rising of relatively warm air parcels. During the night, total net radiation is negative for each month (in the range of 30 - 50Wm^{-2}) and leads to a cooling of the surface and a stable boundary layer. The ratio of day and night values is larger in EM. Whereas night values of both models coincide, EM produces higher values during day (up to more than 20Wm^{-2} for monthly means). Night values show almost no annual cycle while the monthly means for daytime have a marked annual cycle, which is due to stronger turbulence and stronger shortwave radiation heating.
Ground heat flux also changes its direction from day to night (Figure (4.1)). At daytime, ground heat flux is directed into the soil in both models. Only a small annual cycle is observed. This cycle is more visible at night. It is rather surprising that absolute values during the night are

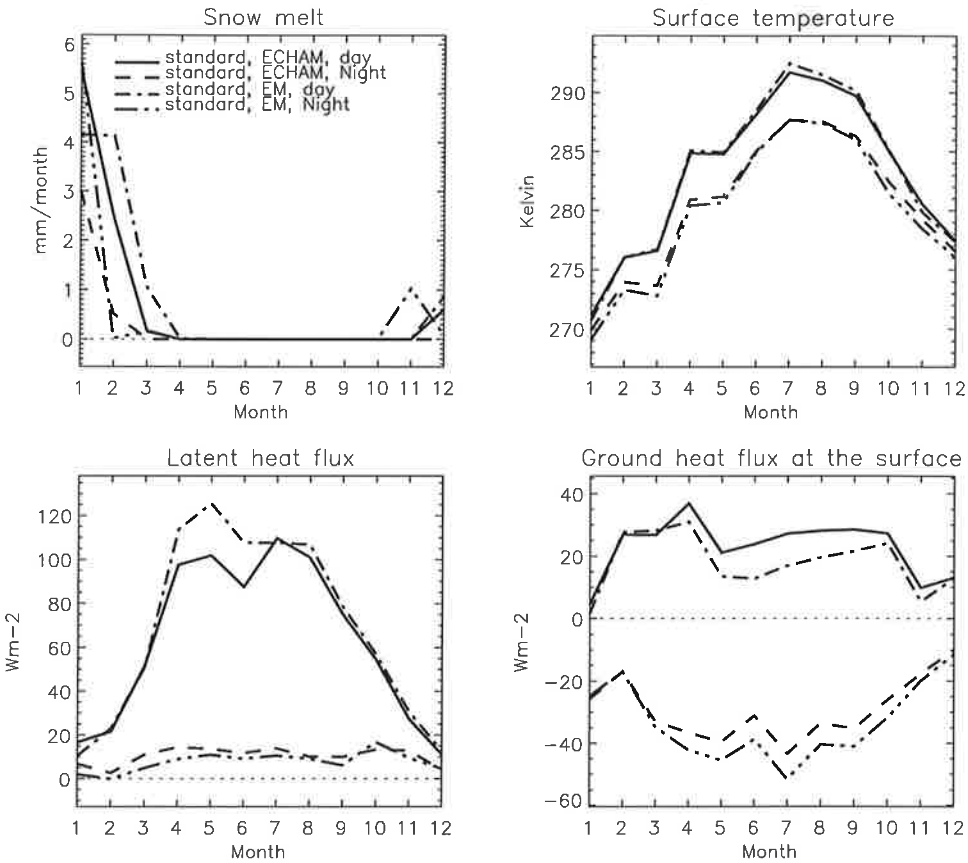

Figure 4.1: *Monthly averages of day- and nighttime for latent heat flux, surface temperature, ground heat flux and snow melt for the ECHAM and EM.*

mostly larger than corresponding data at daytime. For the EM, this result can be directly derived from Equation (1.13) and the evolution of the surface and soil temperature. During the night, the surface temperature is distinctly lower than the soil temperature, and the second term in Equation (1.13) is more important because the difference between T_M and T_U is smaller than T_S - T_U. This is also clear from a physical point of view: During the night, the net radiation balance is negative and thus the heat stored in the soil during the day flows upward to warm the surface. For daytime, conditions are opposite and so is the ground heat flux.

The observed ground heat fluxes and turbulent fluxes can also be divided into 'day' and 'night' (not graphically shown). The modeled ground heat fluxes during the night are roughly three times higher than the observed ones whereas absolute differences during the day are much lower. The overestimation of the amplitude is mainly due to the inertia of the too deep upper soil layer of both models. The sensible heat flux is overestimated during the day but underestimated at night. The underestimation lies in the order of 5-10Wm^{-2} for both models whereas at daytime, ECHAM works less efficiently. The main reasons are incorrect surface temperatures and uncertainties with the stability function for stable conditions which often occur during the night (see also Chapter (5.2)).

The snow melt shows clear differences in ECHAM and EM. The most striking feature is the

ratio of snow melt during the night and day. In January, the snow melt of ECHAM at daytime is nearly fourfold more efficient during the day than during the night. The error introduced by the different length of day and night in January has been previously eliminated. The same ratio is determined for EM to be slightly more than 1.5. This means that the EM-parameterization also melts snow during night very efficiently. The reason can be found when analysing the formulae: Snow melt at the lower boundary of the snow deck is also calculated in EM. If snow melts at the upper boundary of the snow pack, water can infiltrate and possibly refreeze. These processes reduce differences between day and night. Snow depth is almost the same at day and night. The same is valid for snow sublimation in the ECHAM, while EM shows slightly higher values during the day which is expected because of the higher wind speeds.
The drainage processes and surface runoff are not very strongly dependent on daytime. Differences in surface runoff and drainage during winter can mostly be explained by comparison with precipitation distribution and soil moisture content. Differences between day and night show more scattering for surface runoff than for drainage. This is due to a larger inertia of the drainage processes. The annual mean day/night ratios of both quantities are at first approximation equal to 1.
Instead of only analysing the day and night values, it is also worthwhile to plot diurnal cycles. The diurnal cycle has been calculated for each month separately. In the following, only the four quantities which can be validated against Cabauw observations are presented: sensible and latent heat flux, surface ground heat flux and surface temperature.

The mean diurnal sensible and latent heat fluxes are shown in Figures (4.2) and (4.3).

The most striking characteristic of the latent and sensible heat fluxes is the phase-lag of the ECHAM model of the order of two hours compared to the observational data (Figure (4.2) and (4.3)). The reason can be found in the large ground heat flux in the morning hours (Figure (4.4)). After sunrise, far too much energy goes into the soil to warm the first soil layer: The thermal inertia of the too deep soil layer causes a delayed rise in the latent and sensible heat flux. Another reason for the overestimation of the ground heat flux is the so-called time-truncation problem in ECHAM (Betts et al., 1993).
A backward shift in the modeled diurnal cycles allows a reasonable fit of latent heat. This backward shift is also typical for EM. However, the phase lag is somewhat smaller. During the night, the latent heat flux is overestimated by the ECHAM model. This may be attributed to features not yet understood which reflect on the parameterization of fluxes under stable conditions. The measured latent heat seldom exceeds 10Wm^{-2} during the night whereas the model occasionally reaches values of 25Wm^{-2}. The observed latent heat flux is also directed to the ground (formation of dew) which is not the case in the model results. This applies to monthly means of diurnal cycles but not to a single day.
The deviation of modeled sensible heat fluxes from the observed ones (Figure (4.2)) show a large variability from month to month. The observation shows a clear and smooth diurnal cycle while the cycle of both models is less smooth. In April and October, the EM fits the observations much better than ECHAM, but in late summer EM produces a too high maxima. This overestimation can be explained with the strong overestimation of surface temperature at noon (Figure (4.5)). It seems that the EM produces better results in spring and autumn. It has to be emphasized that EM results could strongly be improved by taking a more reasonable lower boundary condition for the temperature T_U.
The modeled ground heat flux (Figure (4.4)) rises very steeply after sunrise and reaches its highest value three hours after sunrise. The maximum value is about 100Wm^{-2}. This far too high value is reached more than two hours too early. This is inherent in both models. The measured ground heat fluxes have smaller maximum values (maximum summer values not over 50Wm^{-2}) and a smoother diurnal cycle. Obviously, too much heat can flow into the ground during the morning hours. Consequently, during the night, the heat flux from the ground to the atmosphere is overestimated by a factor of two to three. The main reason for this result is

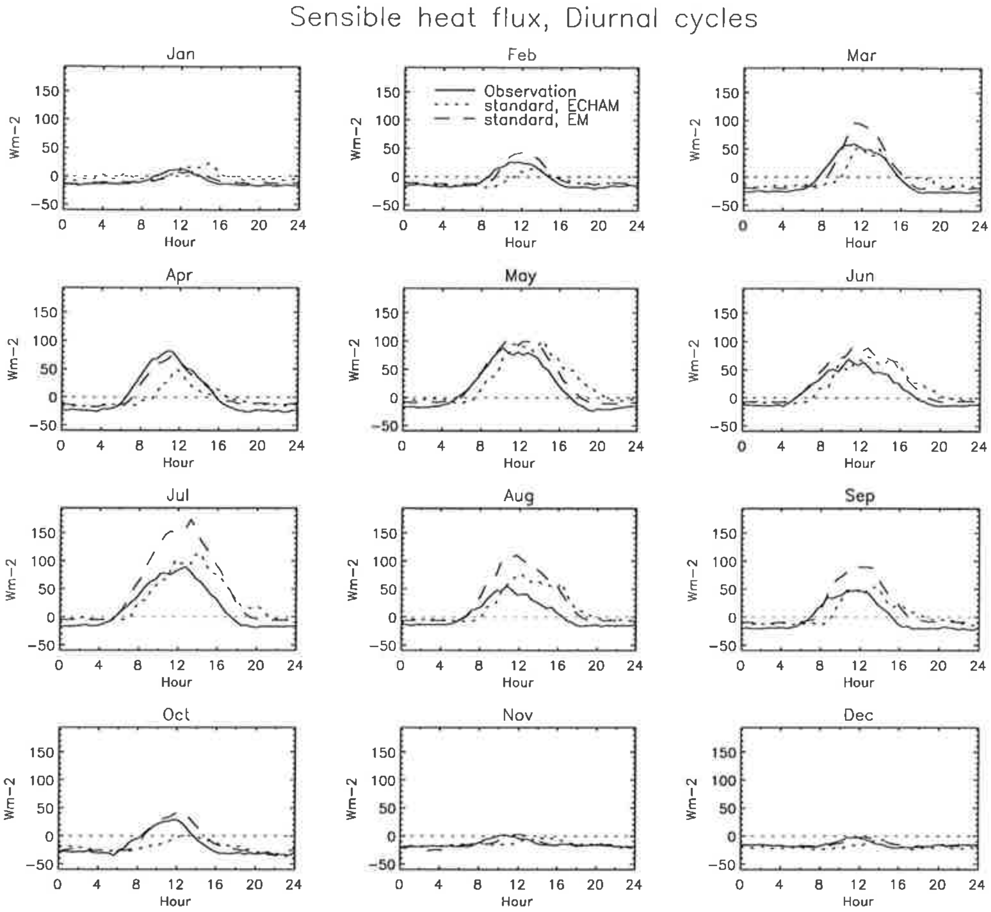

Figure 4.2: *Comparison of the diurnal cycles (sensible heat flux, averages for each month) of both models with observation.*

the thermal inertia of the first soil layer, which has a thickness of 6.5cm in ECHAM and about 10cm (soil type 3) for EM. The second reason is the above mentioned time-truncation problem in ECHAM. This first problem can be partly eliminated by reducing the deepness of the uppermost soil layer. Therefore, an (ECHAM) experiment was performed with a halved thickness of the uppermost soil layer (Figure (4.6)). We can recognize a clear improvement in the soil heat flux. The results are more reasonable and are in better agreement with the observations. The ground heat flux 6.5cm under the surface shows a very similar characteristic and a somewhat smaller amplitude than the ground heat flux at the surface. This is to be expected because the heat which can be stored in the uppermost soil layer is small.
The comparison of the surface temperature is a very delicate matter. The surface temperature which has been chosen for comparison is the temperature measured at a depth of 2cm. The ECHAM model calculates (for snow free conditions) a temperature which is equal for the surface and the whole upper soil layer, while EM determines a temperature valid only for the surface. So the representation of the temperature at the surface and the uppermost few centimetres of the soil is very poor in the ECHAM. Nevertheless, results should be briefly discussed. The modeled surface temperature performs a much higher amplitude and increases faster after sunrise than the observation. The thermal inertia of the first soil layer mainly leads to this effect. Moreover,

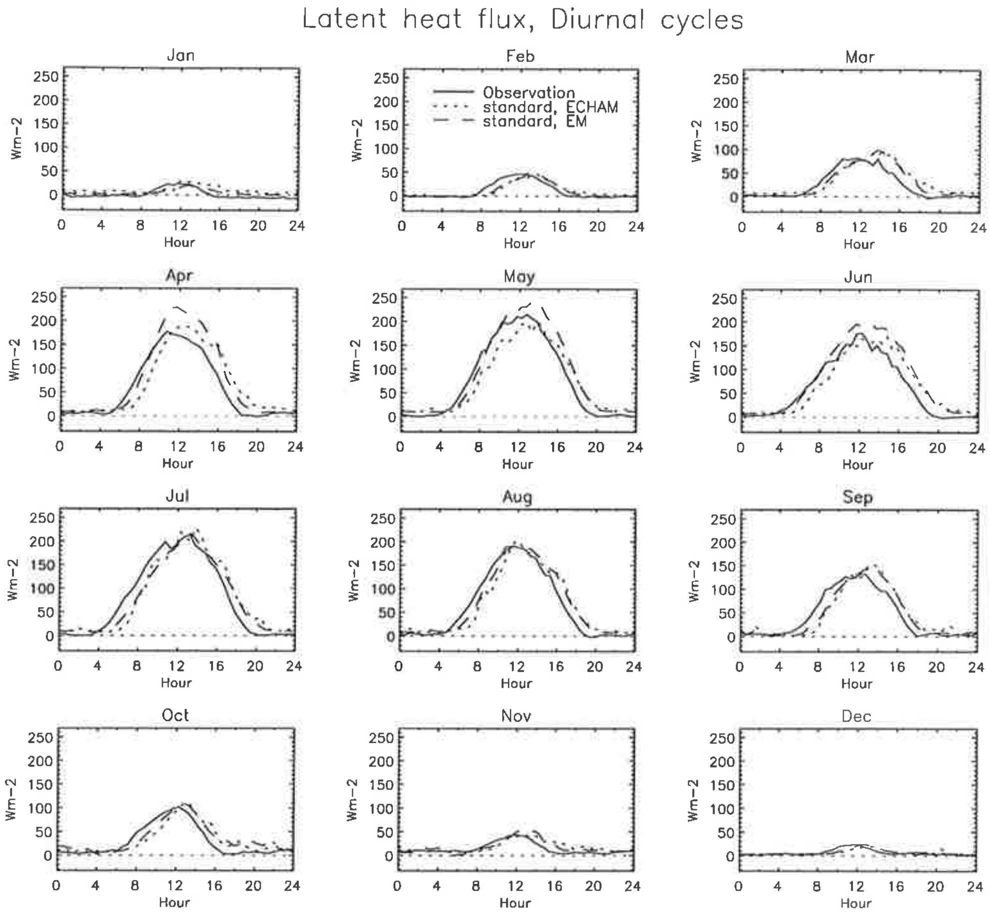

Figure 4.3: *Comparison of the diurnal cycles of latent heat flux (averages for each month) of both model with observations.*

there is grass vegetation at the Cabauw site which prevents the radiation from penetrating and warming the soil. During the night, cooling is slowed under grass and in the soil. This leads to a significantly lower modeled than observed temperature during the night for all months and both models. The effective skin temperature, computed with the upward longwave radiation shows large differences to the models' surface temperature (Fig. (3.3)). The EFR-method in the EM is able to simulate the surface temperature for two preselected frequencies of harmonic forcing without amplitude or phase errors as compared to the equation of heat conduction. Therefore, the phase error of the surface temperature is due to the corresponding error in the forcing, i.e. the ground heat flux. The deviation of the forcing from a harmonic function probably contributes only slightly to the observed phase error. The phase error may also be somewhat influenced by the assumption of homogeneous soil.

For transpiration and bare soil evaporation, no measurements are available. Nevertheless, it is of some interest to show differences in both models. Transpiration starts to increase earlier in the morning in the EM. The phase lag amounts to about one hour. Maximum transpiration is also often reached earlier for EM, but differences are not as clear as for the onset in the morn-

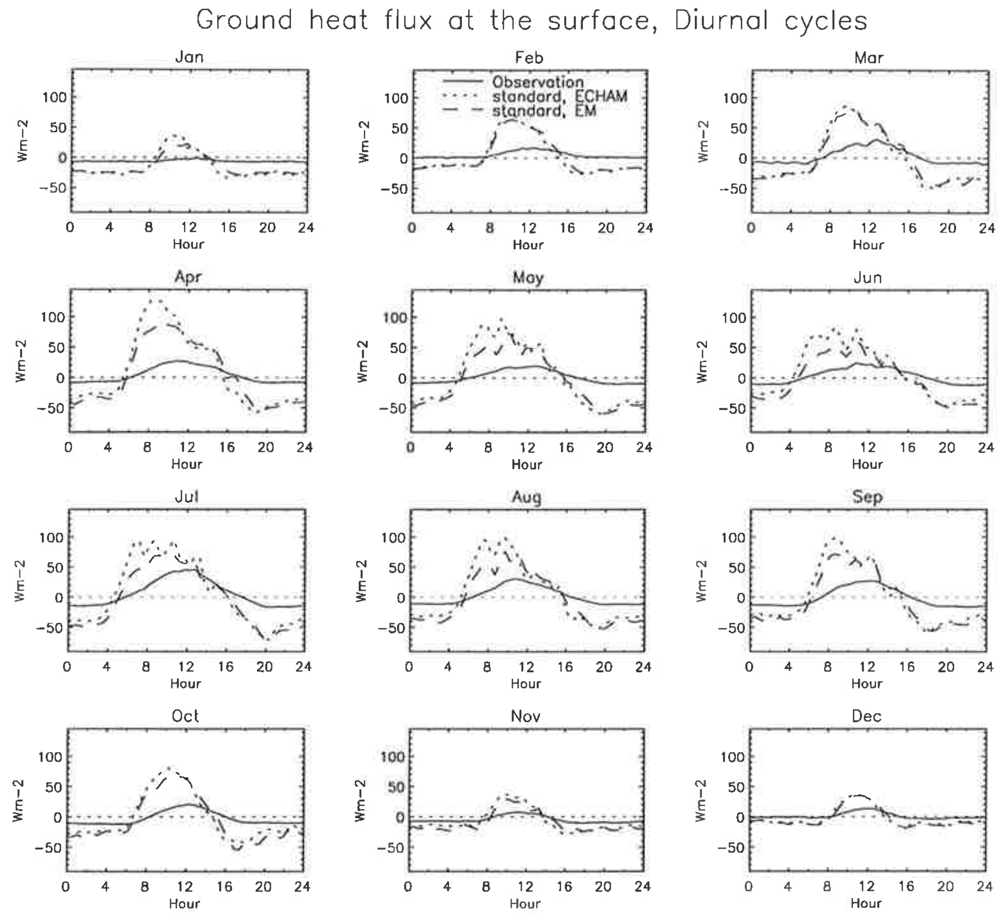

Figure 4.4: *Comparison of the diurnal cycles of surface ground heat flux (averages for each month) of both models with observations.*

ing. Maximum values are distinctly higher for EM in late spring (April to June) but slightly lower in summer (July - September). It seems that transpiration in EM is too high in spring and therefore falls below ECHAM values for late summer because of limited soil water. The diurnal cycle of transpiration follows very well the cycle of potential evaporation because EM - parameterization only takes potential evaporation, soil moisture and root depth into account. Soil moisture for the uppermost soil layer performs only a very weak diurnal cycle and the root depth is a constant. For ECHAM, the evaporation efficiency E (Equation (1.47)), which has a clear diurnal cycle, is also important.
A phase lag of bare soil evaporation is observed in both models. This quantity increases about one to two hours earlier in the EM. Moreover, maximum values are much smaller for the ECHAM model (mainly during late summer). The reason is mainly the different parameterization and not the lower soil moisture content in the ECHAM model. This will be shown in Chapter (5).
How fast can the surface runoff and drainage follow the precipitation? Surface runoff follows the precipitation pattern very well whereas drainage shows only a small or no diurnal cycle (Figure (4.7)). This is physically correct because surface runoff is a direct consequence of precipitation while drainage is a slow process and includes the whole soil. The same is found for EM. However, individual months partly show rather large differences in the evolution of the diurnal cycle of

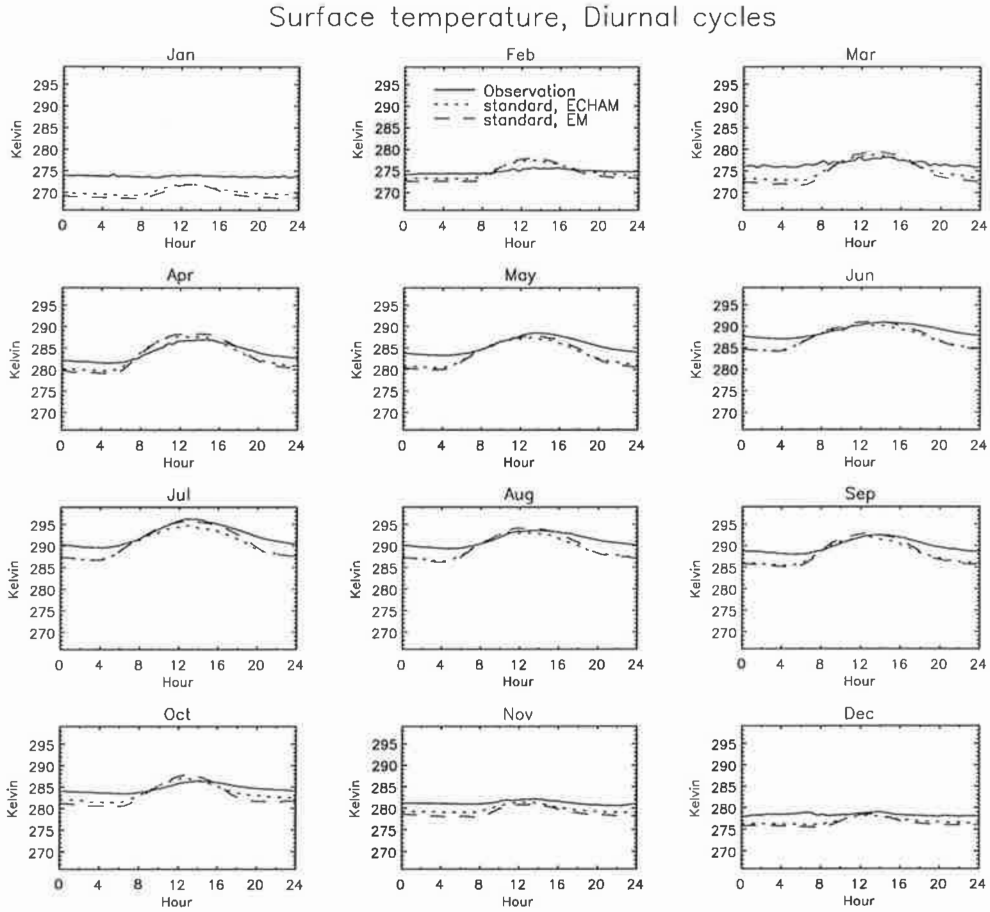

Figure 4.5: *Comparison of the diurnal cycles of the surface temperature (averages for each month) of both models with observations.*

runoff. Besides that, surface runoff in the EM does not follow the precipitation as instantaneously as in ECHAM because surface runoff in EM includes the lateral water flow out of the uppermost soil layer.

The phase shift between the total energy flux at the surface, the surface temperature and soil heat fluxes will be treated both theoretically and experimentally. The results of the experiments for the EM and ECHAM are shown in Fig. (4.8) and (4.9). We recognize that the surface temperature reaches its daily maximum about three hours later than the surface soil heat flux and roughly one to two hours later than the soil heat flux at a depth of 6.5cm. The total energy flux (net radiation plus turbulent heat fluxes) is in phase with the surface soil heat flux in both models. Whereas in EM the curves lie exactly upon another, the ECHAM total energy flux has a distinctly higher amplitude than the surface soil heat flux (for ECHAM shown in Fig. (4.9)). If one assumes a period of the total energy flux at the surface of P=24 hours, the surface temperature has a phase shift of about P/8 to the total energy flux at the surface. Moreover, one recognizes the decreasing amplitude of soil heat flux with increasing soil depth. These results show the inertia of the soil very well. This phase shift is also observed on an annual basis. The highest surface energy fluxes are simulated in May, whereas the highest surface temperature

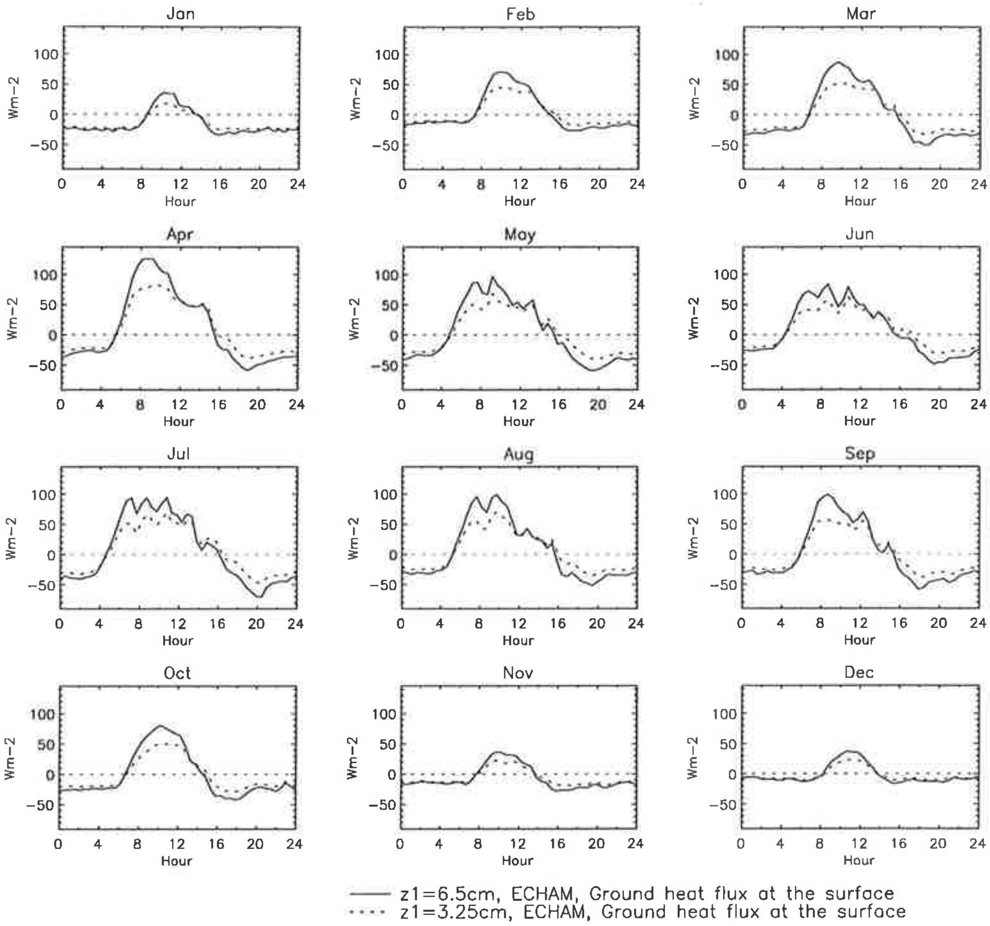

Figure 4.6: *Comparison of the diurnal cycles of the ground heat flux for the ECHAM model with a thickness of the first soil layer of 6.5cm and 3.25cm.*

occurs about two months later.

The heat conduction equation for a homogeneous soil can be formulated in one dimension as

$$\frac{\delta T}{\delta t} = k\frac{\delta^2 T}{\delta^2 z} \tag{4.1}$$

with

k	Thermal diffusivity [$m^2s^{-1}K^{-1}$]
t	Time [s]
T	Surface temperature [K]
z	Depth (zero point at the soil surface) [m]

leads with the following statement of the temperature for z < 0

$$T(0,t) = T_0 + \Delta T_0 sin(\omega t) T(\infty, t) \tag{4.2}$$

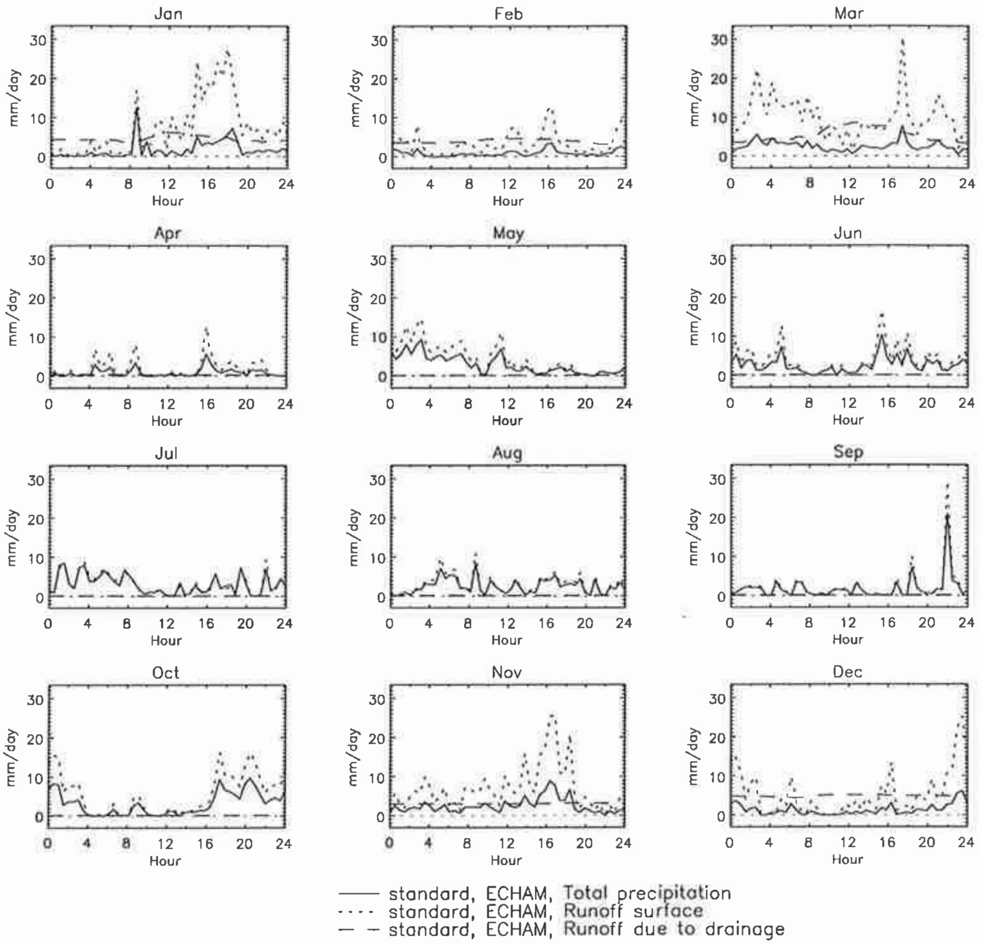

Figure 4.7: *Monthly averages of diurnal cycles of precipitation, surface runoff and drainage for the ECHAM model. Values of drainage and surface runoff are multiplied by 10.*

to the following solution

$$T(z,t) = T_0 + \Delta T_0 exp(-z)\sqrt{\frac{\omega}{2k}} sin\left(\omega t - z\sqrt{\frac{\omega}{2k}}\right) \tag{4.3}$$

with

$T(z,t)$	Temperature at depth z and time t
ω	Frequency of the surface temperature.

The thermal diffusivity can be written as $k = \frac{\lambda}{\rho c}$ where λ is thermal conductivity, c the heat capacity and ρ the density of the soil.
The maximum temperature in a certain depth can be determined by setting the first derivative with respect to z equal to 0. This leads to

$$t_{max} = \frac{1}{\omega}\left(\pi/2 + z\sqrt{\frac{\omega}{2k}}\right) \tag{4.4}$$

This equation expresses the increasing phase shift of the temperature (and so heat flux) with soil depth. Typical values for the Cabauw site are

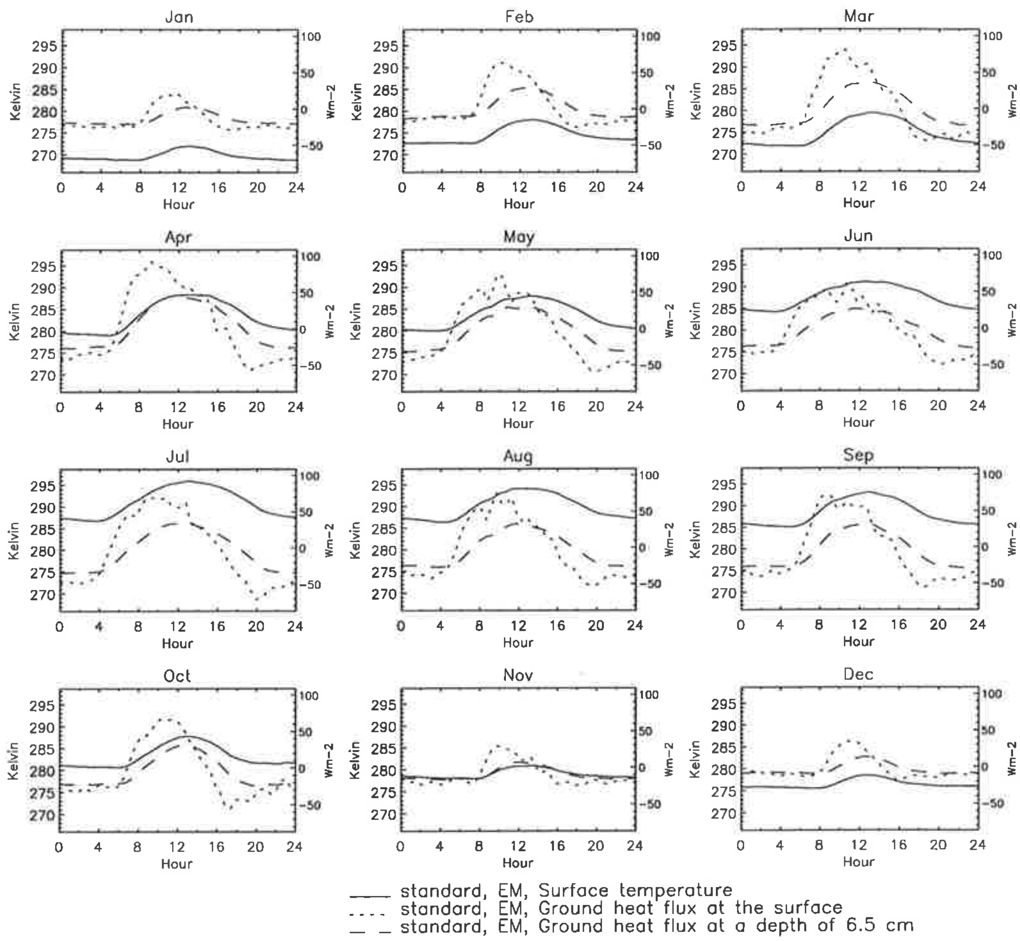

Figure 4.8: *Monthly averages of diurnal cycles of surface temperature, ground heat flux at the surface and at a depth of 6.5cm for EM.*

$$\begin{aligned} \lambda &= 1.4\mathrm{Wm}^{-1}\mathrm{K}^{-1} \\ \rho c &= 2.43\ 10^6\ \mathrm{Jm}^{-3}\mathrm{K}^{-1}\ \text{(loamy sand)} \end{aligned}$$

and lead to a phase shift between temperature at the surface and a depth of 6.5cm of about two hours. This agrees quite well with the modeled difference of the phase shift of ground heat fluxes. It can be easily shown that the phase shifts of the soil temperature and the soil heat flux are the same.
The ground heat flux G(z,t) at the depth z in a homogeneous soil is

$$G(z,t) = -k\rho c \frac{\delta T}{\delta z} \tag{4.5}$$

The use of the solution (4.3) in Equation (4.5) yields a result that surface ground heat flux is a maximum for $t_{max} = \frac{\pi}{4\omega}$. If we compare the maxima of the surface temperature and the surface ground heat flux we get

$$\Delta t_{max} = t_{max}(temp.) - t_{max}(heatflux) = \frac{\pi}{2\omega} - \frac{\pi}{4\omega} = \frac{\pi}{4\omega} = P/8 \tag{4.6}$$

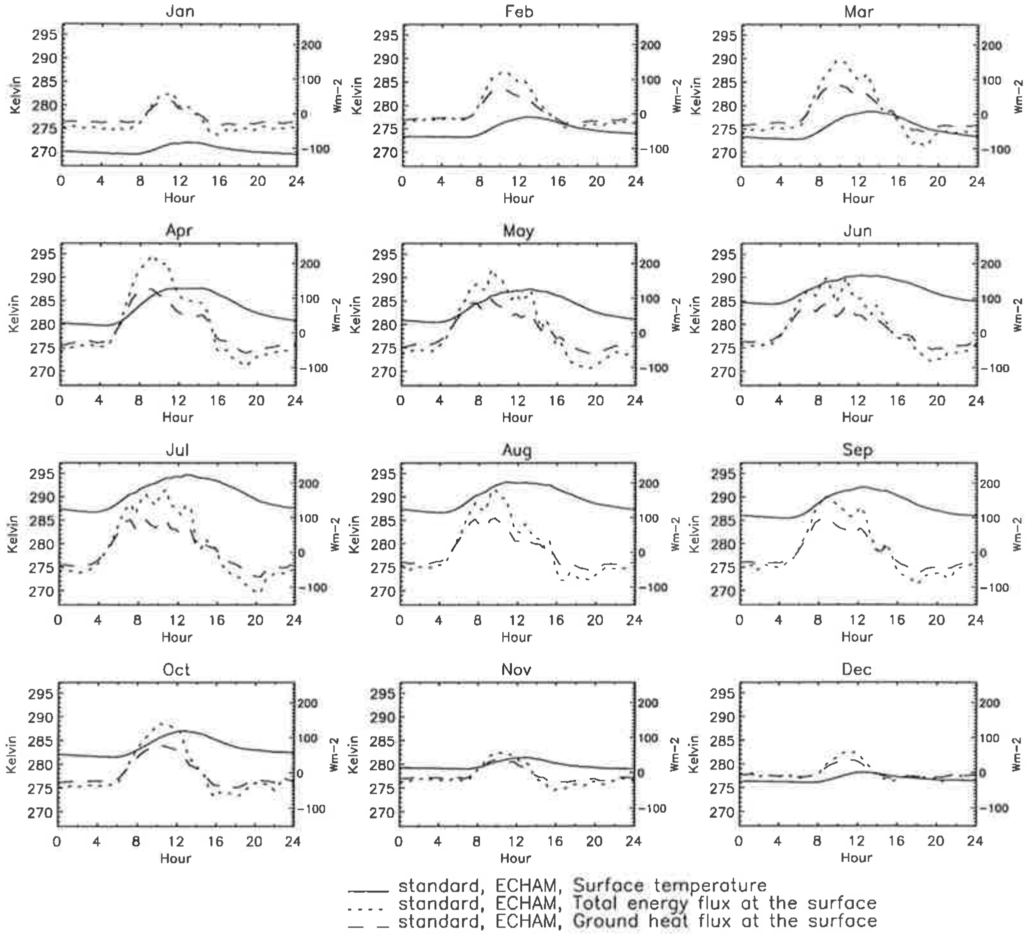

Figure 4.9: *Diurnal cycles of surface temperature, total energy flux and surface ground heat flux for the ECHAM model.*

where P is the period of surface temperature (P=24 hours). This means that the maximum surface soil heat flux occurs 3 hours earlier than the maximum surface temperature. This important result is confirmed by both models. Moreover, the observational data of Cabauw shows this characteristic. The phase shift seems to be slightly smaller in the measurements, but the differences are not significant.

A short calculation leads to the soil depth in which the soil temperature and the heat flux are in phase: $z = 33600s\sqrt{2k\omega}$ and with the above supposed soil parameters to z=10cm.

It is a somewhat surprising result that both models are able to capture these relations of phase shifts. However, it confirms again that the EFR-method of EM is a useful tool to calculate surface soil heat fluxes.

Chapter 5

Comparison of the ECHAM- and EM-parameterizations with other parameterization formulae

In this Chapter, the impact of different parameterizations on the simulation results will be investigated. For this reason, we examine the influence when replacing an EM-parameterization by the ECHAM one. For this study, the parameterization of bare soil evaporation and the stability function has been chosen to show which differences can appear when using different parameterizations.

5.1 Bare soil evaporation

Evaporation over bare soil involves very complex mechanisms so a lot of parameterizations can be found to treat this problem. The modeling of evaporation requires a good resolution close to the soil-atmosphere interface in order to ensure the continuity of water fluxes. However, these models are not suitable for use within large scale models because they need very short time steps and large memory storage. Therefore, simpler parameterizations must be used. The available parameterizations can be divided into

- bulk aerodynamic methods and
- threshold formulations.

The bulk aerodynamic methods provide an explicit relation between the bare soil evaporation E_g and the near-surface water content w_g by using a parameterization of the surface specific humidity. In the threshold formulation method, evaporation proceeds at the potential rate until the soil moisture supply is sufficiently depleted. Mahfouf and Noilhan (1991) (see for references therein) compares the formulae with in situ data (located in Montfavet, France) from bare soil. The conclusion is that the formula of Noilhan and Planton (Eq. (5.2)) fits the data the best while the threshold methods strongly underestimate surface evaporation. The bulk-aerodynamic formulation can be divided into the so-called 'α-methods' and 'β-methods'. In the β-method, the whole process of evaporation is described from the water level to the atmosphere. All methods used in this study are shortly described.
The α-method needs the determination of the factor α in the formula

$$E_g = \frac{\rho}{R_a}[\alpha q_{sat} - q_a] \tag{5.1}$$

with

E_g	Bare soil evaporation [mms^{-1}]
q_a	Specific humidity of air [$kgkg^{-1}$]
q_{sat}	Saturated specific humidity at the surface temperature [$kgkg^{-1}$]
R_a	Aerodynamic resistance [sm^{-1}]
α	Relative humidity of air at the land surface [mm^{-1}].

The factor α is computed as

$$\alpha = \min\left(1, \frac{1.8w_g}{w_g + 0.3}\right) \quad \text{(Barton, 1979)} \tag{5.2}$$

$$\alpha = \min\left(1, \frac{1.8w_g}{0.7w_g + 0.4}\right) \quad \text{(Yasuda and Toya, 1981)} \tag{5.3}$$

$$\alpha = \frac{1}{2}\left[1 - \cos(\frac{w_g \pi}{FC})\right] \quad \text{(Noilhan and Planton, 1989)} \tag{5.4}$$

with

FC	Field capacitity
w_g	Near-surface water content.

The β-formulation is based on

$$E_g = \frac{\rho}{R_a}\beta[hq_{sat} - q_a] \tag{5.5}$$

h	Relative humidity of the air adjacent to the water
β	Moisture availability parameter.

The factor β is computed as

$$\beta = \min\left(1, \frac{w_g}{0.75PV}\right) \quad \text{(Deardorff, 1978)} \tag{5.6}$$

$$\beta = \frac{R_a}{R_a + R_{soil}} \quad \text{(Sun, 1982)} \tag{5.7}$$

and

$$R_{soil} = 3.5\left(\frac{PV}{w_g}\right)^{2.3} + 33.5. \tag{5.8}$$

R_{soil} is the resistance to water diffusion in the large soil pores.
The threshold formulations are based on

$$E_g = \min\left[\rho_w E_t, \frac{\rho}{R_a}(q_{sat} - q_s)\right] \tag{5.9}$$

with

ρ_w	densitiy of water [kgm^{-3}],

and the water flux

$$E_t = 2D\frac{w_g - PWP}{d_1} - K \quad \text{(Mahrt and Pan, 1984)} \tag{5.10}$$

$$E_t = \frac{Dw_g\pi^2}{4d_1} \quad \text{(Abramopoulos et al., 1988)} \tag{5.11}$$

with

D	Near-surface hydraulic diffusivity $[m^2 s^{-1}]$
d_1	Depth of the top soil layer [m]
K	Near-surface hydraulic conductivity $[ms^{-1}]$
PWP	Permanent wilting point.

The relative humidity of the air adjacent to the water h is set to 1 in both models described above. Therefore, the difference in the presented α- and β-models is that α is multiplied by q_{sat} but β by the saturation deficit $(q_{sat} - q_a)$.
Figure (5.1) shows the evolution of α (thin curves), β (thick lines) and E_t for the soil type of loamy sand which is the most frequent soil type in Central Europe. The aerodynamic resistance R_a was set to $50sm^{-1}$. We recognize that the models of Barton (1979) and Yasuda and Toya (1981) lie close together, the first gives slightly higher values for α. The model of Noilhan and Planton (1989) gives distinctly lower values for α for very dry soils but higher values for soil moisture contents normally observed over Central Europe. The soil in this model already evaporates at a potential rate when the soil moisture equates the field capacity whereas for the other models this is only true for soil moistures close to the volume of pores. The cosine evolution of α in Noilhan and Planton (1989) is very similar to the parameterization implemented in ECHAM (Eq. (1.44)).
The β factor of the two presented models differs quite strongly. For low soil moistures, the model of Sun (1982) produces a higher water vapour flux whereas for wetter soils, the reverse is true. The model of Sun (1982) is the only model which does not reach potential evaporation even for totally water filled soils.
The threshold formulation models incorporate a linear increase of E_t with increasing soil moisture content, but the model of Mahrt and Pan (1984) assumes lower threshold values. The Dickinson model, which can be switched on in EM, is also a threshold formulation.

It is now of some interest to see how the different parameterizations work in the real model environment. Since the EM includes several soil layers for water, it is better to test the influences of different formulae in the EM.
Figure (5.2) depicts the influence of the different parameterizations on the monthly means of bare soil evaporation for the Cabauw site. It is straightforward to notice that huge differences occur. This indicates how difficult and uncertain the parameterization of bare soil evaporation is currently. We recognize that the 'standard-case' calculates a bare soil evaporation which coincides with the maximum curve of the bulk aerodynamic formulation. The threshold formulations seem to overestimate bare soil evaporation. The bare soil evaporation lies close to the potential rate during the period October to June which is unrealistic. The ECHAM formula produces, in the monthly average, no downward directed bare soil evaporation (formation of dew) while the models of Barton (1979) and Yasuda and Toya (1981) do. The two models using the α method give very low evaporation rates which are surely too low for Central Europe. The ECHAM parameterization produces lower evaporation than the EM formulation. Above all, during winter and spring, potential evaporation is reached for the EM formula but not for the ECHAM parameterization. During July, the absolute difference is largest. The ECHAM parameterization seems to be influenced more by warm and sunny weather with high net shortwave radiation which is the characteristic of July. According to the paper of Mahfouf and Noilhan

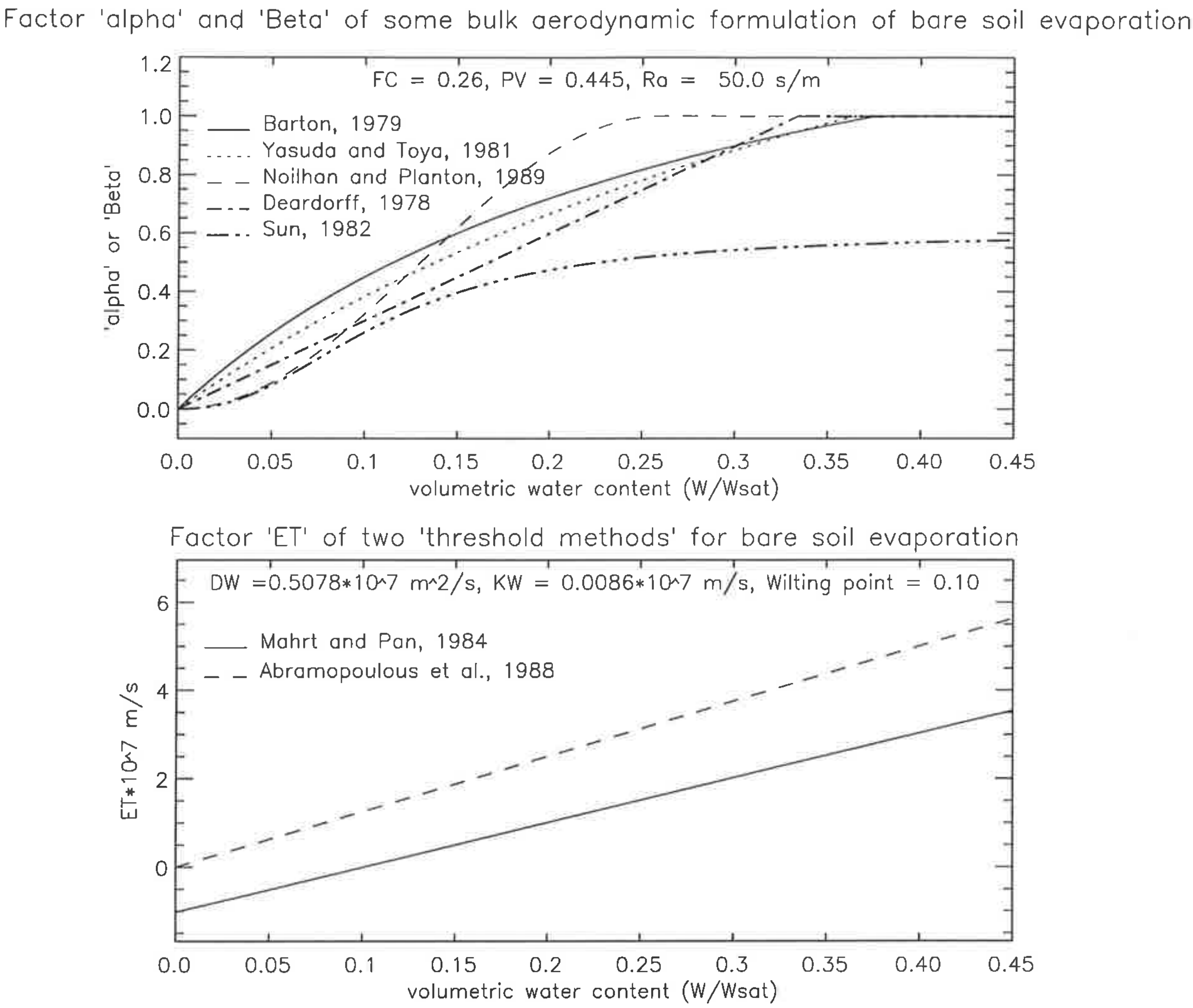

Figure 5.1: *Relative humidity of air at the land surface α, moisture availability parameter β and E_t as a function of relative water content. FC is the field capacity, PV the porosity (total water-holding capacity) and R_a the aerodynamic resistance. The hydraulic diffusivity D_W and the hydraulic conductivity K_W have been defined in Equation (1.31). The equation defining α β are given in Eq. (5.1) - (5.6); whereas E_t is given in Eq. (5.10). Soil type is loamy sand.*

(1991), the method of Noilhan and Planton (1989) fits the results the best. Therefore, we can assume that the ECHAM parameterization is more efficient to catch the right rate of bare soil evaporation because these two formulae are very similar.

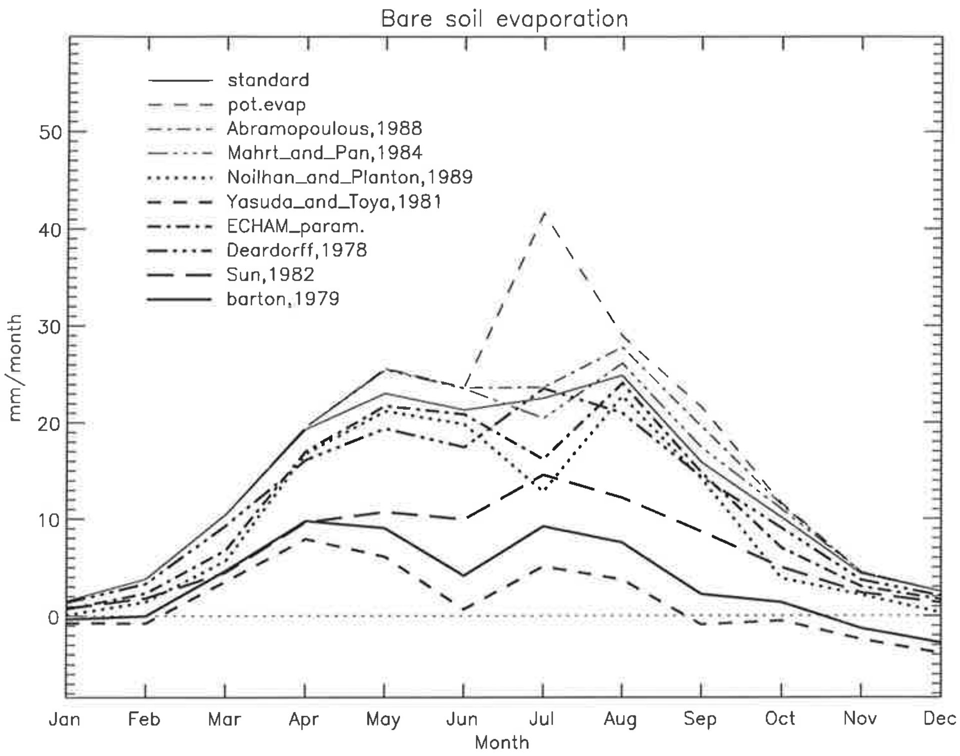

Figure 5.2: *Monthly means of bare soil evaporation for different parameterizations of bare soil evaporation. The formulae all are built in the EM. For comparison the standard version of EM is also shown. The abbrevation 'pot.evap' means that potential evaporation is always assumed and the curve 'ECHAM_param.' shows the result when using the ECHAM parameterization for bare soil evaporation within EM.*

5.2 Stability function

Measurements in Greenland during the year 1991 suggest that for stable situations the use of Webb's formula (Webb, 1970) for the stability function is preferred to the formulation by Louis (Louis, 1979) which is used in the ECHAM and EM. The stability functions for stable situations are

$$\Phi_h = \left(1 + \frac{15Ri}{\sqrt{(1+5Ri)}}\right)^{1/2} \qquad (Louis,\ 1979) \tag{5.12}$$

$$\Phi_h = (1 - 5.2Ri)^{-1} \qquad (Webb,\ 1970) \tag{5.13}$$

where Ri is the Richardson number. These two curves are plotted in Figure (5.3). We recognize the very steep increase in the Webb parameterization for increasing stability whereas the Louis version shows nearly a linear increase as a function of the Richardson number.

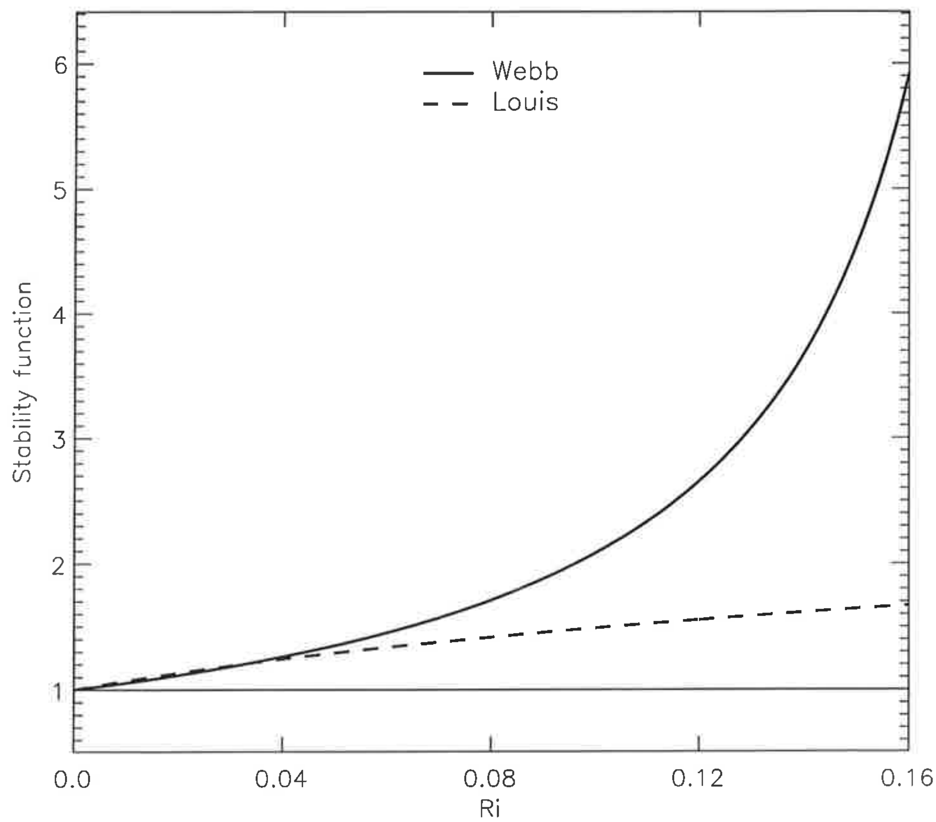

Figure 5.3: *Stability function Φ_h of Webb and Louis as a function of the Richardson number Ri.*

One can show that the correction function f_h in Equation (1.51) can be written as

$$f_h = [\Phi_m \Phi_h]^{-1} \tag{5.14}$$

We can therefore conclude that Webb's correction function f_h decreases much faster to zero than Louis' formulation. Differences are larger the more stable the situation is. We therefore expect larger differences of turbulent heat fluxes during night and winter. This is presented for the latent heat flux in Figure (5.4). We observe the lower fluxes during the colder season when using Webb's formulation which suppresses turbulence more efficiently than the alternative theory. This leads to a decreased drying of the soil during winter and therefore, in summer, Webb's formulation is able to evaporate more. The difference in relative soil moisture amounts to about 10% in winter and 5% in summer which is in the order of the influence of a change of the leaf area index from 1 to 5. Surface temperature is also strongly dependent on the chosen formulation: Winter values (monthly averages) differ by one half to one degree. The reduction of turbulence and the exchange of air when using Webb's formula leads to lower winter temperatures. This illustrates that the replacement of the stability function has an enormous influence on the model results.

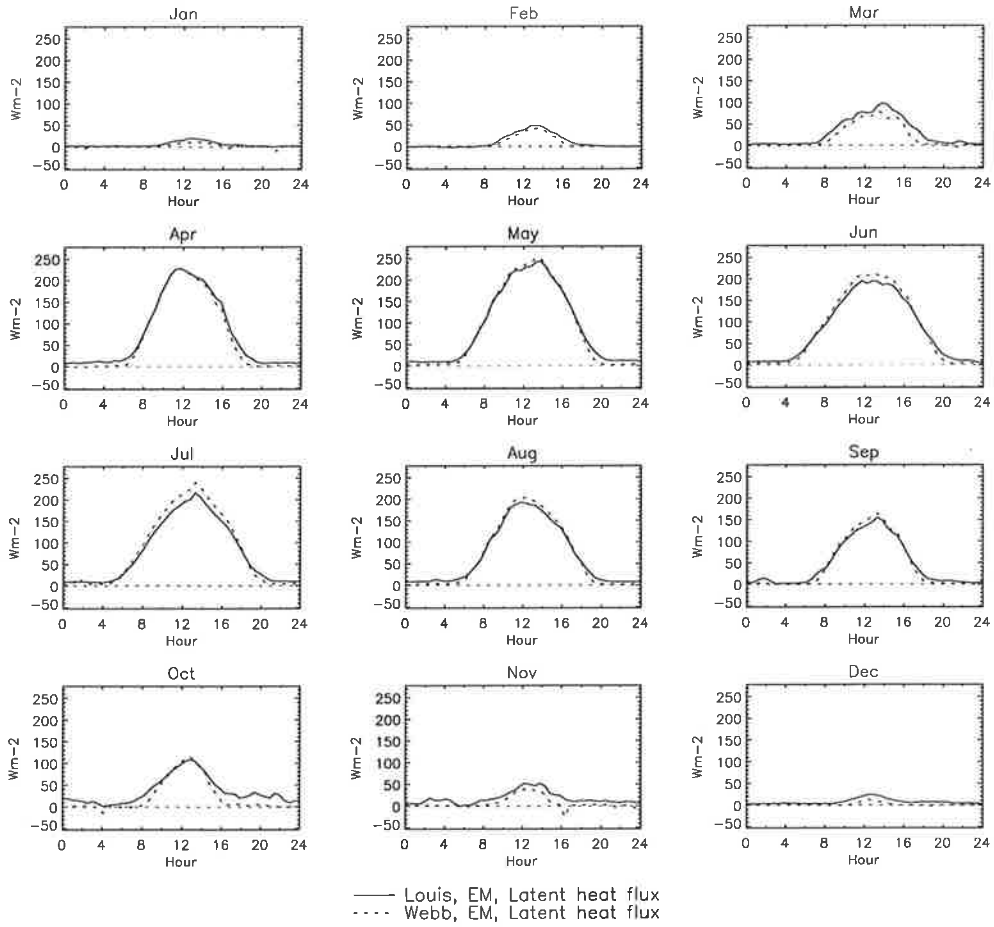

Figure 5.4: *Diurnal cycles of latent heat flux (monthly means) for the Louis (1979) and Webb (1970) parameterizations for stable situations (EM).*

Chapter 6

Comparison of the ECHAM3 and ECHAM4 land-surface schemes

The land-surface schemes of ECHAM3 and ECHAM4 have only minor differences.
An effective modification consists of a new definition of the relative humidity h at the surface (Eq. (1.44)). The new formulation for h has been implemented to avoid unrealistically large evaporation rates at grid points with a large field capacity W_{smax}:

$$h = \left[1 - \cos\left\{\pi \frac{W_s - (W_{smax} - W_{top})}{W_{top}}\right\}\right] / 2 \tag{6.1}$$

for $W_s > W_{smax}$ - W_{top}, and h=0 otherwise. This parameterization allows evaporation only from the upper reservoir W_{top} which is specified as W_{top}=0.1m for $W_{smax} \geq$ 0.1m and W_{top}=W_{smax} otherwise. Figure (6.2) shows the substantial differences of h for W_{smax}=0.2m (standard value of ECHAM3) and W_{smax}=0.364m (PILPS (Project for Intercomparison of Land-surface Parameterization Schemes, see e.g. Henderson-Sellers et al. (1993) for Cabauw)).

The second modification of the land-surface deals with two parameters controling transpiration: The critical value W_{cr} and the permanent wilting point W_{pwp}. In ECHAM4, the value where plants begin to suffer from water stress is taken as W_{cr}=75% and transpiration is supposed to stop if the soil moisture is lower than W_{pwp}=35%. These values were clearly lower in ECHAM3 (50% compared to 20%). In PILPS, W_{cr} is taken as 90% and W_{pwp} as 59%. Figure (6.2) illustrates the water stress factor $F(W_s)$, which controls transpiration according Equation (1.47), for the standard values of ECHAM3, ECHAM4 and Cabauw (PILPS).

The effects on the model results are discussed making use of Figure (6.3) and (6.4).
The modification of h leads to a strong decrease of the evaporation from bare soil. The unrealistic high maximum (ECHAM3) in late spring is clearly reduced. During summer there is almost no bare-soil evaporation. This significant reduction leads to a wetter soil: During summer and autumn, the relative soil moisture content is about 15% higher in the modified model version. Model experiments have shown that the modification of h generates almost the whole observed differences between the ECHAM3 and ECHAM4 simulation whereas the definition of new (higher) values of W_{cr} and W_{pwp} lead only to minor changes in the model results. This is due to the relative soil moisture content which barely falls lower than 75% of the field capacity. Therefore, plants do not suffer from significant water stress during summer for both the ECHAM3 and ECHAM4 value of W_{cr} and this again is the reason why the transpiration is only sligthly different between ECHAM3 and ECHAM4.
The higer soil moisture content in ECHAM4 leads to significantly higher surface runoff (Fig. (6.3)). Drainage is strongly increased in November in ECHAM4 because the relative soil mois-

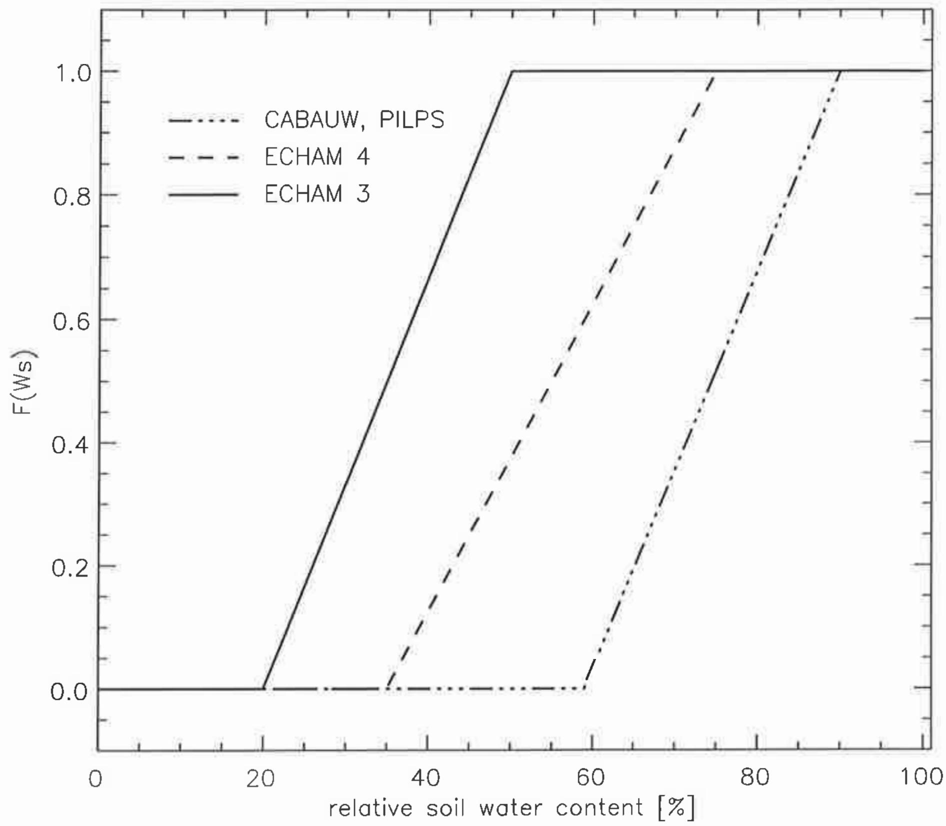

Figure 6.1: *Water stress function $F(W_s)$ for ECHAM3, ECHAM4 and PILPS (Cabauw).*

ture content is higher than 90%, which leads to fast drainage whereas in the ECHAM3 control simulation, slow drainage predominates. The difference in the latent heat flux between the ECHAM3 and ECHAM4 control simulation is mainly influenced by the evolution of bare soil evaporation (Fig. (6.4)). During summer, the latent heat flux in ECHAM3 lies closer to the measurements than ECHAM4. ECHAM3 tends to slightly overestimate, while ECHAM4 clearly underestimates the monthly evapotranspiration from May to August. It should be mentioned that the ECHAM4 run is based on the same input parameters as described in the ECHAM3 experiment (table (2.2)) with the exception of W_{cr} and W_{pwp}.
The sensible heat flux amounts to somewhat unrealistically high values during summer (nearly $40 Wm^{-2}$). These high values are necessary to balance the decrease in the water vapour flux, because changes in surface temperature (and therefore radiation fluxes) are small. This is mainly due to the described temperature on the lowest model level which makes it impossible for the surface to interact with the atmosphere. Differences in both model versions are negligible for ground heat fluxes, soil temperatures, skin resevoir content (and evaporation from this reservoir), albedo and snow conditions.

Finally, it is shown how the ECHAM4 model results are changed when using the PILPS values for Cabauw instead of the standard values of ECHAM3 applied in the control experiments

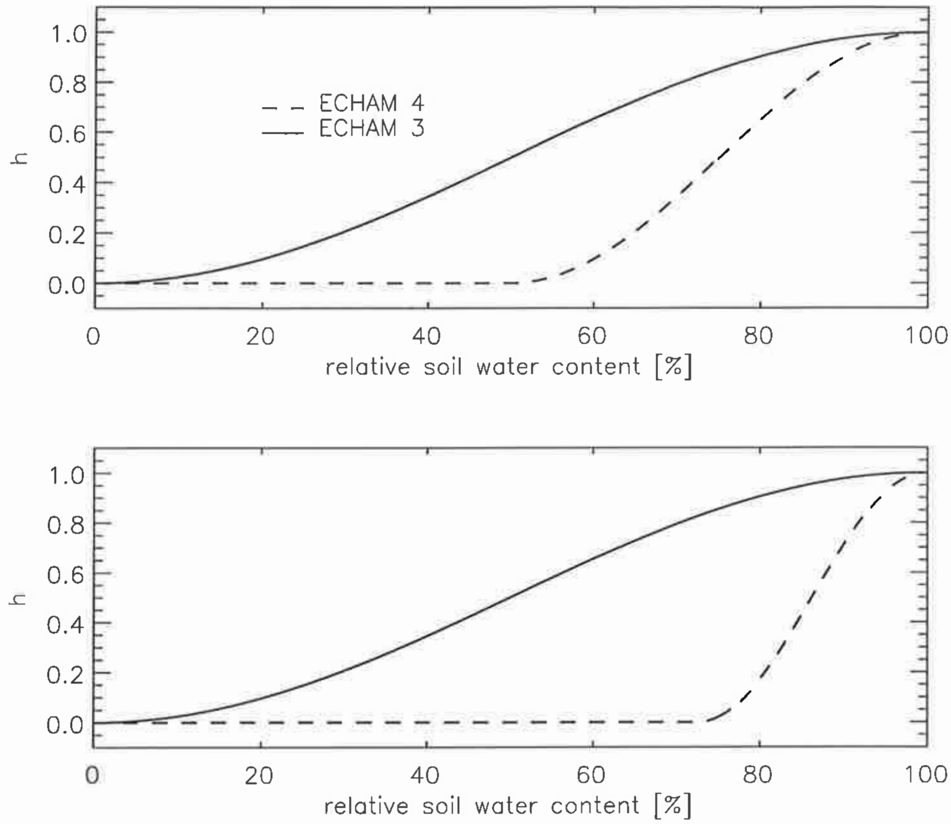

Figure 6.2: *Relative humidity h at the surface for ECHAM3 and ECHAM4. The upper panel is based on W_{smax}=0.2m, the lower one refers to W_{smax}=0.364m.*

(with exception of LAI which is set to 2 instead of 4). The land surface parameters adapted for Cabauw according to PILPS are presented in Table (6.1).

Table 6.1: *List of parameters used for Cabauw in PILPS.*

parameter	**value**
leaf area index	1.3
vegetation ratio	0.956
field capacity	0.364m
wilting point	0.59 x W_{smax}
critical value	0.90 x W_{smax}

The results of this experiment are shown in Fig. (6.3) and (6.4). The influence of most land surface parameters that are listed in Table (6.1) on the model output is described in detail in Chapter (2). The overall effect of the new land surface parameters (ECHAM4 version) is presented here.
The assumption that water stress applies for relative soil moisture contents less than 90% leads

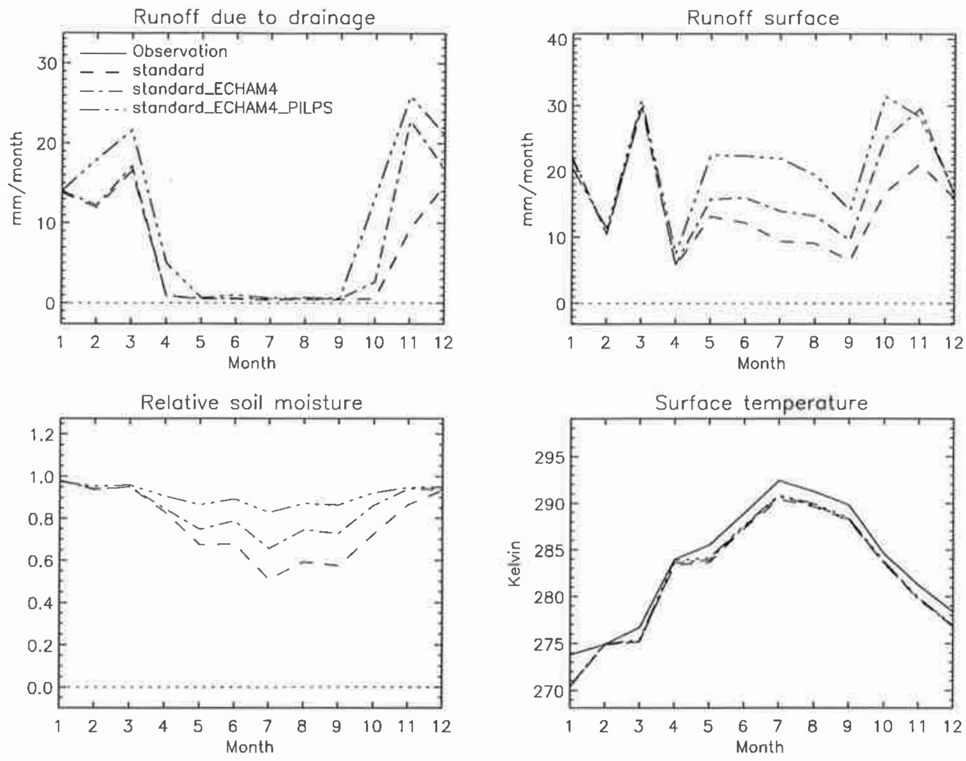

Figure 6.3: *Monthly means of drainage, surface runoff, relative soil moisture for ECHAM3, ECHAM4 and ECHAM4 with PILPS configuration. The standard version sets the parameter as in table (6.1)*

to a significantly reduced transpiration. Bare soil evaporation is also efficiently reduced and becomes negligible for relative soil moisture contents less than about 80% (Fig. (6.2)), lower panel). The reduction of transpiration and evaporation from bare soil leads to a distinct lower latent heat flux because the slight change in the skin reservoir evaporation due to the change of the leaf area index from LAI=2.0 to LAI=1.3 is negligible for the total water vapour flux. The latent heat flux of ECHAM4 with PILPS parameters clearly underestimates the observation (Fig. (6.4)).

The lower latent heat flux leads to an increased soil moisture content W_s. The soil is wet during almost the entire year. This is consistent with the results from Beljaars and Bosveld (1997). Surface runoff increases during May to October due to an enhanced soil moisture. Drainage is strongly increased during the period from October to April because the very efficient fast drainage occurs more often. Similarly to the ECHAM4 simulation, using ECHAM3 land-surface parameters, the sensible heat flux increases to sustain a correct energy balance and leads to a strong overestimation of the observation.

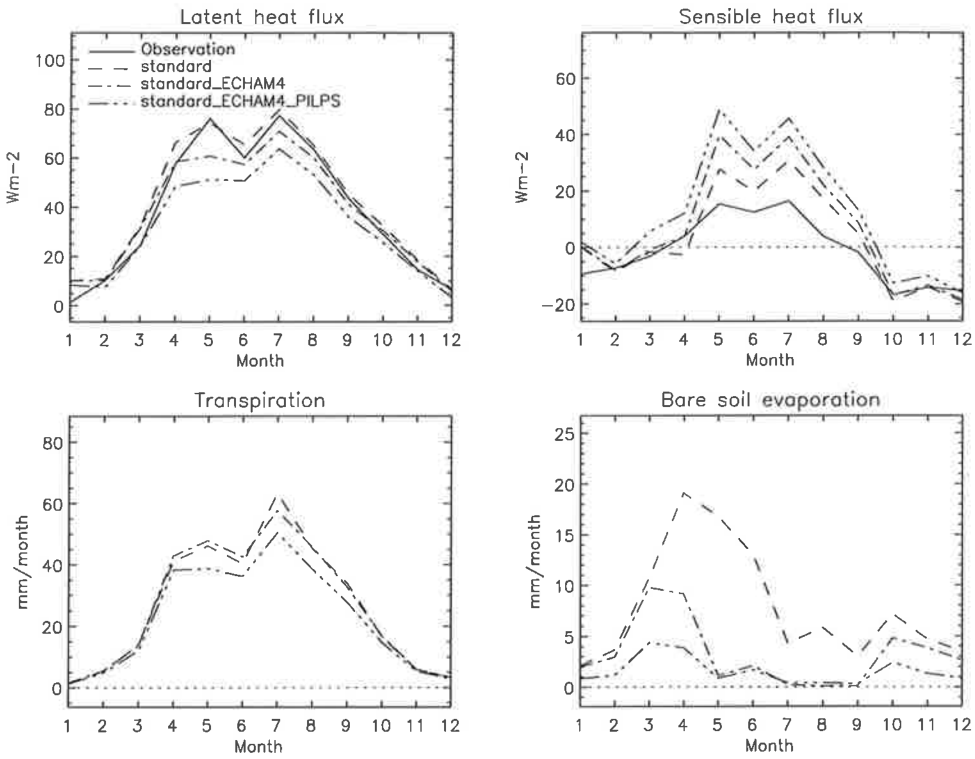

Figure 6.4: *Monthly means of latent and sensible heat flux, transpiration and bare soil evaporation for ECHAM3, ECHAM4 and ECHAM4 with PILPS configuration.*

Chapter 7

Summary and conclusions

In this study we have presented the results of a comparison of the land-surface schemes of ECHAM and EM. The experiments were performed with one-dimensional model versions with fixed upper boundary conditions at the lowest atmospheric level. Emphasis was placed on the comparison of annual and diurnal cycles of the surface energy and water budget. Differences are explained by looking very closely at the parameterization formulae. With the variation of the input parameters, a detailed sensitivity study was performed which shows the impact of changing parameters on the results.
Some general statements can be made:
(1) The results of this study indicate the importance to account for variation of surface and soil parameters in a one-dimensional model. The influence on the surface energy balance and water cycle has important implications to the land surface parameterizations which can directly influence the performance of large-scale models.
(2) The difference between the two examined models are often larger than the differences caused by a variation of a certain input parameter over a physically reasonable range.
(3) The comparison of two models should contain several aspects. This has been done by using a comparison of annual and monthly means, diurnal cycles and phase shifts of different quantities. In addition, the output was divided into 'day' and 'night' values. Moreover, the influence of changed input parameters has been examined by a detailed sensitivity study. Interpretation of the results with the parameterization formulae is more easily achieved by using 1-dimensional version of the models and would be nearly impossible for 3-dimensional versions. Moreover, computer time for so many model experiments would exceed computer capacity because at least 5-year runs are necessary for reliable results. However, 3-dimensional simulations are necessary to capture the very important feedback between surface and atmosphere.
(4) The replacement of a certain parameterization formula often has a large influence on the results which sometimes is larger than the variation of an input parameter over the whole physically possible range. Parameterization swhich are too simple (e.g. transpiration in EM) have the disadvantage of not capturing the physics in a correct manner. Parameterization formulae including parameters which are difficult to determine produce unreliable results. One has to find a compromise between an accurate description of the main physical processes and restriction of the number of prescribed input parameters.
(5) Testing sensitivity by using the derivative of parameterization formulae can often be a useful tool.
(6) Individual components of a quantity (e.g. bare soil evaporation) often have large differences between both models whereas the averaged quantity (e.g. total evapotranspiration) sometimes shows a rather high correlation.
(7) Both models can be tuned to approximately follow the observations. With standard input parameters, ECHAM results are in better agreement with the observations.

The main differences of the two models, based on the control experiments, are:
- Surface temperature in EM is higher during summer and lower in winter. This higher amplitude is mainly due to the climatology which describes the lower boundary condition for the ground temperature.
- Ground heat fluxes in EM show an unexpected evolution (monthly averages are directed upward during summer), whereas ECHAM fluxes follow the observations quite well (when monthly means are considered). The main reason is the prescription of the lower boundary condition for temperature of the EM. If one forces the surface temperature to be the same, both the explicit EFR-method of EM and the implicit computation of ECHAM yield almost the same soil heat fluxes.
- Albedo shows larger values in EM during winter. This can be explained by the strongly different snow covered grid fraction for thin snow layers (less than critical snow depth). This leads to a lower net shortwave radiation.
- Skin reservoir evaporation and skin reservoir content are mostly more than twice as high in ECHAM than in EM. The reason is the fast infiltration of the skin reservoir water in EM whereas ECHAM allows the water to remain on leaves.
- Transpiration is higher in EM during winter and spring. The missing influence of the photosynthetically active radiation (PAR) on stomata closure must be the main reason.
- Bare soil evaporation is hard to parameterize correctly. The ECHAM values break down during April whereas EM shows the expected annual cycle with a summer maximum. The main reason is not the drying of the soil but the structure of the parameterization formulae which leads to a near zero evaporation if the specific humidity h is close to the ratio of specific humidity and the value for saturation.
- Sensible heat flux is mostly higher in EM (with the exception of winter) because of higher surface temperature and thus more unstable conditions.
- Total annual runoff is larger in ECHAM. This is necessary to fulfill the water balance because EM is more efficient in evaporating water. The main differences occur in winter because of the introduction of fast drainage in ECHAM which starts to work above an empirically chosen threshold of 90% relative soil water content. ECHAM surface runoff also increases rapidly for nearly saturated soils. The EM contains two or more soil layers for soil water which enables the model to compute runoff processes more steadily and physically based. Large differences are found for the partition between total runoff into surface runoff and drainage. This is caused by the capability of the EM to exchange the soil water between the different layers. Both models do not include any dependence on the forest fraction which is able to break peaks in surface runoff.

In the following, main differences in the sensitivities are shortly described.

Before describing the single parameters, two general remarks can be made:
- Ground heat fluxes in EM show a much higher sensitivity than in ECHAM because there is no possibility to change fixed temperature at the lower boundary condition.
- The sensitivity of the skin reservoir content and evaporation is about an order higher in ECHAM. This is due to the fast infiltration of skin reservoir water in the weather model.

A summary of the results (only for annual means) is given in the following:

- Roughness length (z_0): The formulation of the transfer coefficients are explicitly dependent on the roughness length. In ECHAM, the evaporation efficiency again includes z_0. Turbulent heat fluxes increase with the roughness length because of higher turbulence over rougher surfaces. ECHAM shows larger sensitivities for most calculated output quantities. The decrease in sensitivity is reversed proportionally to z_0 because of the logarithmic dependence of C_h on z_0. The examined range causes about a halvening of the sensitivity.
- Leaf area index (LAI): For EM-experiments the Dickinson parameterization was chosen to

compute evaporation. Transpiration, evaporation from the skin reservoir and latent heat flux increase with increasing LAI whereas runoff, soil moisture, bare soil evaporation and surface temperature decrease. Transpiration is an exponential function of LAI in ECHAM but a rational one in EM. The sensitivity of almost all quantities is decreasing with increasing LAI. The reason is that lower leaves in the canopy receive less shortwave radiation because of absorption and reflection. The exponential law of penetrating radiation also suggests an exponential law for transpiration. The EM-experiments show a strong decrease of most quantities for LAI values between 1 and 3 while for LAI values over 4 the model is reaching a state where results are nearly independent on LAI. This is mainly caused by the very strong drying of the soil for higher leaf area indices. Transpiration seems to draw too much water out of the soil. ECHAM does not reach such an equilibrium.

- Vegetation ratio (σ_{PLNT}): In ECHAM, the leaf area index and vegetation ratio are closely connected but this is not the case in EM (operational version) because there is no dependence on the LAI. The vegetation is poorly modeled in both models. Only transpiration and skin reservoir content are dependent on the vegetation ratio in the two models. EM introduces a further explicit dependence on σ_{PLNT} for surface albedo and maximum infiltration rate. EM mostly shows a more than double the sensitivity compared to ECHAM because more parameterization formulae take into account the vegetation ratio. An interesting feature is that, for some quantities (e.g. soil moisture), the smallest sensitivity is reached for grid elements that are half vegetated. However, most quantitites show the largest sensitivity for a vegetation ratio equal to 1.

- (snow free) albedo (α): Albedo is one of the most important parameters in climate models. Nevertheless, the parameterization of albedo is very poor in both models. For snow free conditions, ECHAM assumes the albedo to be a constant and the formulation for snow covered grid elements is very empirical and not physically based. A higher albedo lowers net radiation, surface temperature and turbulent energy fluxes. To conserve the water balance, runoff and soil moisture are raised. Sensitivity is approximately constant for most quantities on a annual basis. Most output quantities show a larger sensitivity for ECHAM. One of the main reasons is the consideration of net shortwave radiation in the computation of transpiration in the ECHAM scheme.

- snow albedo (α_s): Absolute sensitivity of (total surface) albedo is about three times higher in EM than in ECHAM. The reason is the difference in the computation of albedo for snow depths below the critical snow depth. Whereas sensitivities are rather constant for ECHAM, EM shows more scattering. Other conclusions are similar as for surface albedo α.

- maximum soil water content (w_{smax}): The soil water content takes a key position in the determination of processes in the soil and close to the surface. Many formulae (transpiration, bare soil evaporation, drainage, surface runoff) explicitly include the water content. Most parameterizations relate to the relative soil moisture content rather than to absolute values. Since different processes originate from different soil depth, one should include several soil layers for water to give the possibility for more physical formulation of the processes.

Sensitivity normally decreases with higher maximum soil moisture content because limiting effects have a higher influence for low maximum water contents with less efficient storage possibilities. Sensitivities of ECHAM and EM are rather different. Besides the different parameterizations, the difficulty to compare the two models directly concerning soil parameters must not be forgotten.

It could be an aim to build up a new model of both models, although this is certainly not the right method to improve models. However, a short overview of what the results and the experience of the whole study would suggest is given.

A combined scheme should include:

Representation as in ECHAM:

- Albedo of snow covered forest
- Dependence of snow albedo on temperature

- Skin reservoir content (dependent on leaf area index)
- Depths and numbers of soil layers for temperature (to avoid artificial boundary conditions)
- Boundary layer parameterization (the same for both models)
- Numerical method (implicit because of better stability)
- Transpiration (EM is too simple, Dickinson has too many badly known parameters)
- Soil heat fluxes (although the EFR-method of EM gives very similar and encouraging results)

Representation as in EM:
- Soil water (for bare soil evaporation, it may be an advantage to better resolve the soil close to the surface)
- Runoff/ drainage (possibility to compute runoff from different soil layers)
- Infiltration rate
- Bare soil evaporation (inspite of the fact that the ECHAM parameterization gives better results in the EM environment, the strong decrease in summer bare soil evaporation in ECHAM experiments, even for field capacities of 0.4m, indicates there are severe deficiencies and problems in the ECHAM parameterization)
- Dependence of albedo on soil moisture and vegetation ratio
- Parameterization of snow (and water) covered grid fraction
- Snow melt (melt from lower and upper boundary of snow pack, redistribution of heat)
- Surface temperature and temperature of uppermost soil layer
- Allowance of transpiration and skin reservoir evaporation from vegetation at the same time.

In addition, the following points should be improved:

- Introduction of a simple physically based canopy model for a correct description of radiation and temperature within the vegetation (and therefore the surface temperature, albedo and snow melt).
- Introduction of a very thin uppermost soil layer (for temperature and water) to better determine surface temperature and evaporation from bare soil. However, it must be ensured that the implemented numerical method does not produce instabilities.
- Physically based parameterization of albedo for snow covered conditions.
- Taking into account the balancing effects of forests concerning runoff processes (introduction of a soil moisture for the forest fraction of the grid element and a different one for the non-forested part).
- A replacement of the stability function for vertical diffusion in stable conditions.

Acknowledgements:

The first author thanks Dr. E. Heise from the German Weather Service for the assistance to run the Europa-Modell. Much thanks is extended to Prof. A. Ohmura, Prof. M. Beniston, Dr. D. Jacob, Dr. E. Heise and R. Sheppard for a critical reading of the manuscript. Many thanks for the possibility to frequently visit the MPI and to discuss with many researchers.

Bibliography

Barnett, T., L. Dümenil, U. Schlese, E. Roeckner, and M. Latif, 1989: The effect of Eurasian snow cover on regional and global climate variations. *J. of the Atmospheric Sciences* **46**, 661–685.

Beljaars, A. and F. Bosveld, 1997: Cabauw data for the validation of land surface parameterization schemes. *Journal of Climate* **10**, 1172–1193.

Betts, A., A. Beljaars, and J. Ball, 1993: Comparison between the land surface response of the ECMWF model and the FIFE-1987 data. *Q.J.R.Meteorol.Soc.* **119**, 975–1001.

Bonan, B., D. Pollard, and S. Thompson, 1992: Effects of boreal forest vegetation on global climate. *Nature* **359**, 716–717.

Dickinson, R., 1978: Efficient prediction of ground surface temperature and moisture with inclusion of a layer of vegetation. *J. Geophys. Res* **20**, 1889–1903.

Dickinson, R., A. Henderson-Sellers, and P. Kennedy, 1993: Biosphere-Atmosphere Transfer Scheme (BATS) Version 1e as Coupled to the NCAR Community Climate Model In *NCAR/TN-387+STR*. National Center for Atmospheric Research, Boulder, Colorado.

Dickinson, R., A. Henderson-Sellers, P. Kennedy, and M. Wilson, 1986: Biosphere-Atmosphere Transfer Scheme (BATS) for the NCAR community Climate Model In *NCAR/TN-275+STR*. National Center for Atmospheric Research, Boulder, Colorado.

Driedonks, A., H. van Dop, and W. Kohsiek, 1978: Meteorological observations on the 213 m mast at Cabauw in the Netherlands. *Preprints, 4th Symp. Meteor. Observ. and Instrum., Denver, USA, Amer. Meteor. Soc.*, 41–46.

Ducoudré, N., K. Laval, and A. Perrier, 1993: SECHIBA, a new set of parameterizations of the hydrologic exchanges at the land-atmosphere interface within the LMD atmospheric general circulation model. *Journal of Climate* **6**, 248–273.

Dümenil, L. and E. Todini, 1992: A rainfall-runoff scheme for use in the Hamburg Climate model. In J. O'Kane (Ed.), *Advances in theoretical hydrology. A tribute of James Dooge*, European Geophysical Society Series on Hydrological Sciences, pp. 129–157. Elsevier Science Publishers B.V., Amsterdam.

Edelmann, W., D. Majewski, E. Heise, P. Prohl, G. Doms, B. Ritter, M. Gertz, and T. Hanisch, 1995, 6) *Dokumentation des EM/DM-Systems*. DWD.

Gallimore, R. and J. Kutzbach, 1989: Effects of soil moisture on the sensitivity of a climate model to earth orbital forcing at 9000 YR BP. *Climatic Change* **14**, 175–205.

Garratt, J., 1993: Sensitivity of Climate Simulations to Land-Surface and Atmospheric Boundary-Layer Treatments- A Review. *Journal of Climate* **6**, 419–449.

Henderson-Sellers, A. and V. Gornitz, 1984: Possible climatic impacts of land cover transformations, with particular emphasis on tropical deforestation. *Clim. Change* **6**, 231–257.

Henderson-Sellers, A., Z.-L. Yang, and R. Dickinson, 1993: The Project for Intercomparison of Land-surface Parameterization Schemes (PILPS). *Bull. Amer. Meteor. Soc.* **7**, 1335–1349.

Jacobsen, I. and E. Heise, 1982: A new economic method for the computation of the surface temperature in numerical models. *Beitr. Phys. Atmosph.* **155**, 128–141.

Jacquemin, B. and J. Noilhan, 1990: Sensitivity study and validation of a land surface parameterization using the HAPEX-MOBILHY data set. *Boundary-Layer Meteorol.* **52**, 93–134.

Louis, J.-F., 1979: A parametric model of vertical eddy fluxes in the atmosphere. *Boundary-Layer Meteorol.* **17**, 187–202.

Louis, J.-F., 1982: A short history of the PBL parameterization at ECMWF In *Proceedings, ECMWF workshop on planetary boundary layer parameterization, Reading, 25-27 Nov. 81*, pp. 59–80. ECMWF.

Mahfouf, J. and J. Noilhan, 1991: Comparative study of various formulations of evaporation from bare soil using in situ data. *Journal of Applied meteorology* **30**, 1354–1365.

Meehl, G. and W. Washington, 1988: A comparison of soil-moisture sensitivity in two global models. *J. of the Atmospheric Sciences* **45**, 1476–1492.

Mylne, M. and P. Rowntree, 1991: Deforestation of Amazonia-Modelling the effects of albedo change Technical Report Clim. Res. Tech. Note CRTN 7, Hadley Centre, UK Met. Office, Bracknell.

Pitman, A., 1994: Assessing the sensitivity of a land-surface scheme to the parameter values using a single column model. *Journal of Climate* **7**, 1856–1869.

Pitman, A., Z.-L. Yang, J. Cogley, and A. Henderson-Sellers, 1991: Description of bare essentials of surface transfer for the Bureau of Meteorology Research Centre AGCM Technical Report BMRC Res. Rep., Res. Cent., Melbourne.

Roeckner, E., K. Arpe, L. Bengtsson, L. D. S. Brinkop, M. Esch, E. Kirk, F. Lunkeit, M. Ponater, B. Rockel, R. Sausen, U. Schlese, S. Schubert, and M. Windelband, 1992: Simulation of the present day climate with the ECHAM model: impact of model physics and resolution. *Max Planck Institute for Meteorology Report No. 93, 171 pp.*

Rowntree, P., 1983: Sensitivity of general circulation models to land surface processes pp. 107–166. ECMWF.

Sellers, P., Y. Mintz, Y. Sud, and A. Dalcher, 1986: A simple biosphere model (SiB) for use within general circulation models. *J. of the Atmospheric Sciences* **43**, 505–531.

Siebert, J., U. Sievers, and W. Zdunkowski, 1992: A one-dimensional simulation of the interaction between land surface processes and the atmosphere. *Boundary-Layer Meteorol.* **59**, 1–34.

Verseghy, D., 1991: CLASS -A Canadian Land Surface Scheme for GCMs. I Soil model. *International Journal of Climatology* **13**, 111–133.

Verstraete, M., 1994: *Retrieving Canopy Properties from Remote Sensing Measurements* Imaging Spectrometry - a tool for environmental observations. Kluwer Academic Publishers, Dortrecht.

Viterbo, P. and A. Beljaars, 1995: An improved land surface parameterization scheme in the ECMWF model and its validation. *Journal of Climate*, 1–50.

Webb, E., 1970: Profile relationships: the log-linear range, and extension to strong stability. *Quart. J. R. Met. Soc.* **96**, 67–90.

Wetzel, P. and J. Chang, 1987: Concerning the Relationship between Evapotranspiration and Soil Moisture. *Journal of Climate and Applied Meteorology* **26**, 18–27.

Wetzel, P. and J. Chang, 1988: Evapotranspiration from nonuniform surface: A first approach for short term numerical weather prediction. *Journal of Climate and Applied Meteorology* **116**, 600–621.

Yamazaki, K., 1989: A study of the impact of soil moisture and surface albedo changes on global climate using the MRI GCM-I. *J. Meteorol. Soc. Jpn* **67**, 123–146.